THE MEF2 TRANSCRIPTION FACTOR IS AN ESSENTIAL

REGULATOR OF BONE DEVELOPMENT

APPROVED BY SUPERVISORY COMMITTEE

Eric N. Olson, Ph.D.

Jane E. Johnson, Ph.D.

Melanie H. Cobb, Ph.D.

Dennis McKearin, Ph.D.

To my many supportive friends and family,
especially my wife Christina,
and my daughter Madelyn.

THE MEF2 TRANSCRIPTION FACTOR IS AN ESSENTIAL REGULATOR OF BONE DEVELOPMENT

by

Michael Andrew Arnold

DISSERTATION

Presented to the Faculty of the Graduate School of Biomedical Sciences

The University of Texas Southwestern Medical Center at Dallas

In Partial Fulfillment of the Requirements

For the Degree of

DOCTOR OF PHILOSOPHY

The University of Texas Southwestern Medical Center at Dallas

Dallas, Texas

June, 2006

THE MEF2 TRANSCRIPTION FACTOR IS AN ESSENTIAL REGULATOR OF BONE DEVELOPMENT

Michael Andrew Arnold

The University of Texas Southwestern Medical Center at Dallas, 2006

Eric N. Olson, Ph.D.

MEF2 transcription factors are essential regulators of muscle and cardiovascular development. Mice lacking *Mef2c* die during early embryogenesis due to cardiovascular abnormalities. Using a conditional *Mef2c* null allele, I show that MEF2C plays an essential and unexpected role in the development of both neural crest derived and mesoderm derived bones. Deletion of MEF2C from the cartilaginous precursors of endochondral bones causes a delay in chondrocyte maturation, resulting in persistent endochondral cartilage, decreased bone growth and short stature. Further, transgenic over expression of a dominant negative or constitutively active MEF2C causes a block in chondrocyte hypertrophy or premature ossification, respectively. HDAC4, a known

repressor of MEF2 proteins, inhibits chondrocyte maturation by repressing the Runx2 transcription factor. Intercrosses of the null alleles of *Mef2c* and *HDAC4* reveal that the dynamics of chondrocyte hypertrophy in the endochondral growth plate is controlled by a balance between the positive transcriptional effects of MEF2C against the repressive activity of HDAC4. Misregulation of signaling pathways that influence growth plate dynamics results in dwarfisms and bone deformations due to either accelerated maturation of the growth plate cartilage, characteristic of achondroplasia, or delayed or absent chondrocyte maturation, characteristic of many chondrodysplasia syndromes. MEF2C is capable of directly activating the promoter of *collagen α1(X)*, which marks hypertrophic chondrocytes. I therefore conclude that the association of HDAC4 with MEF2C serves as a switch to directly control gene expression in hypertrophic endochondral cartilage, and therefore the interaction of HDAC4 and MEF2C in chondrocytes may be an opportunity for pharmacologic intervention in disorders of growth plate maturation.

Table of Contents

Prior Publications

Davis CA, Haberland M, **Arnold MA**, Sutherland LB, McDonald OG, Richardson JA, Childs G, Harris S, Owens GK, Olson EN. (2006). PRISM/PRDM6, a Transcriptional Repressor That Promotes the Proliferative Gene Program in Smooth Muscle Cells. Mol Cell Biol. *26*, 2626-36. PMID: 16537907

Durham JT, Brand OM, **Arnold M**, Reynolds JG, Muthukumar L, Weiler H, Richardson JA, Naya FJ. (2006). Myospryn Is a Direct Transcriptional Target for MEF2A That Encodes a Striated Muscle, {alpha}-Actinin-interacting, Costamere-localized Protein. J Biol Chem. *281*, 6841-9.

Nakagawa O, **Arnold M**, Nakagawa M, Hamada H, Shelton JM, Kusano H, Harris TM, Childs G, Campbell KP, Richardson JA, Nishino I, Olson EN. (2005). Centronuclear myopathy in mice lacking a novel muscle-specific protein kinase transcriptionally regulated by MEF2. Genes Dev. *19*, 2066-77.

Bush E, Fielitz J, Melvin L, **Martinez-Arnold M**, McKinsey TA, Plichta R, Olson EN. (2004). A small molecular activator of cardiac hypertrophy uncovered in a chemical screen for modifiers of the calcineurin signaling pathway. Proc Natl Acad Sci U S A. *101*, 2870-5.

List of Figures

List of Tables

List of Abbreviations

MEF2,	Myocyte Enhancer Factor 2
HDAC,	Histone Deacteylase
E,	Embryonic Day
P,	Postnatal day
bHLH,	basic Helix-Loop-Helix
MAPK,	Mitogen-activated protein kinase
OSC,	Osteocalcin
BSP,	Bone Sialoprotein
MMP13,	Matrix metalloproteinase 13

Chapter I

Introduction

The MEF2 Family of Transcription Factors

Members of the Myocyte Enhancer Factor 2 (MEF2) family of transcription factors are known to be essential transcriptional regulators of striated muscle development, and key mediators of histone deacetylase (HDAC) signal dependent gene regulation in cardiac hypertrophy. The family of MEF2 factors is composed of four members in vertebrates, MEF2A, MEF2B, MEF2C and MEF2D, which have emerged from a common ancestor represented in insects by the single D-MEF2 gene of *Drosophila* (Reviewed in Molkentin and Olson 1996). MEF2 proteins are members of the MADS box family of transcription factors, which bind DNA as dimers through a hallmark amino-terminal DNA binding domain. The MADS box of each MEF2 protein is immediately followed by the MEF2 domain, which mediates dimerization. The remaining protein sequence encodes the transactivation domain, which mediates interaction with both activators, such as p300 (Ma et al., 2005), and the signal responsive repressors of the Class II HDAC family (Lu et al., 2000a, Lu et al., 2000b, McKinsey et al., 2000, reviewed in McKinsey et al., 2001).

MEF2 proteins were first identified as a muscle enriched DNA binding activity, and are generally enriched in striated muscle (Gossett et al., 1989). In the developing heart, *Mef2c* is the first *Mef2* gene to be detected in the early precardiac mesoderm of the primary and secondary heart fields at E7.5 (Dodou et al., 2004). Expression of *Mef2a* and *Mef2d* follows, beginning at E8.0. *Mef2c* expression diminishes and is undetectable beyond E13.5 (Edmondson et al., 1994). Similarly in skeletal muscle, *Mef2c* is the first to be detected in somites at E8.5, followed by *Mef2a* and *Mef2d* at E9.5. The expression of MEF2 family members is not limited to muscle during later development and

throughout adulthood. *Mef2* expression is detectable in many regions of the brain (Lyons et al., 1995), neural crest derivatives in the head, skin and enteric nervous system, and arterial and visceral smooth muscle (Edmondson et al., 1994).

All four of the *Mef2* transcripts in mammals are encoded by genes of similar exon structure. In each case, the transcript contains one or more 5' untranslated exons initiated from one or more different promoters. The first protein coding exon encodes the first 18 amino acids of the MADS box, and the second coding exon encodes the remainder of the MADS box and the entire MEF2 domain. Since the critical DNA binding activity of the MADS and MEF2 domains is encoded almost entirely by a single exon that is never alternatively spliced, the second coding exon has been the target of *Mef2* gene disruption studies.

The function of several *Mef2* family members has been analyzed by gene deletions in mice. Null alleles of *Mef2a*, *Mef2c*, and *Mef2d* have been generated by gene targeting to disrupt the second coding exon. A null allele of *Mef2b* has been cited in the literature as unpublished data, which remains unpublished (Lin et al., 1997).

The majority of *Mef2a* null mice die suddenly in the first two weeks of postnatal life. The lethality of these mice was highly sensitive to the genetic background. All *Mef2a* null mice died in a pure 129SvEv background before postnatal day (P) seven, while more than 50% of the *Mef2a* null mice survived in subsequent intercrosses of mice from a C57B6 genetic background. Death of the null mice was attributed to dilation and failure of the right ventricle, leading to arrhythmia and sudden death. Analysis of the cardiac muscle of these mice demonstrated a decrease in the number and function of mitochondria. Surprisingly, crosses of the *Mef2a* null allele to mice bearing the MEF2

sensor LacZ transgene indicated that the activity of the MEF2 sensor transgene increased (Naya et al., 2002). This suggests that MEF2D, which is the only other MEF2 protein significantly expressed in the adult heart, attempts to compensate for the absence of MEF2A, but is unable to sustain normal cardiac function in some genetic backgrounds.

Mef2d null mice have been recently generated in the Olson lab, resulting in normal, viable adult homozygous null animals (Kim, Phan and Olson unpublished data). Surprisingly, animals heterozygous for both *Mef2c* and *Mef2d* exhibit significant perinatal lethality, demonstrating that members of the *Mef2* family can function redundantly in essential developmental roles.

MEF2C is essential for cardiac development, as *Mef2c* null embryos die of cardiovascular defects at approximately embryonic day (E)9.5 (Lin 1997, Lin 1998). The cardiovascular system develops from tissues arising from several regions of the embryo. Much of the heart is derived from mesodermal precursors which are initially specified in the mouse embryo at E7.5 (Reviewed in Srivastava and Olson 2000). This crescent shaped region, the primary heart field contributes cells to all four chambers of the mature heart. Additional contributions to the right side of the heart are made by a secondary region of mesoderm which is specified at E7.5 and expresses *Mef2c* (Dodou et al, 2004). These cells migrate to the midline of the embryo and form the heart tube, a rudimentary one chambered heart which begins to beat. This tube is connected to the vasculature by vessels which will become the aorta and pulmonary artery, and are derived from the neural crest, a migratory population of mesenchyme originating from the neural tube (Jiang et al., 2000). As development continues, the four morphologically distinct chambers of the adult heart begin to become distinct during the process of cardiac

looping. Rightward looping of the heart tube is accompanied by reconnection of segments of the looped heart tube to each other and to the vasculature. This process results in four distinct chambers, the right ventricle and atrium and the left ventricle and atrium, which are separated from each other by the ventricular septum and atrial septum, and the atrioventricular valves. Defective cardiovascular development of *Mef2c* null embryos includes a failure of cardiac looping, pericardial effusion and disorganized vessel formation. Analysis of cardiac gene expression demonstrated that markers of cardiac development such as cardiac α–actin, MLC1A and HAND2 are significantly down regulated in the hearts of null embryos. The expression of *Mef2b* was significantly increased, while the expression of *Mef2d* was slightly increased and the expression of *Mef2a* was unchanged. The upregulation of some *Mef2* family member genes again suggests a failed attempt to compensate for the absence of a *Mef2* gene, as seen in *Mef2a* null hearts. One possible explanation for the failure of other *Mef2* genes to compensate for the absence of *Mef2c* in early cardiac development is the relative timing of gene expression in the *Mef2* family. *Mef2c* is the first to be expressed in the precardiac mesoderm at 7.5, a day before the expression of other *Mef2* genes. It is possible that the loss of *Mef2c* in the early stages of cardiac differentiation results in an irreversible insult in cardiac development, which cannot be rescued by subsequent up regulation of other *Mef2* family members. An alternative explanation is that the lethality of *Mef2c* null embryos is the result of the observed defects in vascular development. Recently, this issue has begun to be addressed both by my own work (Appendix), and the publication of mice in which *Mef2c* was conditionally deleted from the developing heart using a Cre recombinase transgene driven by the *α-myosin heavy chain* promoter (Vong et al., 2005).

This Cre line results in deletion of *Mef2c* at approximately E9.5, after looping has taken place and the expression of other *Mef2* genes are established. The resulting mice are viable, with no apparent cardiac defects. This result does not however distinguish between the possibilities of functional redundancy in the *Mef2* family during late cardiac development, or a requirement for *Mef2c* in vascular development.

MEF2 and HDAC Regulate Cardiac Hypertrophy

Since the initial identification of MEF2 DNA binding activity in muscle, MEF2 proteins have been shown to activate many striated muscle genes in cooperation with tissue restricted factors such as the bHLH factors MyoD and Myogenein (Molkentin and Olson 1996). MEF2 dependent transcription has also been shown to be responsive to various stimuli, including calcineurin and MAPK signaling (Wu et al., 2001, Flavell et al., 2006, Han el at. 1997, Stanton et al., 2004). The activity of MEF2 proteins is regulated by a repressive association with class II histone deacetylase (HDAC). Class II HDAC proteins directly associate with and repress MEF2, and are exported to the cytoplasm as a consequence of signal responsive phosphorylation and binding by 14-3-3, relieving MEF2 repression (Lu et al., 2000a, Lu et al., 2000b, Grozinger et al., 2000, McKinsey et al., 2000). The repressive effects of Class II HDACs on MEF2 can be exerted independent of HDAC catalytic deacetylase activity, by recruiting co-repressors and competing with transcriptional co-activating factors for binding sites on the MEF2 protein (Zhang et al., 2001).

The class II HDACs include HDAC4, HDAC5, HDAC7 and HDAC9. These genes are expressed in many tissues and, like the *Mef2* family, are expressed

predominantly in cardiac and skeletal muscles and in the brain (Grozinger et al., 1999, Fischle et al., 1999, Verdel and Khochbin 1999). Targeted deletions of HDACs 4, 5 and 9 have been produced in mice. HDAC5 and HDAC9 are not individually required for normal development, however the absence of both can result in cardiovascular defects including cardiac septal defects and thinning of the ventricular wall (Chang et al., 2004). The absence of either of these genes confers extreme sensitivity to stimuli which induce cardiac hypertrophy, accompanied by strong activation of MEF2 dependent transcription during hypertrophic growth (Zhang et al., 2002, Chang et al., 2004).

HDAC4 Regulates Bone Development

Mice which lack HDAC4 display an unexpected phenotype due to abnormal bone development. At birth, HDAC4 null mice appear grossly normal. However, during the first week of postnatal life these mice develop abnormal skeletal structures due to premature ossification of the endochondral skeleton (Vega et al., 2004).

All bones of the vertebrate skeleton are formed by either endochondral or membranous ossification. Membranous bones, which include flat bones of the skull and craniofacial structures, are formed from a mesenchymal precursor. The mesenchymal cells, usually of neural crest origin, differentiate directly into osteoblasts and deposit the matrix of the mature bone. Endochondral bones are initially formed as a patterned cartilaginous template. The formation of the mature bone requires the chondrocytes in these templates to undergo hypertrophy, apoptosis and replacement by invading osteoblasts. Chondrocyte hypertrophy is an essential process in endochondral ossification, as it provides the force for elongation of the bone during development.

Chondrocyte hypertrophy first begins in the middle of the long bones and progresses towards each end of the bone during development and bone growth. Each end of the developing bone contains proliferating chondrocytes which exit the cell cycle, undergo hypertrophy and apoptosis. This process continuously supplies the growing bone with hypertrophic chondrocytes, creating a growth plate at each end of the bone which contains chondrocytes at all stages of maturation and hypertrophy. Hypertrophic chondrocytes also produce signals which recruit osteoblasts to deposit a bony collar around the developing bone. The bone collar is first formed in the middle of the bone and continues to form towards each end of the bone, corresponding with the position of the hypertrophic chondrocytes. Bone growth is completed when the proliferating chondrocytes in the ends of the bone exit the cell cycle, undergo hypertrophic differentiation and apoptosis. The resulting mature bone contains no cartilage and is largely hollow to accommodate the bone marrow (Reviewed in Lefebvre and Smits 2005).

HDAC4 is expressed in prehypertrophic endochondral cartilage, coinciding with the expression of Runx2 (Vega et al., 2004). Runx2 is a runt domain transcription factor which is necessary for ossification of nearly all bones (Ducy et al., 1997, Kimori et al., 1997, Mundlos et al., 1997, Otto et al., 1997). Runx2 is expressed in prehypertrophic chondrocytes and osteoblasts. It is required for the function of osteoblasts, and is capable of promoting ectopic chondrocyte hypertrophy *in vivo*. Transgenic mice which overexpress Runx2 in proliferating and prehypertrophic chondrocytes using the c*ollagen α1(II)* promoter exhibit premature and ectopic ossification in endochondral bones and skeletal elements which normally remain cartilaginous (Takeda et al., 2001). Mice which lack Runx2 die shortly after birth due to a nearly complete lack of ossification throughout

their skeleton as a result of failed osteoblast differentiation (Komori et al., 1997). Chondrocytes in the endochondral cartilage of *Runx2* mutant mice undergo hypertrophic differentiation, but not apoptosis. However, chondrocyte hypertrophy is completely blocked in mice which are null for both *Runx2* and *Runx3*, suggesting redundant functions among these runt domain transcription factors (Yoshida et al., 2004).

HDAC4 interacts with Runx2 and represses its transcriptional activity. The Runt domain of Runx2 physically interacts with the MEF2 binding domain of HDAC4. Additionally, the interaction of HDAC4 with Runx2 can disrupt Runx2 binding to its target sequences in DNA. The transcriptional activity of Runx2, and its control by HDAC4, has been thought to be the major mechanism of transcriptional control in chondrocyte development (Vega et al., 2004).

MEF2C and HDAC4 Function Antagonistically in Bone Development

My data demonstrates that MEF2C is a major target of HDAC4 repression in the development of hypertrophic chondrocytes. Intercrosses of the existing null alleles of *Mef2c* and *HDAC4* demonstrate a genetic interaction in which removal of a single wild type allele of *Mef2c* from the *HDAC4* null background results in restoration of a normal pattern of postnatal ossification. Conversely, a previously unknown defect in ossification present in early postnatal mice heterozygous for *Mef2c* can be reversed in a dose dependent manner by removal of wild type alleles of *HDAC4*. To further study the role of *Mef2c* in specific tissues during later embryogenesis, I have generated a mouse line with conditional allele of *Mef2c*. I have demonstrated that MEF2C is required specifically for appropriate growth and development of both membranous and

endochondral bones. MEF2C controls the population of osteoblasts in neural crest derived membranous bones, and regulates the hypertrophic differentiation of chondrocytes in endochondral bones of both mesodermal and neural crest origin. However, MEF2C is not required in patterning the template endochondral cartilage. Mice which lack MEF2C in endochondral cartilage are viable with features resembling short-limb dwarfism, due to chondrodysplasia. Further, the activities of multiple MEF2 proteins are required for chondrocyte hypertrophy. I generated transgenic mice which overexpress dominant negative MEF2C protein fused to the *Drosophila* engrailed protein. This MEF2-engrailed fusion protein binds DNA and blocks transcriptional activation by other MEF2 factors. At E18.5, these transgenic mice displayed a severe lack of endochondral ossification and bone growth resulting from a nearly complete block in chondrocyte hypertrophy. Conversely, transgenic mice that express a "super-active" MEF2C-VP16 fusion protein under control of the collagen II promoter display a phenotype opposite to that of MEF2C-engrailed transgenic mice, in which endochondral bones underwent precocious ossification with consequent foreshortening of the limbs and premature fusion of growth plate cartilages. Evidence presented here also demonstrates that MEF2 proteins directly activate the expression of *Collagen α1(X)*, suggesting that MEF2 proteins control the expression of the hypertrophic gene program of chondrocytes and that growth plate dynamics can be modified by the balance of MEF2C and its repressor, HDAC4. Misregulation of signaling pathways that influence growth plate dynamics are responsible for dwarfisms and bone deformations resulting from either premature maturation of the growth plate cartilage, characteristic of achondroplasia (Chen el al., 1999, Li et al., 1999, Reviewed in Horton 2006 and Ornitz 2005), or delayed

or absent chondrocyte maturation, characteristic of many chondrodysplasia syndromes (Reviewed in Schipani and Provot 2003, Cohen 2002). The activation of MEF2C dependent transcription by a variety of signaling pathways, and the ability of MEF2C to directly activate chondrocyte gene expression demonstrates that MEF2C and HDAC4 control a key nodal point in chondrocyte hypertrophy and growth plate dynamics. Further investigation may identify molecules which can influence the interaction of MEF2C and HDAC4 in chondrocytes and make control of growth plate dynamics possible.

Chapter II

MEF2C Regulates Neural Crest Derived Bone Development

MEF2C is an essential factor in early cardiovascular development. Mice which lack MEF2C die at E9.5, displaying cardiovascular defects including failure of cardiac looping, pericardial effusion and disorganized vessel formation (Lin et al., 1997, Lin et al., 1998). To further dissect the role of MEF2C in different tissues that contribute to cardiovascular development, and to study its function in adult tissues, I have generated a loxP conditional allele of *Mef2c* which can be inactivated in mice by the expression of Cre recombinase. Deletion of *Mef2c* from the neural crest was of particular interest given the known role of MEF2C in cardiovascular development (Lin et al., 1997, Lin et al.,1998), the expression of *Mef2c* in neural crest derivatives (Edmondson et al., 1994), and the contribution of neural crest derivatives to cardiovascular outflow structures (Jiang et al., 2000). To determine the role of MEF2C in neural crest derived cardiovascular structures, *Mef2c* was deleted in the neural crest using Cre recombinase driven by the *Wnt1* promoter (Jiang et al., 2000). Surprisingly, the resulting neural crest knockout mice were born with normal cardiovascular structures, but died in the very early postnatal period with a severe defect in bone development effecting both membranous and endochondral bones. Neural crest derived membranous bones in these mice are composed of an abnormally high number of hyperactive osteoblasts, resulting in a thick, disorganized bone matrix. Endochondral bones of neural crest origin are reduced in size and contain underdeveloped growth plate cartilages. These mutant mice reveal a novel role for MEF2C in the regulation of both membranous and endochondral bone development.

Results

Generation and Verification of a Conditional Null Allele of *Mef2c*

To study the role of *Mef2c* in individual cell types that contribute to the cardiovascular system, or to various tissues that arise later in development, I have generated and utilized a loxP conditional allele of *Mef2c* (Figure II.1). The ability of the conditional allele to support normal development in place of wild type alleles of *Mef2c* was verified by crosses to produce mice homozygous for either the $Mef2c^{neo\text{-}loxP}$ or $Mef2c^{locP}$ alleles, as well as crosses to the existing $Mef2c^{KO}$ allele (Lin et al., 1997). The resulting animals were viable and fertile adults, demonstrating that the conditional alleles produced sufficient wild type *Mef2c* to support normal development.

To verify that Cre recombinase could efficiently delete the conditional allele of *Mef2c*, I used a tamoxifen inducible Cre recombinase expressed ubiquitously by the β-actin promoter, called $Cre\text{-}ER^{TM}$ (Hayashi and McMahon 2002). To test if conditional deletion of *Mef2c* during embryonic development was capable of reproducing the phenotypes observed in mice homozygous for the null allele of *Mef2c* (Lin et al., 1997, Lin et al., 1998), I conditionally deleted *Mef2c* in all embryonic tissues and collected embryos at embryonic day 9.5; when the *Mef2c* null phenotype is apparent. $Mef2c^{neo\text{-}loxP/KO}$;$Cre\text{-}ER^{TM}$ mice were generated and were viable, fertile adults in the absence of tamoxifen treatment. Male $Mef2c^{neo\text{-}loxP/KO}$;$Cre\text{-}ER^{TM}$ mice were mated to $Mef2c^{neo\text{-}loxP/KO}$ female mice, and pregnant females were administered 4-hydroxy-tamoxifen at E6.5.

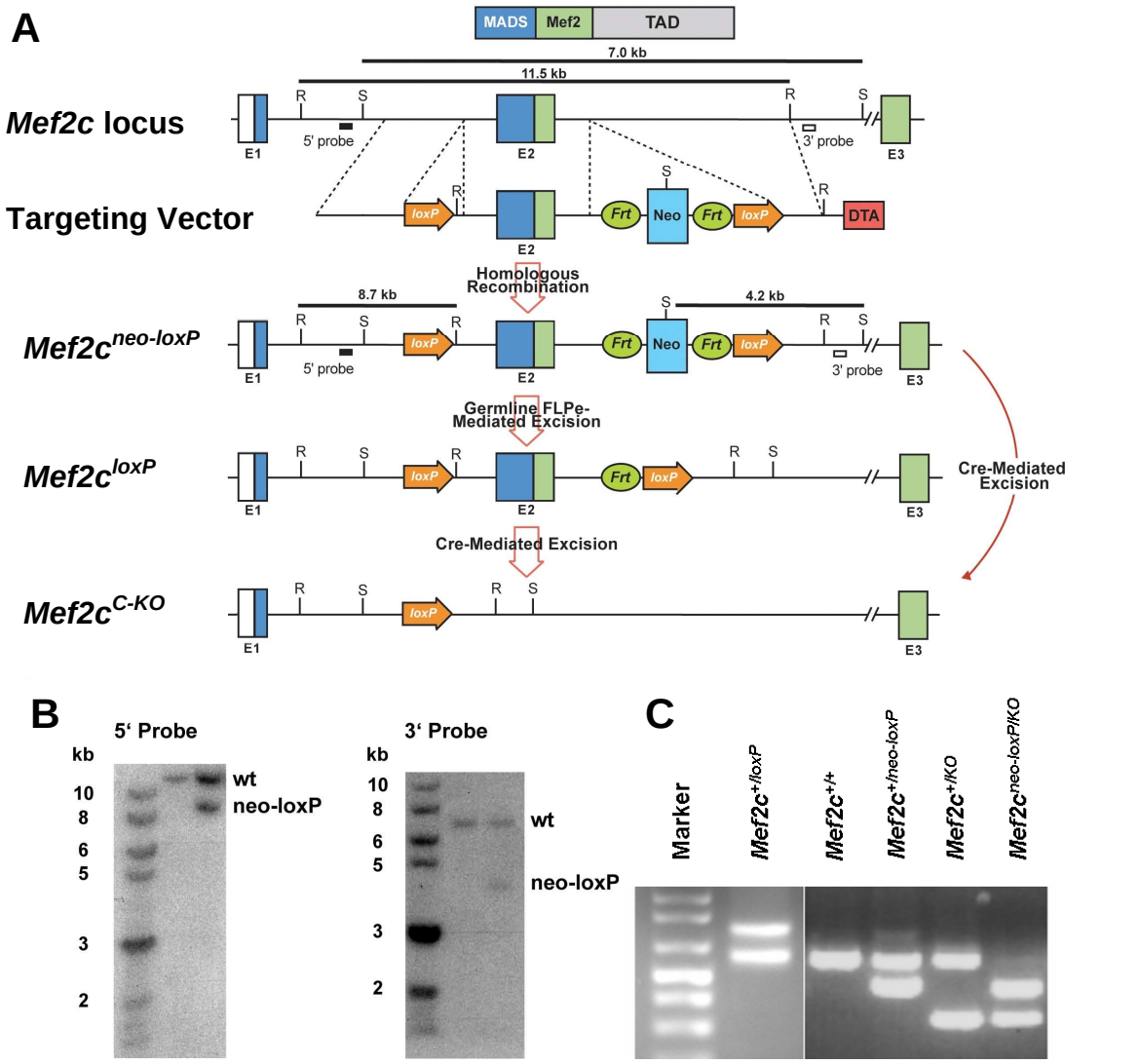

Figure II.1 Design and Genomic Targeting of a Conditional Allele of *Mef2c*.
A. A conditional allele of *Mef2c* was designed to introduce loxP sites on either side of the genomic region previously deleted in the $Mef2c^{KO}$ allele. Mice positive for the $Mef2c^{neo\text{-}loxP}$ allele were bred to mice expressing FLPe recombinase, resulting in mice positive for the $Mef2c^{loxP}$ allele. Either the $Mef2c^{neo\text{-}loxP}$ or $Mef2c^{loxP}$ alleles can be modified by tissue expression of Cre recombinase to excise the targeted genomic region to produce the $Mef2c^{C\text{-}KO}$ allele. The relative position of EcoRI sites (R) and SacI sites (S) are shown. B. Targeting of the *Mef2c* locus to generate the $Mef2c^{neo\text{-}loxP}$ allele was confirmed by Southern blots probed for the genomic region marked 5' probe when genomic DNA samples were digested with EcoRI, or probed for the genomic region marked 3' probe when genomic DNA samples were digested with SacI. C. Multiplex PCR genotyping of mice of the indicated genotypes using the 3'neo genotyping, KO region MEF2C genotyping, and 3'arm MEF2C genotyping primers listed in Table II.1. PCR products are compared to the 1kb plus DNA ladder (Invitrogen). Bands corresponding to each allele are of the following sizes: $Mef2c^{loxP}$ 773bp, $Mef2c^{+}$ 586 bp, $Mef2c^{loxP\text{-}neo}$ 412 bp, and $Mef2c^{KO}$ 253 bp.

Oligonucleotide Name	Sequence
5' Targeting Arm fwd	GGATCCAATGGCTTCTTTGGGTGTGTCTGAAGAGAG
5' Targeting Arm rev	GAGTTTGATTTGTCTTTTAATTACTTGAAGACTAG
KO Region fwd	GATATCTAGTTTTATAATTGGGAGAACTG
KO Region rev	GATATCATTTTGAGGAAAAGCAGTATTTTTATAACTAG
3' Targeting Arm fwd	GTCGACATTGAAAACTGTTAATACACGTGAAGTCAG
3' Targeting Arm rev	AAGCTTTCTGTTAGACCTATTCTAAAAGAGAATTCTCCCAG
5' Targeting Arm seq 1 rev	TGAGGGGCGGAGAAGTGTGAA
5' Targeting Arm seq 1 fwd	CTTATGTTTGCACAGTGGGCA
5' Targeting Arm seq 2 fwd	TAAGAATACTTTAGGAAATAA
5' Targeting Arm seq 3 fwd	GGAAAGAAGGTTCTGTTAAGC
5' Targeting Arm seq 4 fwd	TTAATTCTGAAAACTAGATGT
5' Targeting Arm seq 5 fwd	AGAAGCTATATGCACTGACTT
5' Targeting Arm seq 6 fwd	TGAAAATAAAATGCTAGCTTA
5' Targeting Arm seq 7 fwd	ATTAAGTGGCAGTAAGAAGTT
5' Targeting Arm seq 8 fwd	GAATAGAAGAGACAATGATTC
3' Targeting Arm seq 1 fwd	TTCAGTTAAAAGTCACAGCAT
3' Targeting Arm seq 2 fwd	GGCTCTGATATGAACAGTGGG
3' Targeting Arm seq 3 fwd	TATCATATATACCACTTTTAA
5' Southern Probe fwd	GCTGTTCTCGGGAAAAGGGTCAGG
5' Southern Probe rev	GTAACGTGAATATGGAGAGCAGAG
3' Southern Probe fwd	CCTCTCTCCCTTAAGCCTCTACAAACAGTTTACTTGCAGGAAG
3' Southern Probe rev	GTGAGAGGCTCCGTTGGCCAGCTGCTAAG
3' neo genotyping	GTGGGCTCTATGGCTTCTGAGGCGGAAAG
KO region Mef2C genotyping	GTGATGACCCATATGGGATCTAGAAATCAAGGTCCAGGGTCAG
3' arm Mef2C genotyping	CTACTTGTCCCAAGAAAGGACAGGAAATGCAAAAATGAGGCAG

Table II.1 Oligonucleotide Sequences.
The sequences of all DNA oligonucleotides used in the construction and verification of the *Mef2c* targeting vector, and primers used for PCR genotyping.

The resulting embryos included mice homozygous for the $Mef2c^{KO}$ allele and $Mef2c^{neo\text{-}loxP}$;$Cre\text{-}ER^{TM}$ mice. Mice null for *Mef2c* and mice in which *Mef2c* is conditionally deleted display similar phenotypes; cardiac looping has failed in these mice, and vascular development is abnormal (Figure II.2). However, mice homozygous for the $Mef2c^{neo\text{-}loxP}$ allele and positive for $Cre\text{-}ER^{TM}$ display a milder phenotype in which cardiac looping occurs, but development of the dorsal aortae is abnormal (Figure II.1 panels A4 and B4), suggesting that $Cre\text{-}ER^{TM}$ is not efficient enough to rapidly excise two alleles of $Mef2c^{neo\text{-}loxP}$. Overall, these data demonstrate that the conditional allele of *Mef2c* can fulfill its role

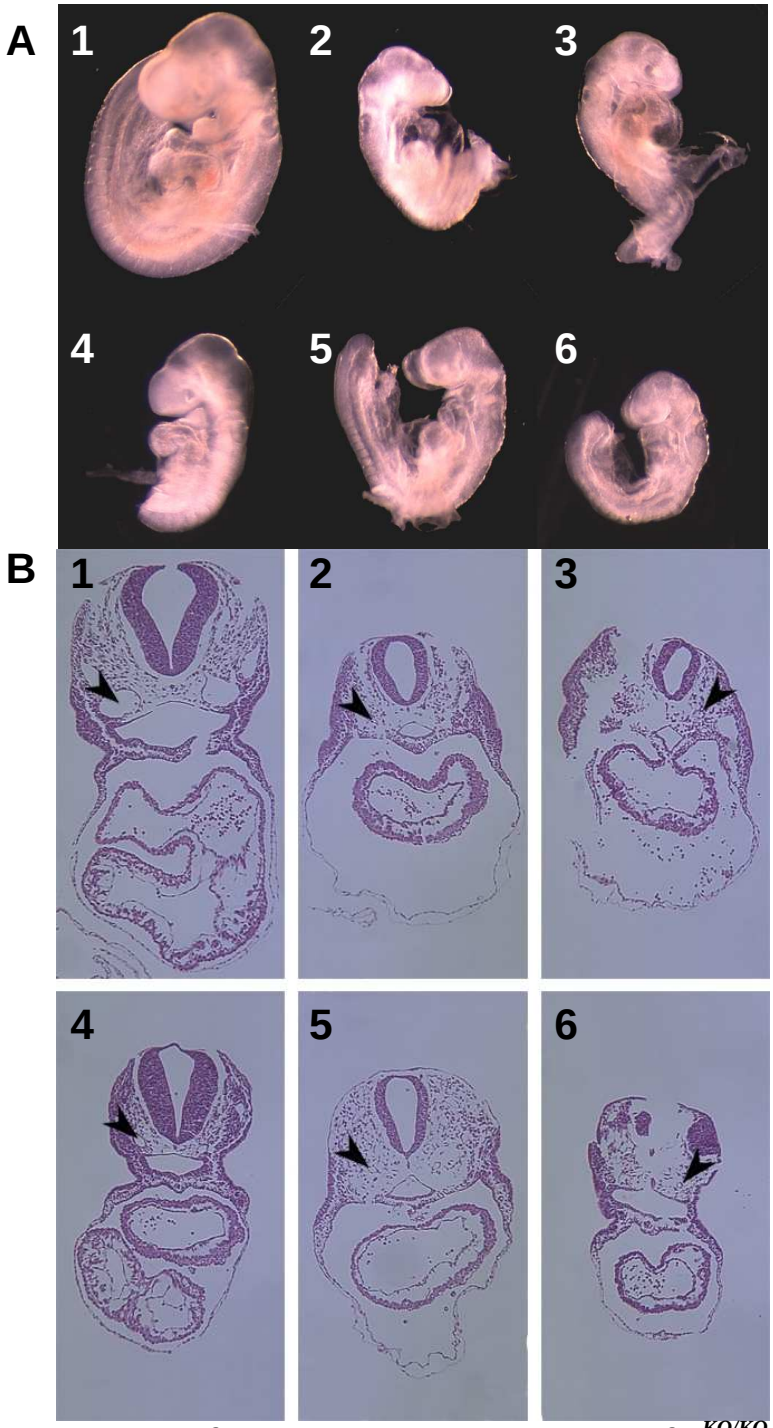

Figure II.2 Conditional *Mef2c* Deletion Recapitulates the *Mef2c*$^{KO/KO}$ Phenotype. Pregnant female mice were administered a single intraperitoneal injection of 4-hydroxy-tamoxifen at embryonic day 6.5. The resulting embryos were collected at embryonic day 9.5 and are shown in whole mount (A) or transverse section (B). The dorsal aortae are marked in panel B (arrowhead). The genotypes of the pictured embryos pictured in each panel are: 1) *Mef2c*$^{neo\text{-}loxP/neo\text{-}loxP}$. 2) *Mef2c*$^{KO/KO}$. 3) *Mef2c*$^{neo\text{-}loxP/KO}$*;Cre-ER*^{TM}. 4) *Mef2c*$^{neo\text{-}loxP/neo\text{-}loxP}$*;Cre-ER*^{TM}. 5) *Mef2c*$^{KO/KO}$*;Cre-ER*^{TM}. 6) *Mef2c*$^{neo\text{-}loxP/KO}$*;Cre-ER*^{TM}.

as a wild type allele in the absence of Cre recombinase activity, and can be efficiently recombined to produce a null allele when Cre recombinase is active.

Deletion of *Mef2c* From Neural Crest Derivatives Results in Membranous Bone Defects

Deletion of *Mef2c* from the neural crest was of particular interest given the known role of MEF2C in cardiovascular development (Lin et al., 1997, Lin et al.,1998), the expression of *Mef2c* in neural crest derivatives (Edmondson et al., 1994), and the

Figure II.3. Deletion of *Mef2c* from Neural Crest Derivatives Results in Early Postnatal Lethality.
Mice which lack *Mef2c* in neural crest derived tissues die shortly after birth. *Mef2c*$^{loxP/KO}$*;Wnt1-Cre* mice display abnormally shaped craniofacial structures, evident by their shortened jaws and sloped foreheads.

contribution of neural crest derivatives to cardiovascular outflow structures (Jiang et al., 2000). Mice homozygous for the *Mef2c*^{loxP} allele of *Mef2c* were crossed to mice heterozygous for *Mef2c*, and bearing a *Wnt1-Cre* transgene (Jiang et al., 2000). The resulting *Mef2c*$^{loxP/null}$*;Wnt1-Cre* mutant mice died on the first postnatal day (Figure II.3). The neural crest mutant mice were grossly abnormal, with an obviously truncated mandible and a long, sloped forehead. Sections taken from these animals demonstrate no architectural abnormalities in neural crest derived vascular structures (Figure II.4). Neural crest mutant mice differ from wild type mice only by a patent ductus arteriosus, reflecting an absence of sufficient postnatal ventilation.

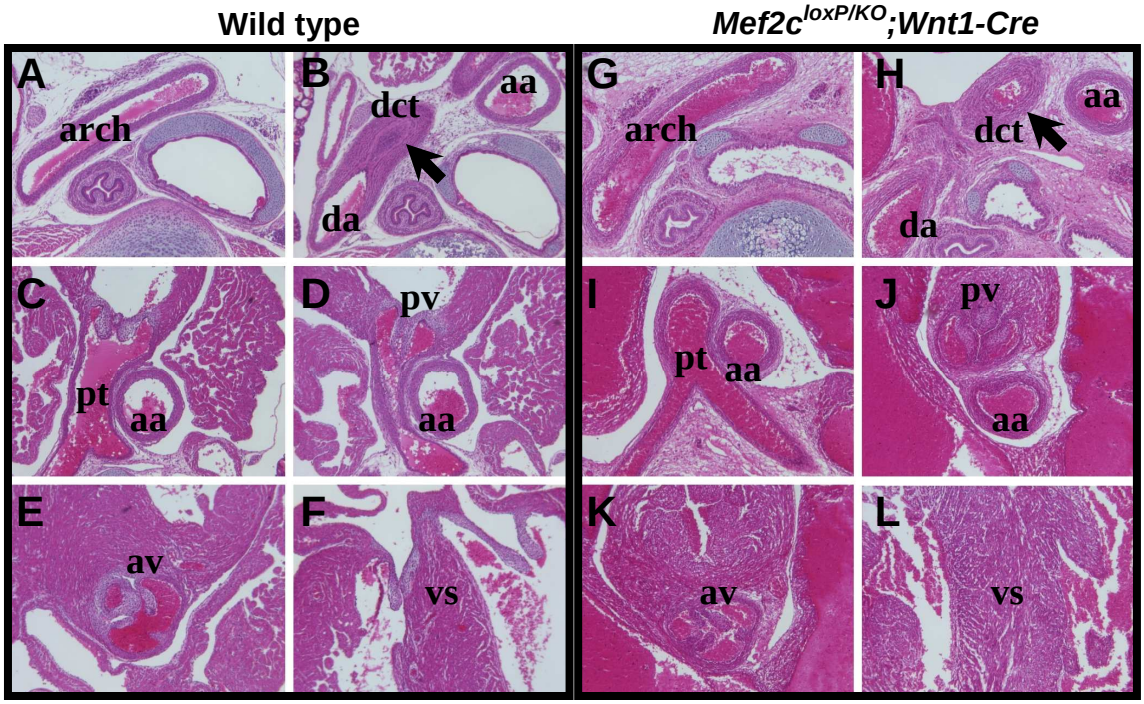

Figure II.4. Normal Vascular Structures Form When *Mef2c* is Deleted From Neural Crest Derivatives.
Transverse sections of thoracic vascular anatomy in wild type (A to F, rostral to caudal) and neural crest mutant mice (G to L, rostral to caudal). The ductus arteriosus remains patent in neural crest mutant mice (arrowhead). Labeled structures; Aortic arch (arch), descending aorta (da), ascending aorta (aa), ductus arteriosus (dct), pulmonary trunk (pt), pulmonic valve (pv), aortic valve (av), ventricular septum (vs).

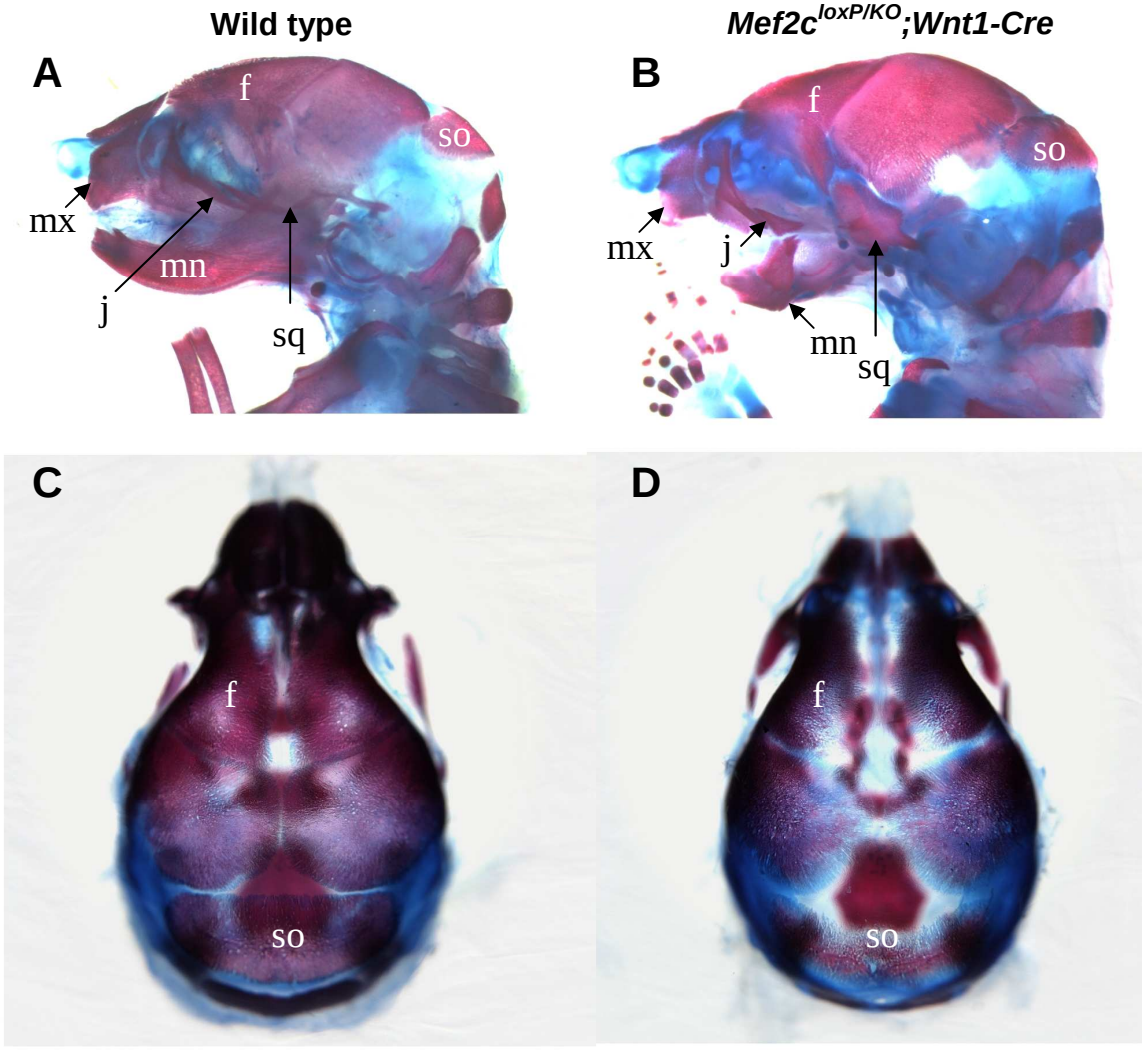

Figure II.5. Abnormal Bone Development of Membranous Bones In The Absence of *Mef2c*.
Lateral views (A and B) and dorsal views (C and D) of skulls of wild type and *Mef2c* neural crest mutant mice stained for bone (red) and cartilage (blue). Defects are seen in the shapes and connections of multiple bones, especially the mandible, and connections of the squamosal bone and neighboring jugal and frontal bones . Labeled bones: mandible (mn), maxilla (mx), frontal (f), supraoccipital (so), jugal (j), and squamosal (sq).

Dissection and staining of bone and cartilage in these mice illustrated the underlying defects in bone development responsible for the abnormal appearance of these mutants (Figure II.5). Several neural crest derived membranous bones are short and mis-shaped. The mandible is severely shortened, as are the maxilla and premaxilla, and the

squamosal bone fails to form appropriate junctions with neighboring bones. To further understand the defects present in these mutants, histological sections of bone from these animals were prepared and examined. Membranous bones of neonatal mice typically contain only a small number of quiescent osteoblasts located near the edge of the bone, however conditional neural crest deletion of *Mef2c* results in a drastic increase in both the number and activity of the osteoblasts found in membranous bones (Figure II.6).

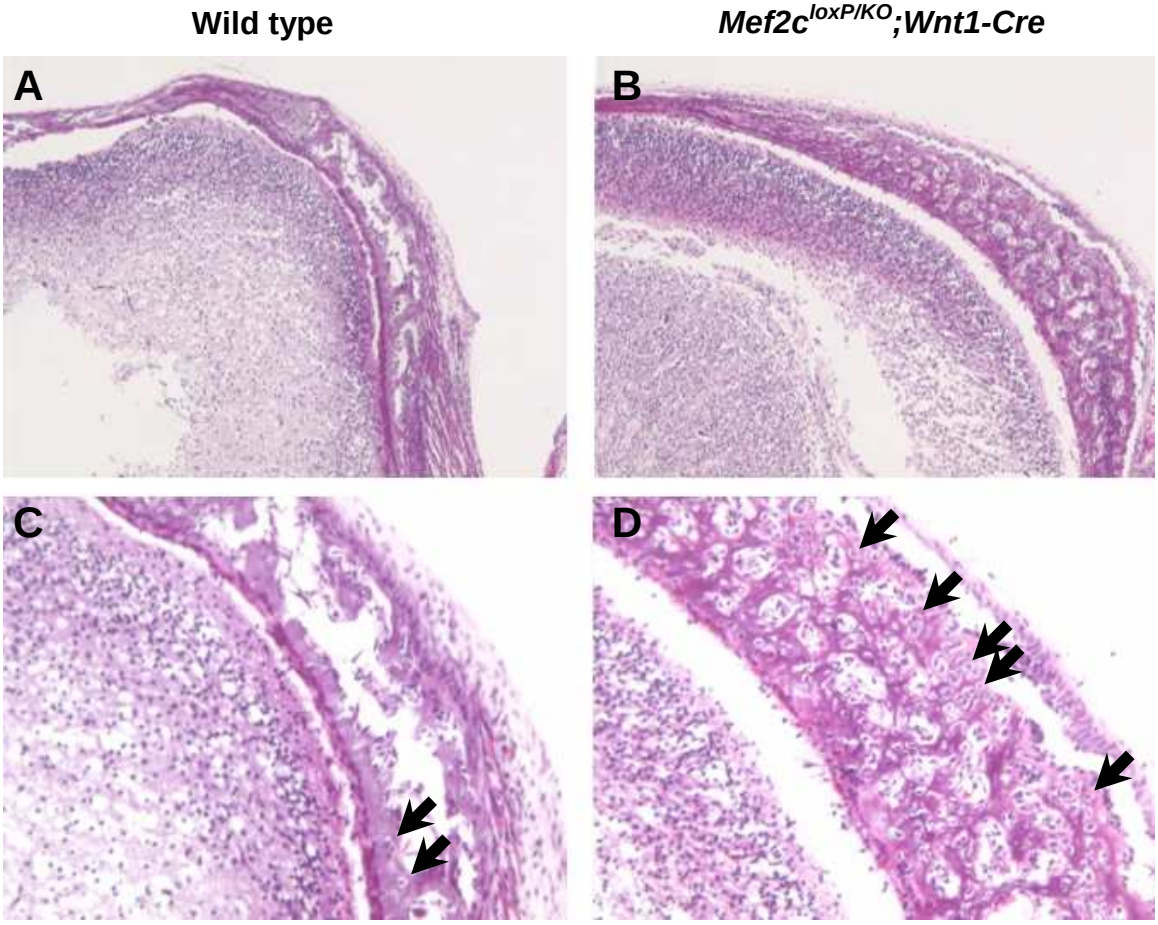

Figure II.6. Excessive Osteoblast Number and Activity in Membranous Bones Lacking *Mef2c*.
Sections of the frontal bones of wild type and *Mef2c* neural crest mutant mice. Osteoblasts in wild type bones are typically small and few in number (arrowhead), but are more numerous in mutant bones.

Mutant osteoblasts appear larger, reminiscent of reactive osteoblasts seen in fractures of mature bones, and are observed throughout the thickness of the bone. These cells are depositing a severely disorganized bone matrix at a significantly increased rate, as seen by the wide, lightly staining areas of unminearlized matrix around these cells (compare Figure II.6C and Figure II.6D). To determine if the osteoblasts in the mutant bones are present in increased numbers due to a lack of apoptosis or an increase in proliferation, sections of these bones were subjected to TUNEL staining and immunohistochemical staining for phosphorylated histone H3 (Figure II.7 and Figure II.8).

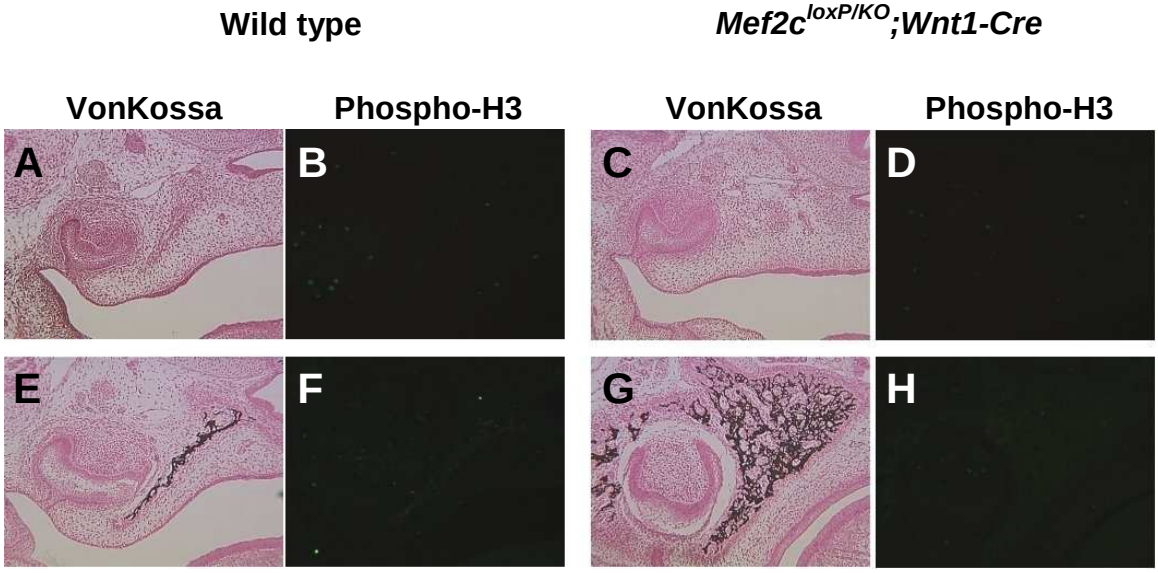

Figure II.7. Detection of Proliferating Cells in Membranous Bones.
Serial coronal sections of the maxilla of wild type and *Mef2c* neural crest mutant mice were stained for calcium deposits in mature bone (black) with VonKossa's method (panels A, C, E and G), or probed for phosphorylated histone H3 (green in panels B, D, F and H)) at embryonic day 14.5 (panels A to D)) or embryonic day 16.5 (panels E to H).

Immunohistochemical staining for phosphorylated histone H3, a marker of proliferating cells, detected only occasional proliferating cells in wild type membranous bones at E14.5 when the morphology of the developing bones is similar (compare Figure II.7A and Figure II.7C), and E16.5 when the mutant bones have significantly expanded

(compare Figure II.7E Figure II.7G). In spite of the significant increase in the number of osteoblasts in the mutant bones, immunohistochemical staining for phosphorylated histone H3 only detected the occasional proliferating osteoblasts. Tunnel staining to detect DNA fragmentation in apoptotic cells was also performed at E14.5, E16.5 and E18.5 (Figure II.8). Wild type bones contained only occasional TUNEL positive cells (Figure II.8E) while mutant bones contained noticeably more positive cells (Figure II.8F), likely related to the increase number of osteoblasts. These assays did not reveal an increase in the rate at which these cells are proliferating nor a decrease in the rate at which these cells are being removed by apoptosis, suggesting that the increase in the number of osteoblasts may be caused by an increase in osteoblast specification or proliferation at another site and migration to the sites of bone formation.

The reactive appearance of the mutant osteoblasts suggests that differentiation of these cells might be incomplete. Mature osteoblasts are marked by the expression of several genes, including *Osteocalcin, Bone Sialoprotein* and *Collagen α1(I)* (Reviewed in Harada and Rodan 2003). To determine if the mutant osteoblasts were of a less differentiated state, sections from mutant and wild type embryos collected at E14.5, E16.5 and E18.5 were probed by radioactive *in situ* hybridization for several markers of the osteoblast lineage (Figure II.9, Figure II.10 and Figure II.11). The expression of *Mef2c* is completely abolished in the developing membranous bones (compare arrow heads in Figures II.9, II.10 and II.11 panels B and J), but remains in the skeletal muscle of the tongue (lower right of Figures II.9, II.10 and II.11 panels B and J). The only detectable changes in osteoblast marker gene expression were decreases in the expression of *Collagen α1(I)* (Figure II.9 panels H and P) and *Bone Sialoprotein* (Figure II.9 panels

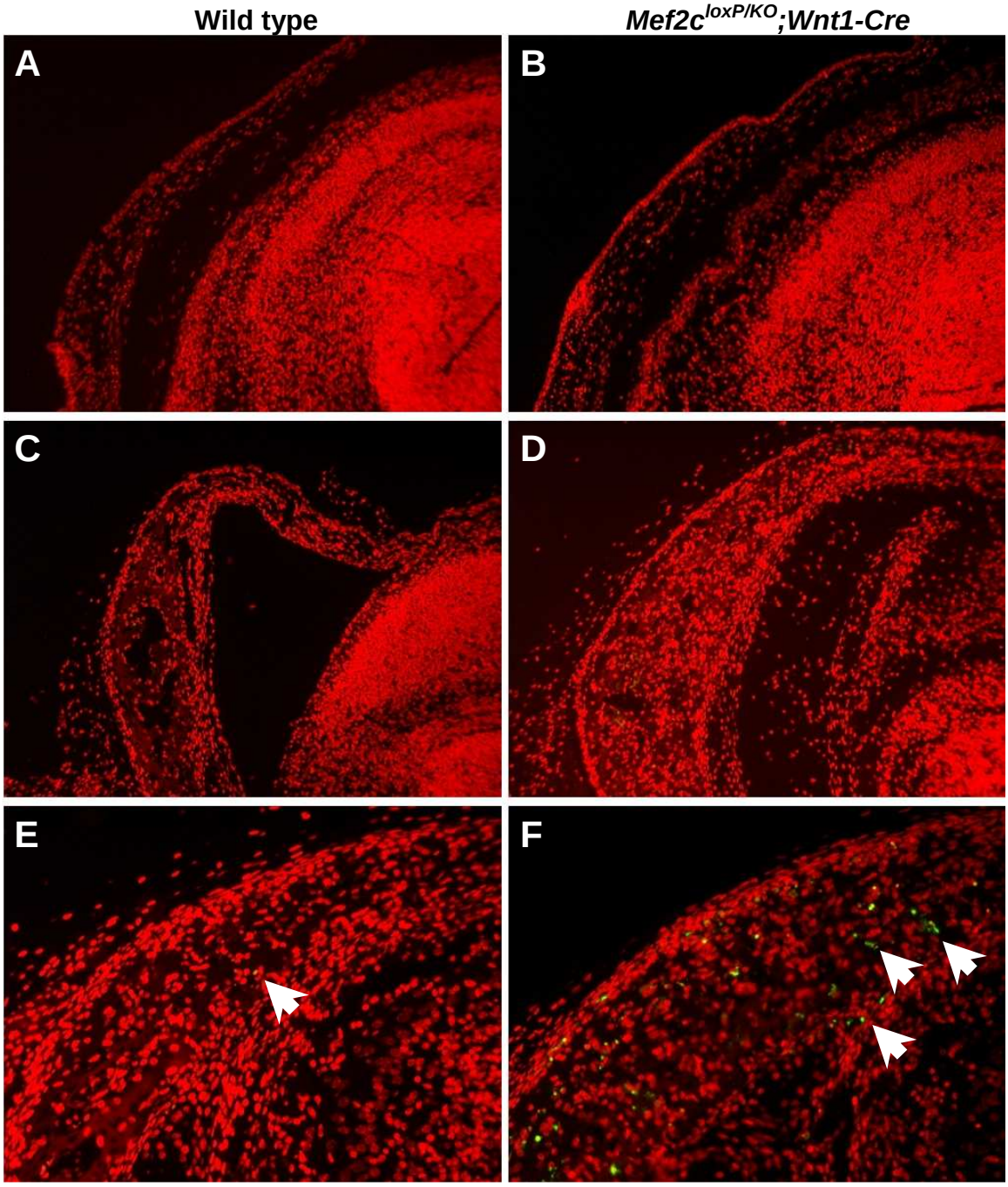

Figure II.8. Detection of Dying Cells in Membranous Bones.
Serial coronal sections of the frontal bone of wild type (panels A, C and E) and *Mef2c* neural crest mutant mice (panels B, D and F) were probed for free DNA ends by terminal deoxyneucleotide transferase labeling (green or yellow) and counterstained for nuclei using propidium iodide (red) at embryonic day 14.5 (panels A and B), embryonic day 16.5 (panels C and D) or embryonic day 18.5 (panels E and F). Occasional staining is seen in wild type samples (arrowhead), and is more frequent in *Mef2c* neural crest mutant mice at late stages of development.

F and N) in the early stages of bone development (Figure II.9). *Collagen α1(I)* expression is decreased, and *Bone Sialoprotein* was not expressed in the mutant maxilla at E14.5. However, at later stages these genes are more highly and broadly expressed in the mutant bones, due to the increased activity and number of these cells (Figure II.10 and Figure II.11). The osteoblasts in the mutant bones therefore appear to be fully differentiated, yet remain inappropriately active during late gestation.

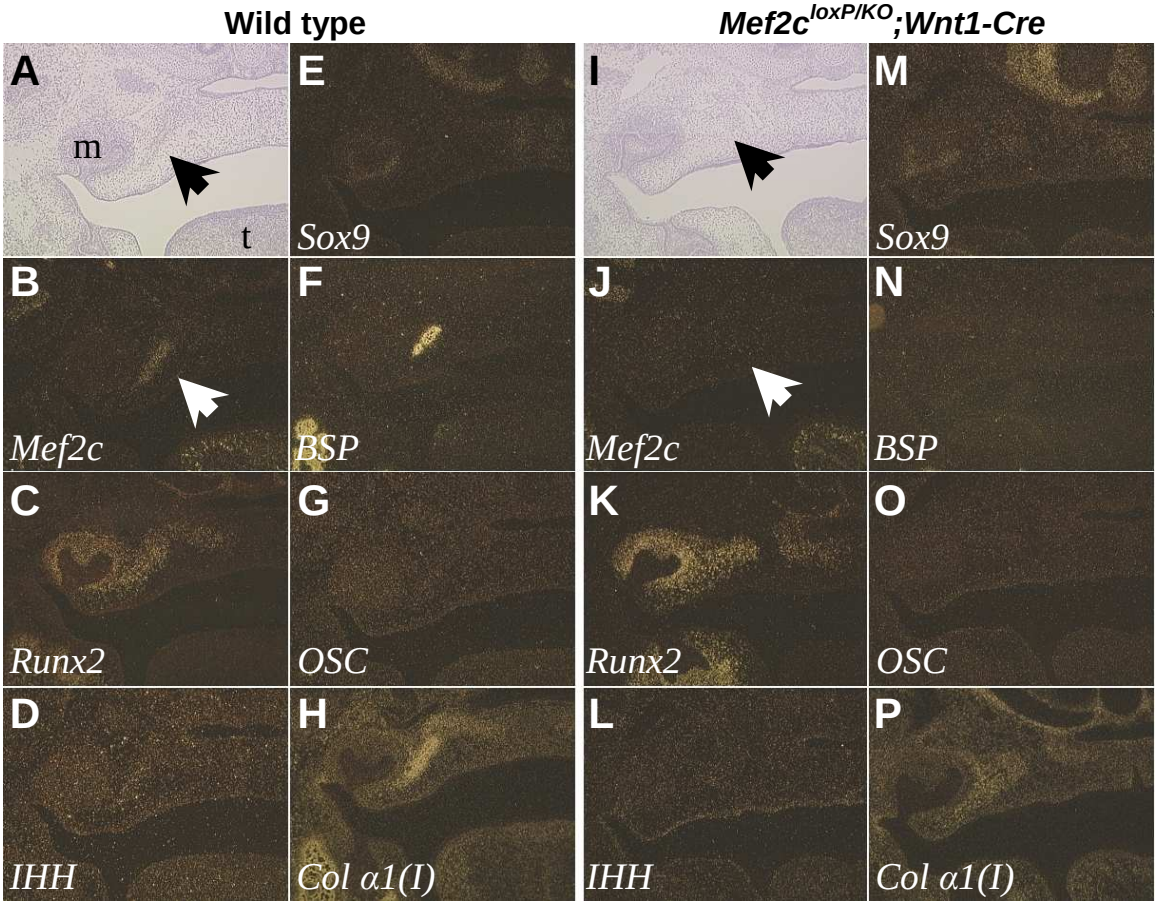

Figure II.9. Detection of Genes Marking Osteoblasts in Wild Type and *Mef2c* Neural Crest Mutant Maxillas at E14.5.

In situ hybridization was performed on serial coronal sections of wild type (panels A to H) and *Mef2c*$^{loxP/KO}$*;Wnt1-Cre* embryos (panels I to P) at the level of the maxillary molar. Sections were probed for the mRNA expression of *Mef2c* (panels B and J), *Runx2* (panels C and K), *Indian Hedgehog* (panels D and L), *Sox9* (panels E and M), *Bone Sialoprotein* (panels F and N), *Osteocalcin* (panels G and O), and *Collagen α1(I)* (panels H and P). Bright field micrographs (panels A and I) illustrate the relative positions of the maxillary molar (m), tongue (t) and developing membranous bone of the maxilla (arrowheads).

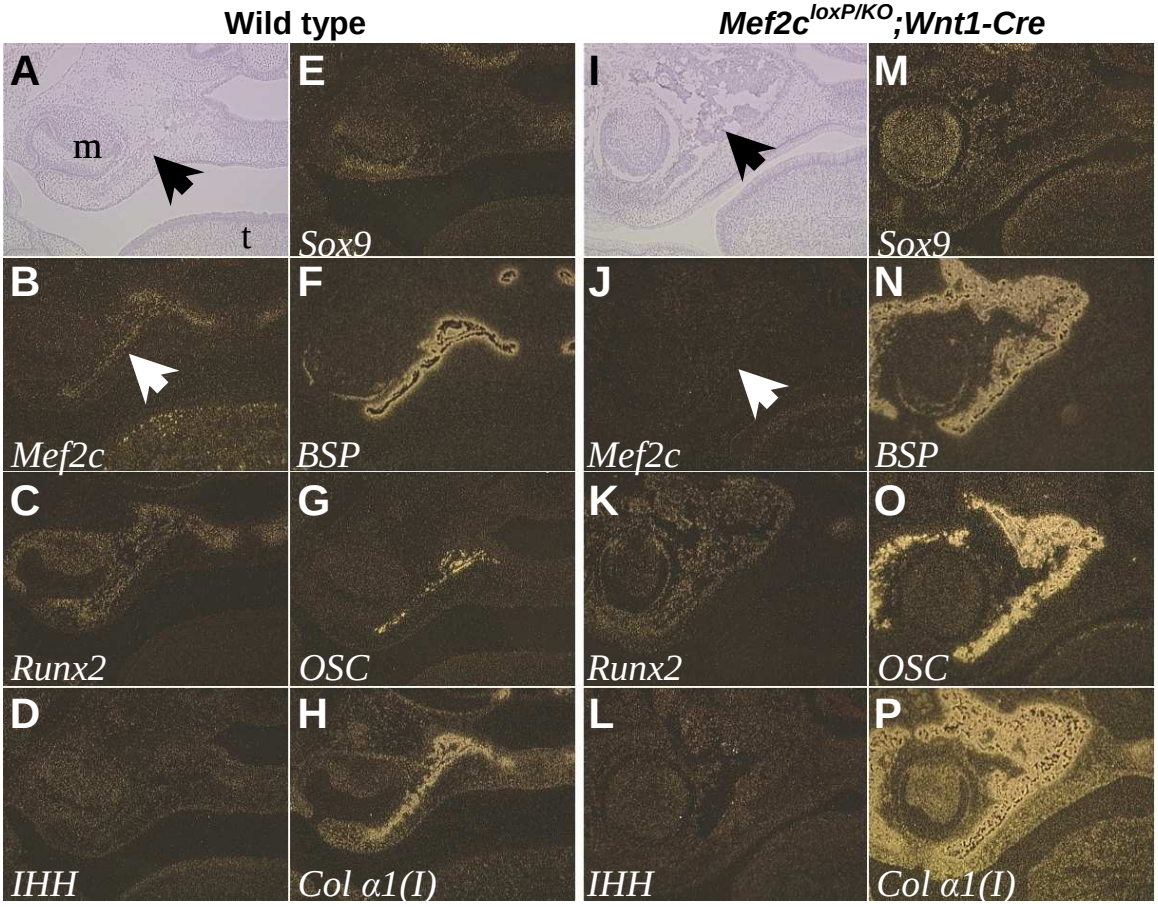

Figure II.10. Detection of Genes Marking Osteoblasts in Wild Type and *Mef2c* Neural Crest Mutant Maxillas at E16.5.

In situ hybridization was performed on serial coronal sections of wild type (panels A to H) and *Mef2c*$^{loxP/KO}$*;Wnt1-Cre* embryos (panels I to P) at the level of the maxillary molar. Sections were probed for the mRNA expression of *Mef2c* (panels B and J), *Runx2* (panels C and K), *Indian Hedgehog* (panels D and L), *Sox9* (panels E and M), *Bone Sialoprotein* (panels F and N), *Osteocalcin* (panels G and O), and *Collagen α1(I)* (panels H and P). Bright field micrographs (panels A and I) illustrate the relative positions of the maxillary molar (m), tongue (t) and developing membranous bone of the maxilla (arrowheads).

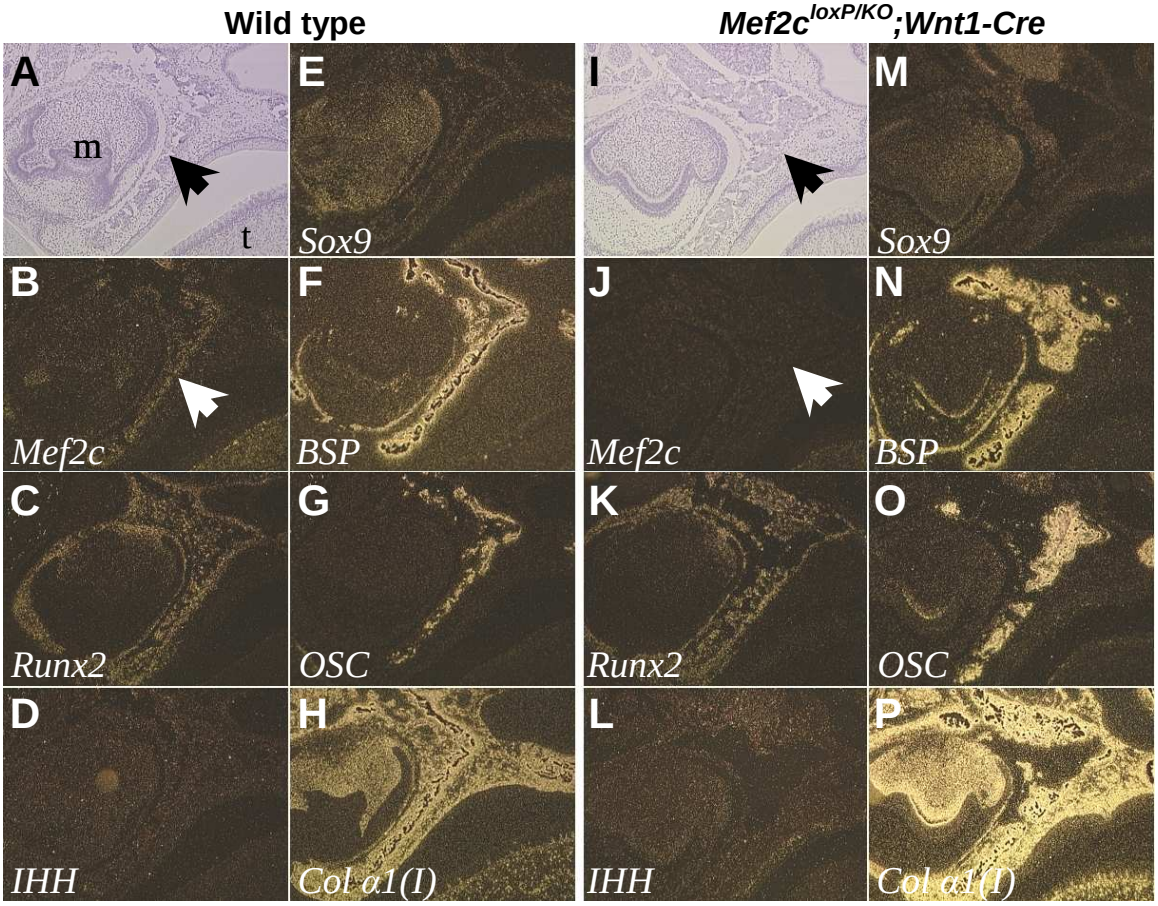

Figure II.11. Detection of Genes Marking Osteoblasts in Wild Type and *Mef2c* Neural Crest Mutant Maxillas at E18.5.
In situ hybridization was performed on serial coronal sections of wild type (panels A to H) and *Mef2c*$^{loxP/KO}$*;Wnt1-Cre* embryos (panels I to P) at the level of the maxillary molar. Sections were probed for the mRNA expression of *Mef2c* (panels B and J), *Runx2* (panels C and K), *Indian Hedgehog* (panels D and L), *Sox9* (panels E and M), *Bone Sialoprotein* (panels F and N), *Osteocalcin* (panels G and O), and *Collagen α1(I)* (panels H and P). Bright field micrographs (panels A and I) illustrate the relative positions of the maxillary molar (m), tongue (t) and developing membranous bone of the maxilla (arrowheads).

The initial delay in the expression of *Collagen α1(I)* and *Bone Sialoprotein* in mutant neural crest derived bones suggested that MEF2 proteins might directly regulate *Collagen α1(I)* expression. The promoters of these genes were examined for consensus MEF2 binding sites which are conserved among mice and humans. The genomic region promoter of the *Collagen α1(I)* gene (Kern et al., 2000) contains two potential MEF2

binding sites which conform to the T A (T/A) (T/A) (T/A) (T/A) T A consensus sequence, and the genomic region upstream of the *Bone Sialoprotein* promoter contains three potential MEF2 binding sites which conform to the T A (T/A) (T/A) (T/A) (T/A) T A consensus sequence. Despite the presence of conserved, consensus MEF2 binding sites these promoters are not activated by MEF2C in COS7 cells (Figure II.12), suggesting that the delay in the expression of these genes is indirectly regulated by *Mef2c*.

Endochondral Bone Defects Caused by *Mef2c* Deletion in Neural Crest Derivatives

Neural crest derived endochondral bones in the ventral cranial vault are severely malformed in neural crest mutant mice (Figure II.13). Endochondral bone defects in mice which lack MEF2C in the developing neural crest demonstrate that *Mef2c* is required for the appropriate development of endochondral cartilage. The ventral cranial vault is composed of a series of endochondral bones which grow in length and later fuse to form the base of the skull. In neural crest mutant mice, staining for bone and cartilage demonstrates that neural crest derived bones are greatly reduced in size, with an increase in the size of the cartilaginous sutures between these bones, while endochondral bones of mesodermal origin develop normally (Figure II.13). Similarly, the hyoid bone fails to ossify at P1. Histological sections of the base of the skull illustrated that the maturation of endochondral cartilage in these bones is delayed (Figure II.14), resulting in the observed decrease in bone size. This phenotype is a sharp contrast to the bone defect observed in mice null for HDAC4, in which chondrocyte maturation is accelerated, resulting in premature ossification and fusion of the cartilaginous sutures between these bones (Vega et al, 2004), suggesting that the repressive effects of HDAC4 in endochondral cartilage might be exerted, at least in part, on MEF2C.

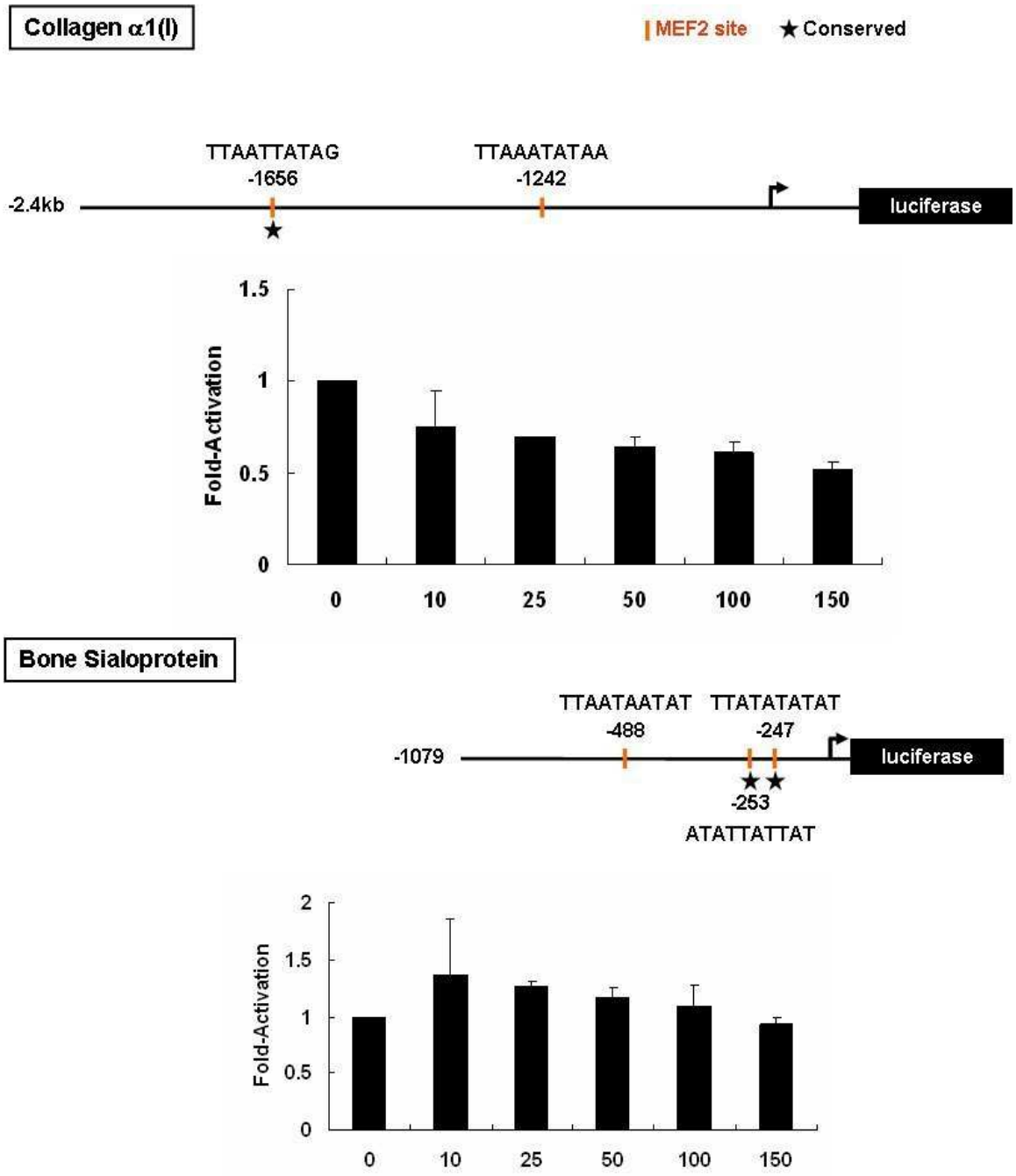

Figure II.12 Potential MEF2 Binding Sites in the Genomic Regions Upstream of the *Collagen α1(I)* and *Bone Sialoprotein* genes.

The genomic sequences upstream of the *Collagen α1(I)* and *Bone Sialoprotein* genes contain putative MEF2 binding sites (orange lines), including sequences where the MEF2 binding consensus sequence is conserved among mice and humans (star). Sequences of the potential MEF2 binding sites are displayed on the same side of the diagram as the number marking the position of the site relative to the start of transcription. These genomic regions are not activated by MEF2 in COS7 cells.

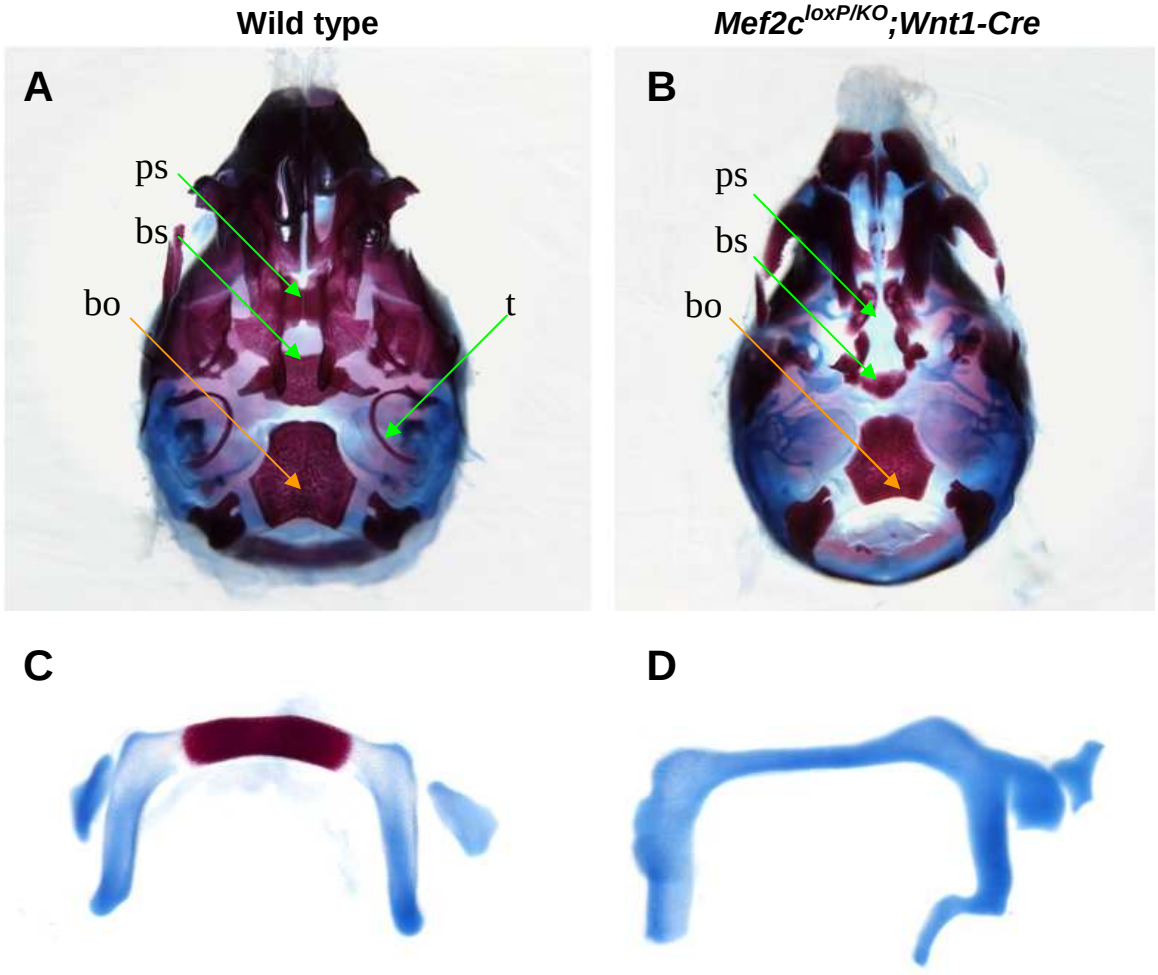

Figure II.13. Defects in Neural Crest Derived Endochondral Bones in *Mef2c* Neural Crest Mutant Mice.
Endochondral bones formed from neural crest derivatives fail to undergo normal ossification before birth. Neural crest derived bones in the base of the cranial vault (panels A and B, green arrows.) and the hyoid bone (panels C and D) are small and misshaped in *Mef2c*$^{loxP/KO}$*;Wnt1-Cre* mice, while the development of mesodermally derived bones is normal (panels A and B, orange arrows). The tympanic ring also fails to form in in *Mef2c*$^{loxP/KO}$*;Wnt1-Cre* mice. Labeled bones are the presphenoid (ps), basisphenoid (bs), basioccipital (bo), and tympanic ring (t).

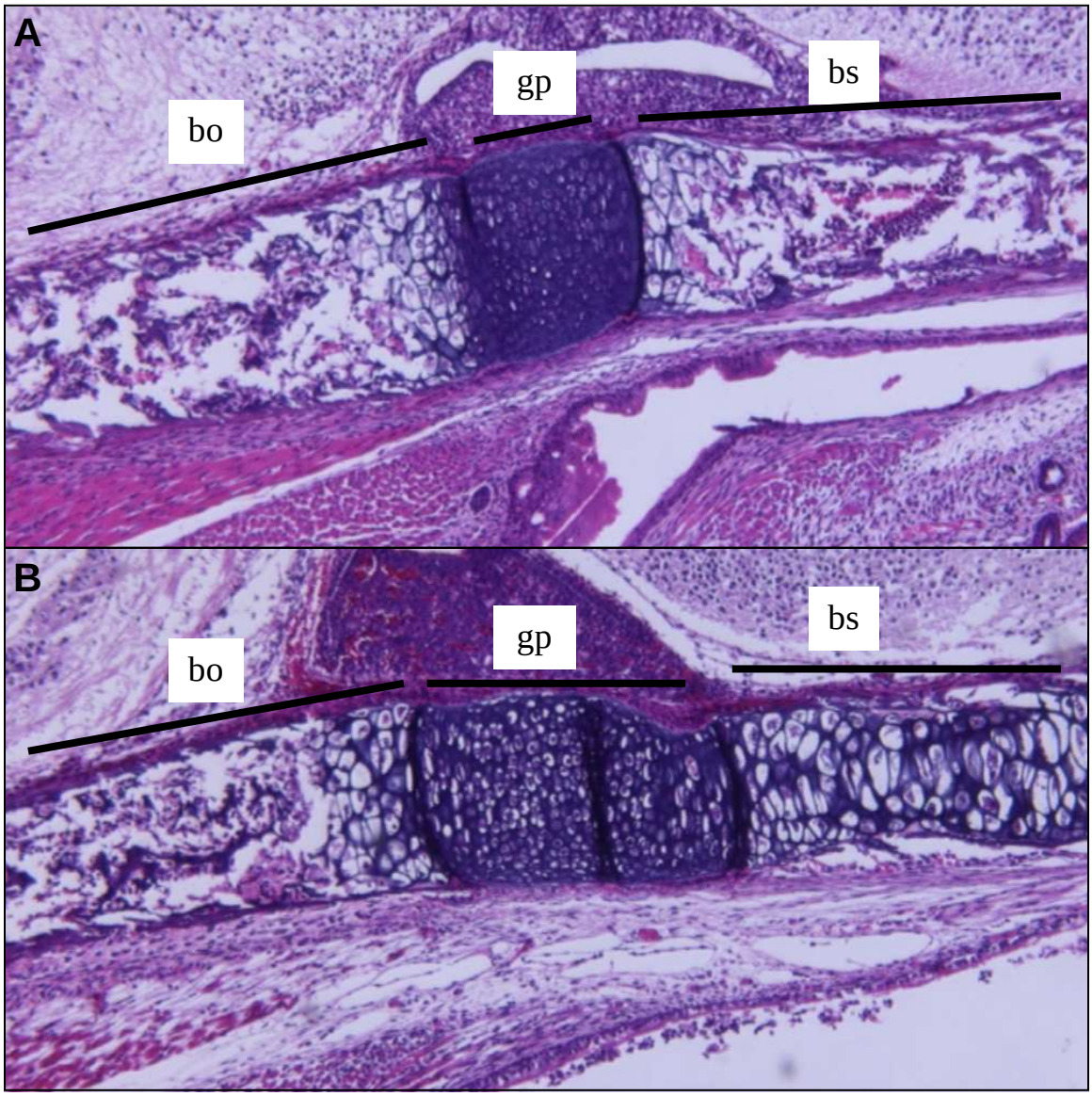

Figure II.14 Persistent Endochondral Cartilage in Neural Crest Derived Endochondral Bones in *Mef2c* Neural Crest Mutant Mice.
Histological sagital sections of wild type (panel A) and *Mef2c*$^{loxP/KO}$*;Wnt1-Cre* (panel B) skulls of postnatal day one mice. Sections at the level of the growth plate cartilage (labeled gp) between the mesodermally derived basioccipital bone (labeled bo) and the neural crest derived basisphenoid bone (labeled bs) demonstrate that growth plate maturation in the mesodermally derived basioccipital bone is normal, but growth plate maturation of the neural crest derived basisphenoid is impaited in *Mef2c*$^{loxP/KO}$*;Wnt1-Cre* mice.

Discussion

To determine the role of *Mef2c* in the development of the major cardiac vessels, a conditional allele of *Mef2c* was generated and deleted from developing neural crest derived tissues. The resulting mice showed no evidence of cardiovascular malformations (Figure II.4), but instead revealed an unanticipated role for MEF2C in the development of membranous and endochondral bones (Figure II.5).

Membranous bone development is dependent on the direct differentiation of mesenchymal precursors to active osteoblasts. In mice conditionally null for *Mef2c* in developing neural crest, active osteoblasts are present in membranous bones and capable of producing osteoid. However, these cells are present in unusually high numbers, and are excessively active, as evidenced by deposition of a thick and disorganized bone matrix. Histologically, the mutant osteoblasts resemble active osteoblasts seen in newly forming woven bone (Figure II.6), characteristic of healing fractures. This appearance suggests that these cells remain in an active state, perhaps due to a failure to completely differentiate into quiescent osteoblasts typical of mature bone. However, the precise cause for this defect remains illusive, as these cells express many of the marker genes characteristic of mature osteoblasts (Figures II.9, II.10 and II.11). Additionally, these cells do not appear to undergo excessive proliferation within the field of the forming bone (Figure II.7), nor do these cells appear resistant to apoptosis within the developing bone (Figure II.8). The increased osteoblast number could be explained if the neural crest derived osteoblasts were specified in abnormal numbers prior to migrating to the site of the forming bone, or were proliferating excessively before entering the developing bone. Perhaps *Mef2c* is required to support the differentiation of neural crest into a lineage

other than osteoblasts, and in its absence, excessive numbers of osteoblasts are specified at the expense of another neural crest derived cell type. However, this may not account for the increased activity of these cells, which suggests that MEF2C is required to regulate the activity of these osteoblasts. Regulation of osteoblast activity by MEF2C may be significant to the study of bone fracture healing and osteoporosis, and requires the further study of MEF2 proteins in osteoblast development and adult function.

Defective endochondral bone growth is also an unexpected consequence of conditional deletion of *Mef2c* from the developing neural crest. Endochondral bones are patterned by a cartilaginous template, in which the osteoblasts undergo proliferation, hypertrophy and apoptosis followed osteoblast invasion and deposition of the mature bone matrix. Conditional deletion of *Mef2c* from the neural crest causes the endochondral bones in the base of the skull to remain small and contain an abnormal amount of growth plate cartilage. This observation not only demonstrates that MEF2C is required for the maturation of chondrocytes (Figure II.14), but the sharp contrast of the growth plate morphology of these mutants when compared to the premature ossification observed in mice null for *HDAC4* (Vega et al., 2004), a known repressor of MEF2 proteins, suggested that MEF2C and HDAC4 might have opposing influences on chondrocyte development in a similar manner to their signal responsive regulation of cardiac myocyte hypertrophy. Previous experiments which I conducted to determine the efficiency of conditional deletion of *Mef2c* in the developing heart unexpectedly identified chondrogenic mesoderm as a site of *Mef2c* expression. Subsequent experiments to examine the expression of *Mef2c* in later stages of chondrocyte development demonstrated that *Mef2c* is expressed in chondrocytes just prior to the

initiation of chondrocyte hypertrophy in the growth plate of the humerus, a mesoderm derived bone. This coincides with the expression of *HDAC4*, confirming that HDAC4 and MEF2C would be present in the same cells and could directly interact to regulate chondrocyte hypertrophy. Further, MEF2C might play a role in endochondral ossification of mesoderm derived bones.

The regulation of chondrocyte hypertrophy by the interaction of MEF2C and HDAC4 would represent a novel mechanism of transcriptional regulation in chondrocytes. *HDAC4* null mice are not viable due to premature and ectopic chondrocyte hypertrophy, which resulted in excessive ossification of endochondral bone and cartilage. The mechanism of premature ossification was attributed to a direct interaction of HDAC4 and Runx2, a known activator of chondrocyte hypertrophy. The co-expression of *HDAC4* and *Mef2c* in prehypertrophic chondrocytes, and the observed delay in chondrocyte maturation observed when *Mef2c* is deleted in the neural crest, suggests that the interaction of MEF2C and HDAC4 in chondrocytes may be of equal or possibly greater significance in chondrocyte development as compared to the interaction of Runx2 and HDAC4. The role of MEF2C in endochondral ossification and its relation to HDAC4 and Runx2 are described in Chapter III of this thesis.

Methods

Creation of a conditional allele of MEF2C

Genomic regions of the *Mef2c* locus were isolated from 129SvEv genomic DNA by high-fidelity PCR (Roche Expand Long Template PCR System or Roche High Fidelity PCR System) and cloned into pGKF2L2DTA (a gift from Philip Soriano, Hoch and Soriano 2006). A 4.6kb genomic sequence (5' targeting arm) upstream of *Mef2c* exon 2, bounded by an upstream BamHI site and a downstream NcoI site, was cloned upstream of the 5' loxP sequence in pGKneoF2L2DTA. A 1.8kb genomic sequence (3' targeting arm) downstream of *Mef2c* exon 2, bounded by an upstream EcoRV site and a downstream HindIII site, was cloned downstream of the 3' loxP sequence. A 1.1kb region (conditional knockout region) corresponding approximately to the region deleted in the *Mef2c* knockout allele (Lin et al., 1997) was cloned between the 5' loxP sequence and the 5' FRT sequence. The resulting vector was verified by DNA sequencing and restriction mapping. The vector was linearized at the SacII site upstream of the 5' targeting arm and electroporated into 129SvEv derived ES cells (Figure II.1). Cells were then treated with G418, and negative selection was accomplished by the diphtheria toxin A cassette (DTA) in the pGKneoF2L2DTA vector. Resistant colonies were screened by Southern blotting using probe sequences isolated form 129SvEv DNA by high-fidelity PCR and cloned into pCRII-TOPO (Invitrogen). Southern blot analysis detected the presence of the EcoRI site adjacent to the 5' loxP site and the SacI site in the neomycin resistance cassette to verify recombination of the 5' and 3' arms, resulting in the $Mef2c^{neo\text{-}loxP}$ allele (Figure II.1B). Germline transmission from chimeric mice was verified by Southern blotting, and genotyping of subsequent mice was performed by PCR

(Figure II.1C). Sequences of DNA oligonucleotides used for PCR, DNA sequencing and genotyping, and Southern probe sequences and plasmids are listed in TABLE II.1.

Inducible Deletion of *Mef2c*.

To delete *Mef2c* in all tissues at a specific time during development, mice heterozygous for the $Mef2c^{KO}$ allele were mated to previously characterized Tamoxifen inducible Cre recombinase transgenic mice, called $Cre\text{-}ER^{TM}$ (Hayashi and McMahon 2002). Matings were continued to produce $Mef2c^{neo\text{-}loxP/KO};Cre\text{-}ER^{TM}$ male mice, which were mated to $Mef2c^{neo\text{-}loxP};Cre\text{-}ER^{TM}$ female mice. Pregnant females were treated with a single intraperitoneal dose of 4-hydroxy-tamoxifen. 4-hydroxy-tamoxifen was diluted in corn oil to 10mg/ml and administered at a dose of 9mg per 40g of body weight. All animal experimental procedures were reviewed and approved by the Institutional Animal Care and Use Committees at the University of Texas Southwestern Medical Center.

Neural Crest-specific Deletion of *Mef2c*.

To generate mice which lack *Mef2c* in neural crest derived tissues, mice heterozygous for the $Mef2c^{KO}$ allele were mated to previously characterized neural crest-specific Cre recombinase transgenic mice, called *Wnt1-Cre* (Jiang et al., 2000). The resulting mice were mated to mice heterozygous for the $Mef2c^{loxP}$ allele to produce neural crest conditional null mice ($Mef2c^{loxP/KO};Wnt1\text{-}Cre$). All animal experimental procedures were reviewed and approved by the Institutional Animal Care and Use Committees at the University of Texas Southwestern Medical Center.

Cartilage and Bone Staining

Euthanized mice were skinned, eviscerated, and fixed in 95% ethanol. Adult animals were additionally incubated overnight in acetone to clear fatty tissues. All specimens were stained using Alcian blue solution. Soft tissues were removed by incubation in 2% KOH as needed, and specimens were stained with Alizarin red solution for 30 to 90 minutes. Tissues were cleared in 1%KOH, 20% glycerol and photographed in 50% ethanol, 50% glycerol. Staining solutions were prepared as described previously (McLeod, 1980). Alcian blue solution is 4 volumes of 95% ethanol, 1 volume of acetic acid and 0.15mg of Alcian blue (Sigma) per ml of total volume. Alizarin red solution is 1% KOH and 0.05 mg of Alizarin red per ml of total volume.

Histology

Tissues were fixed in 10% phosphate-buffered formalin at 4°C. Samples were then embedded in paraffin, sectioned at 5 μm, and stained with hematoxylin and eosin or Von Kossa's method. Briefly, sections were deparaffinized and immersed in 5% Silver Nitrate solution for 30 minutes while exposed to a 100W light bulb. Slides were rinsed in distilled water and immersed in 5% Sodium Thiosulfate for three minutes. Slides were again rinsed in distilled water and counterstained with Nuclear Fast Red for 5 minutes. These protocols were executed by members of the laboratory of Dr. James Richardson.

TUNEL Staining

Tissues were fixed in 10% phosphate-buffered formalin at 4°C. Samples were then embedded in paraffin, sectioned at 5 μm, and stored at -20°C. Free DNA ends were

detected using the DeadEnd Flurometric TUNEL system (Promega) according to the manufacture's protocol.

Immunohostochemistry

Immunohistochemical detection of phosphorylated Histone H3 was performed as previously described (Shin et al., 2002). Briefly, sections were deparaffinized in xylene, rehydrated through graded ethanols to PBS, and permeabilized in 0.3% Triton X-100 in PBS. Nonspecific binding was blocked by 1.5% normal goat serum in PBS and anti-phospho-histone H3 rabbit antibody (Upstate Biotechnology) was applied at a 1:200 dilution in 0.1% BSA in PBS overnight at 4°C. Sections were washed in PBS and fluorescein-conjugated anti-rabbit antibody (Vector Laboratories) was applied at a 1:200 dilution in 1% normal goat serum for 1 hr.

***In situ* hybridization**

Tissue samples were fixed overnight in DEPC-treated 4% paraformaldehyde. Riboprobes were labeled with [α-^{35}S]-UTP using the MAXIscript in vitro transcription kit (Ambion, Austin, Texas). In situ hybridization of sectioned tissues was performed as previously described (Shelton et al., 2000). Briefly, sections were deparaffinized, permeabilized, and acetylated prior to hybridization at 55^{o}C with riboprobes diluted in a mixture containing 50% formamide, 0.3M NaCl, 20mM Tris-HCl, ph 8.0, 5mM EDTA, pH 8.0, 10mM $NaPO_4$, pH 8.0, 10% dextran sulfate, 1X Denhardt's, and 0.5mg/ml tRNA. Following hybridization, the sections were rinsed with increasing stringency washes, subjected to RNAse A (2µg/ml, 30min at 37^{o}C) and dehydrated prior to dipping in K.5 nuclear

emulsion gel (Ilford, UK). Autoradiographic exposure ranged from 14 to 28 days. Signals were pseudocolored as described in figure legends. Hybridizations and slide development were executed by John Shelton, and other members of the laboratory of Dr. James Richardson.

Cell Culture, Reporter Plasmids and Transfection

COS7 cells were grown in DMEM with 10% FBS. Fugene 6 (Roche) was used for transient transfection according to the manufacturer's instructions. A reporter plasmid containing 2.4 kb of the *collagen α1(I)* locus was obtained (Kern et al., 2000), and a genomic region upstream of the *Bone Sialoprotein* promoter was generated by PCR with the upstream primer 5'- GGT ACC GCC TAG TCC ATC ATC AAT GGG ATG AGA AG -3' and the downstream primer 5'- CTC GAG CTT GCC CAT TAC CTT AAC CTT CCT TTC GGC AG -3' and cloned into pGL3 basic (Promega). COS7 cells were transfected with pCDNA Myc-MEF2C. Plasmids were co-transfected with 10ng of a CMV-β-galactosidase reporter plasmid to control for transfection efficiency. Transfections were executed in collaboration with Yuri Kim.

Chapter III

Opposing Influences of MEF2C and HDAC4 Regulate Chondrocyte Hypertrophy

The results described in Chapter II identify a novel role for MEF2C in the development of both membranous and endochondral bones. A recent publication of the Olson lab demonstrated that HDAC4, a known repressor of MEF2 proteins, exerts a critical control on endochondral bone development by inhibiting chondrocyte maturation. The function of HDAC4 in chondrocytes was attributed to repression of the Runx2 transcription factor (Vega et al., 2004). Taken together, these results led me to intercross the existing null alleles of *Mef2c* and *HDAC4*, revealing that chondrocyte hypertrophy is controlled by a balance between the positive transcriptional effects of MEF2C against the repressive activity of HDAC4.

To further investigate the role of MEF2C in chondrocyte hypertrophy, I have utilized the conditional null allele of *Mef2c*. My data shows that MEF2C plays an essential role in the development of all endochondral bones. Deletion of MEF2C from the cartilaginous precursors of endochondral bones causes a delay in chondrocyte maturation, resulting in persistent endochondral cartilage, decreased bone growth and short stature. Further, transgenic over expression of a dominant negative or constitutively active MEF2C causes a block in chondrocyte hypertrophy or premature ossification, respectively.

To determine if MEF2C directly regulates gene expression in hypertrophic chondrocytes, a previously characterized promoter and enhancer of the *Collagen α1(X)* gene which is capable of activating reporter gene expression in hypertrophic chondrocytes was examined. MEF2C is capable of directly activating the promoter of *Collagen α1(X)* in vitro, and assays to determine if this regulation occurs *in vivo* are

ongoing. Therefore MEF2C serves as a critical regulator of chondrocyte hypertrophy by directly activating the hypertrophic gene program of chondrocytes.

Misregulation of signaling pathways that influence growth plate dynamics are responsible for dwarfisms and bone deformations resulting from either premature maturation of the growth plate cartilage, characteristic of achondroplasia (Chen el al., 1999, Li et al., 1999, Reviewed in Horton 2006 and Ornitz 2005), or delayed or absent chondrocyte maturation, characteristic of many chondrodysplasia syndromes (Reviewed in Schipani and Provot 2003, Cohen 2002). My results demonstrate that growth plate dynamics can be modified by the balance of MEF2C and its repressor, HDAC4. The activation of MEF2C dependent transcription by a variety of signaling pathways, and the ability of MEF2C to directly activate chondrocyte gene expression demonstrates that MEF2C and HDAC4 control a key nodal point in chondrocyte hypertrophy and growth plate dynamics. Further investigation may identify molecules which can influence the interaction of MEF2C and HDAC4 in chondrocytes and make control of growth plate dynamics possible.

Results

Bone Development Depends on the Balance of HDAC4 and MEF2C

The results described in chapter II demonstrate that MEF2C has an essential role in the development of endochondral bones which arise from neural crest precursors. Neural crest deletion of *Mef2c* resulted in an endochondral bone defect, which contrasts sharply with that of *HDAC4* null mice (Vega el al., 2004). To determine if *Mef2c* has a general role in endochondral bone development, I tested for a genetic interaction between *Mef2c* and *HDAC4*. Mice heterozygous for both *HDAC4* and *Mef2c* were crossed with mice heterozygous for *HDAC4*. The resulting mice were analyzed by staining for bone and cartilage at postnatal day 1, when *HDAC4* null mice display a mild phenotype and postnatal day eight when the bone defects of *HDAC4* null mice are very pronounced. Surprisingly, mice heterozygous for *Mef2c* display a moderate defect in endochondral ossification of the sternum at postnatal day one, which remains observable at postnatal day eight (Figure III.1). Ossification in the sternum of *Mef2c* heterozygous mice is most pronounced in the first sternebra which fails to ossify by postnatal day one and is partially ossified at postnatal day eight. Similarly, ossification of the xiphoid process is significantly decreased. The defect in *Mef2c* heterozygous mice could be reversed in a dose dependent manner by removal of wild type alleles of *HDAC4.* Deletion of a single allele of *HDAC4* from *Mef2c* heterozygous mice restored some ossification to the first sternebra and increased ossification in the xiphoid process, while removal of both wild type alleles of *HDAC4* resulted in a nearly normal pattern of ossification. Conversely, deletion of a single allele of *Mef2c* from *HDAC4* null mice restored the pattern of

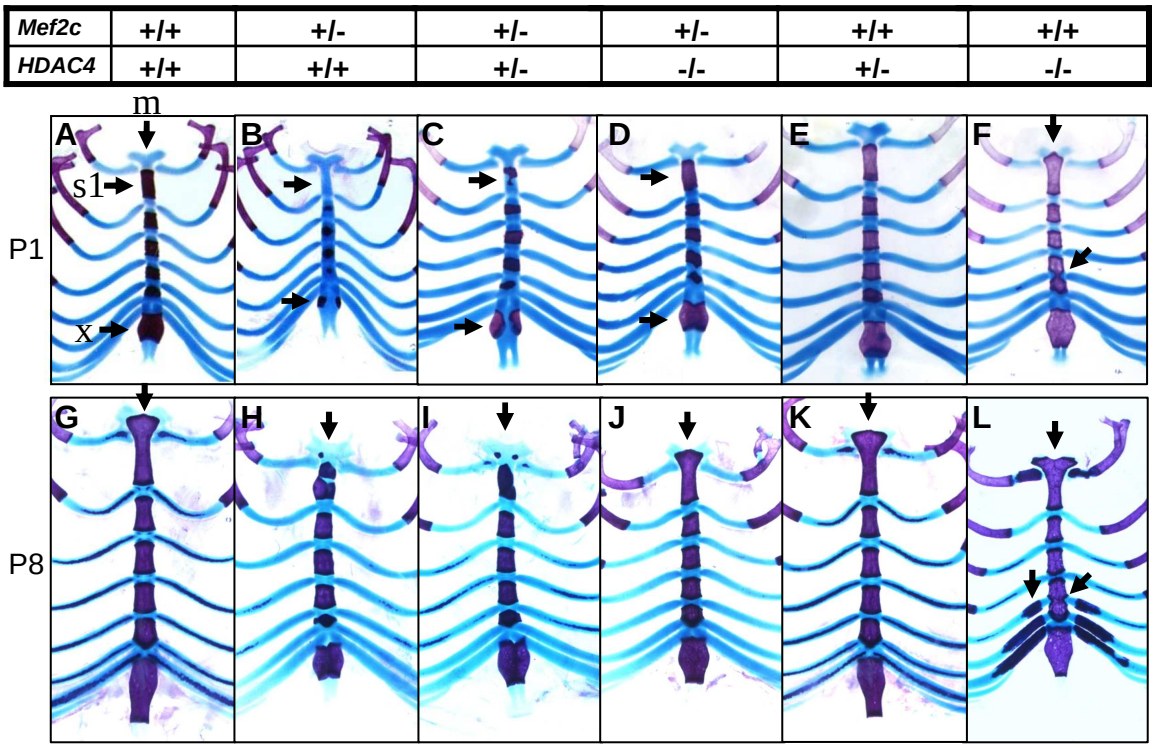

Figure III.1 Genetic Interactions of *Mef2c* and *HDAC4*.
Ribs and sternums of mice of the indicated genotypes were stained for bone (Alizarin red) and cartilage (Alcian blue) at postnatal day one (panels A to F) or postnatal day eight (panels G to K). *Mef2c* heterozygous mice display defects in endochondral ossification at postnatal day one (panel B) and postnatal day eight (panel H). These defects can be rescued in a dose dependent manner by removal of alleles of *HDAC4* (panels C and D or panels I and J). Conversely, premature and ectopic ossifications that occur in *HDAC4* null mice can be rescued by removal of a single allele of *Mef2c* (compare panels F and D or panels L and J). Structures in panel A are labeled; xiphoid process (x), manubrium (m), and first sternebra (s1).

ossification to approximately normal morphology. At postnatal day one, premature ossification of the manubrium and premature fusion of the sternebrae which occurs in *HDAC4* null mice is rescued by removal of a single allele of *Mef2c* (compare Figure III.1 panels F and D). Similarly, at postnatal day eight, *HDAC4* null mice which are heterozygous for *Mef2c* do not develop ectopic ossification of the chondrocostal cartilage, nor premature fusions of growth plates in the sternum or the manubrium (compare Figure III.1 panels L and J). Similar patterns of ossification are seen in other endochondral

bones, such as the base of the skull and hyoid bone, demonstrating that MEF2C is a critical target for HDAC4 repression in endochondral cartilage.

The ability of *Mef2c* and *HDAC4* to interact genetically in regulating endochondral ossification suggests that MEF2C is a major target of HDAC4 repression in chondrocytes. Since Runx2 was reported to interact with HDAC4 and mediate its repressive effects on chondrocyte development, I began to address the extent to which *Runx2* and *Mef2c* act in parallel, by intercrossing the existing alleles of *Runx2* and *Mef2c*. *Runx2* heterozygous mice display a significant defect in the ossification of neural crest derived membranous bones of the skull, and an absence of clavicles (Komori et al., 1997). In endochondral bones, *Runx2* heterozygous mice display subtle defects in ossification, limited to bones of neural crest origin (Figure III.2). Ossification of the hyoid bone is decreased (Figure III.2 panel F), and growth of the basisphenoid bone along the rostral-caudal axis is slightly decreased (Figure III.2 panel J). Ossification of neural crest derived endochondral bones appears normal in mice heterozygous for *Mef2c* (Figure III.2 panels G and K), but ossification in the mesoderm derived sternebrae is greatly decreased (Figure III.2 panel C). Mice heterozygous for both *Mef2c* and *Runx2* display significantly exacerbated defects in endochondral ossification, but defects in the shape and size of membranous bones are similar to those seen in *Runx2* heterozygous mice. In $Mef2c^{+/-};Runx2^{+/-}$ mice at postnatal day one, endochondral ossification of the sternum of is nearly abolished (Figure III.2 panel D), ossification of the hyoid and presphenoid bones has failed (Figure III.2 panels H and L), and lengthwise growth of the basisphenoid bone along the rostral-caudal axis is decreased (Figure II.2 panel L). This suggests that *Mef2c* and *Runx2* may function redundantly, cooperatively or in parallel in endochondral

Runx2	**+/+**	**+/-**	**+/+**	**+/-**
Mef2c	**+/+**	**+/+**	**+/-**	**+/-**

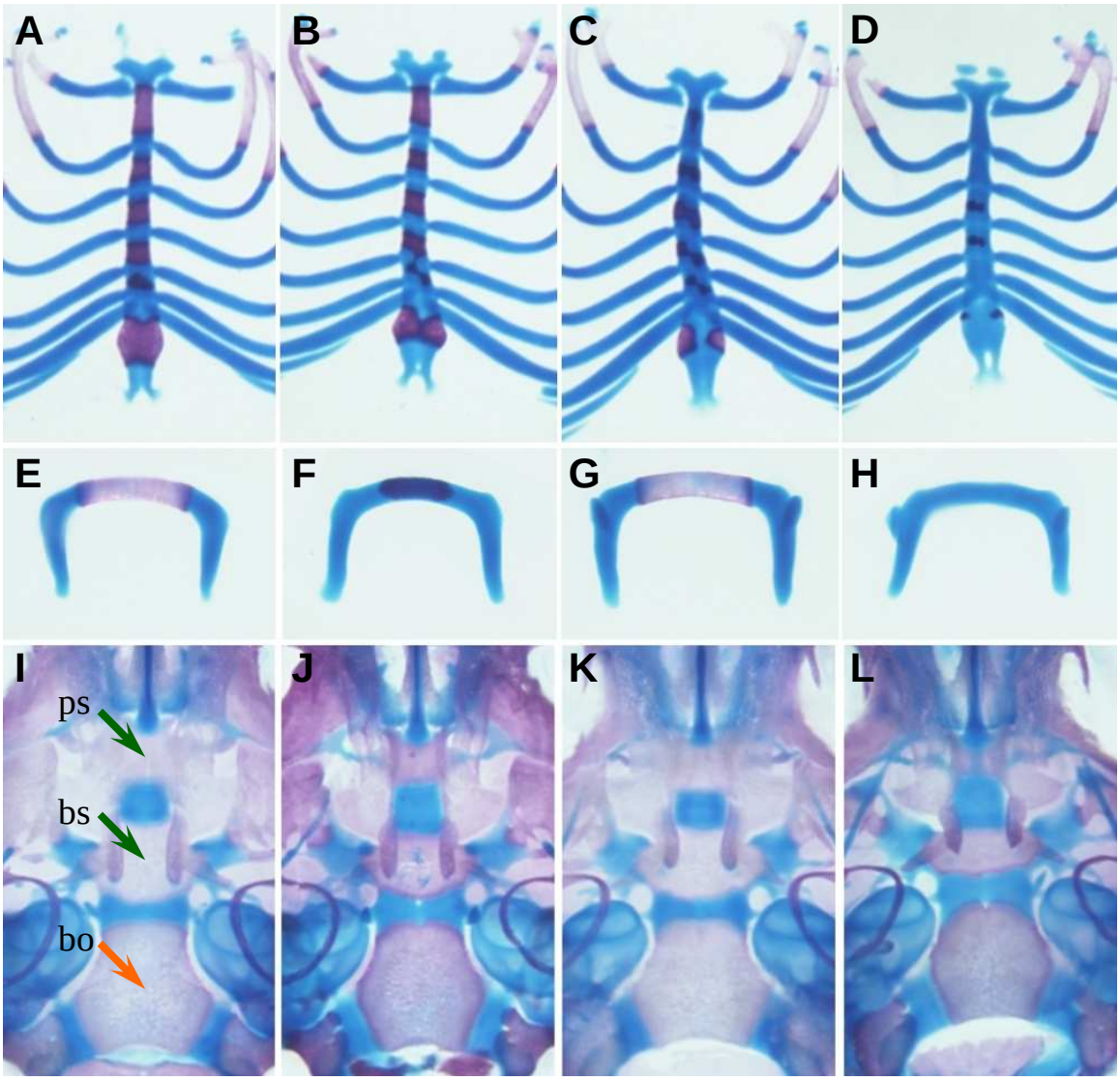

Figure III.2. Genetic Interactions of *Mef2c* and *Runx2*.
Skeletons of neonatal mice of the indicated genotypes were stained for bone (Alizarin red) and cartilage (Alcian blue), and dissected to illustrate the sternum (panels A to D), hyoid bones (panels E to H) and the base of the cranial vault (panels I to L). Bones labeled in panel I are: presphenoid (ps), basisphenoid (bs) and basioccipital (bo). Bones of neural crest origin are marked with green arrows, and mesodermally derived bones are marked with orange arrows.

ossification. The exact mechanism by which MEF2C and Runx2 genetically interact is complicated by the critical contribution of Runx2 to osteoblast development. However,

the significant rescue of endochondral ossification defects in *HDAC4* null mice by *Mef2c* demonstrates that MEF2C is a critical target of HDAC4 repression in chondrocytes since HDAC4 is excluded from osteoblasts.

MEF2C is an Essential Regulator of Endochondral Bone Development

To determine if *Mef2c* is required for the development of mesoderm derived endochondral bones, I have conditionally deleted *Mef2c* using a *twist2-Cre* knock-in (Yu et al, 2003), which is expressed in mesenchymal precursors of endochondral bone, including chondrocytes within growth plate cartilage and in osteoblasts in the perichondrium, periosteum, and endosteum. The resulting mutant mice were readily identifiable at birth by their shortened limbs (Figure III.2). A fraction of these conditional *Mef2c* mutants also displayed difficulty breathing, evidenced by gasping and accumulation of air in their intestines. These mice did not survive beyond the first week of postnatal life, presumably due to deletion of *Mef2c* in skeletal muscle precursors, which also results in perinatal lethality (Appendix). Analysis of the skeletons of postnatal day (P) one $Mef2c^{loxP/KO}$*;twist2-Cre* mice revealed severe defects in nearly all endochondral bones. The ventral vertebral bodies of the spine failed to ossify, as did the supraoccipital bone which surrounds the dorsal edge of foramen magnum (Figure III.3). This phenotype was especially pronounced in the sternum, which was completely devoid of trabeculated bone at P1 (Figure III.4). The truncated limbs of these mutants were also seen to contain significant defects (Figure III.5). Bone stains of the forelimbs of the mutant mice demonstrate the absence of ossification in many phalangeal bones of the fingers, and severe growth plate defects in remaining bones. The radius, ulna, humerus

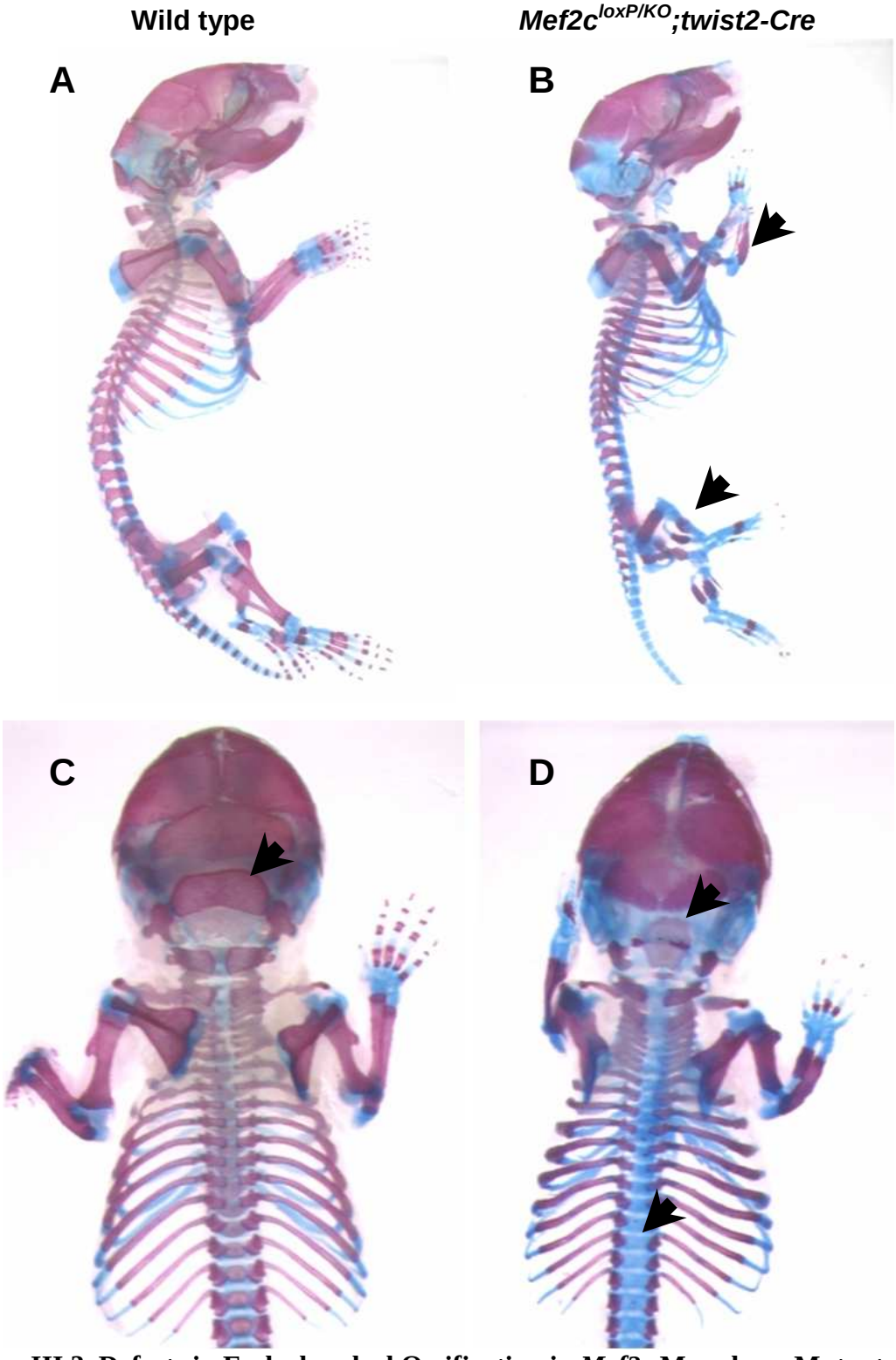

Figure III.3. Defects in Endochondral Ossification in *Mef2c* Mesoderm Mutants. Skeletons of wild type (panels A and C) and *Mef2c*$^{loxP/KO}$*;twist2-Cre* mice (panels B and D) at postnatal day one were stained for bone (Alizarin red) and cartilage (Alcian blue)and photographed in lateral (panels A and B) and dorsal views (C and D). Multiple defects in endochondral ossification are seen in the limbs, skull and spine (arrowheads).

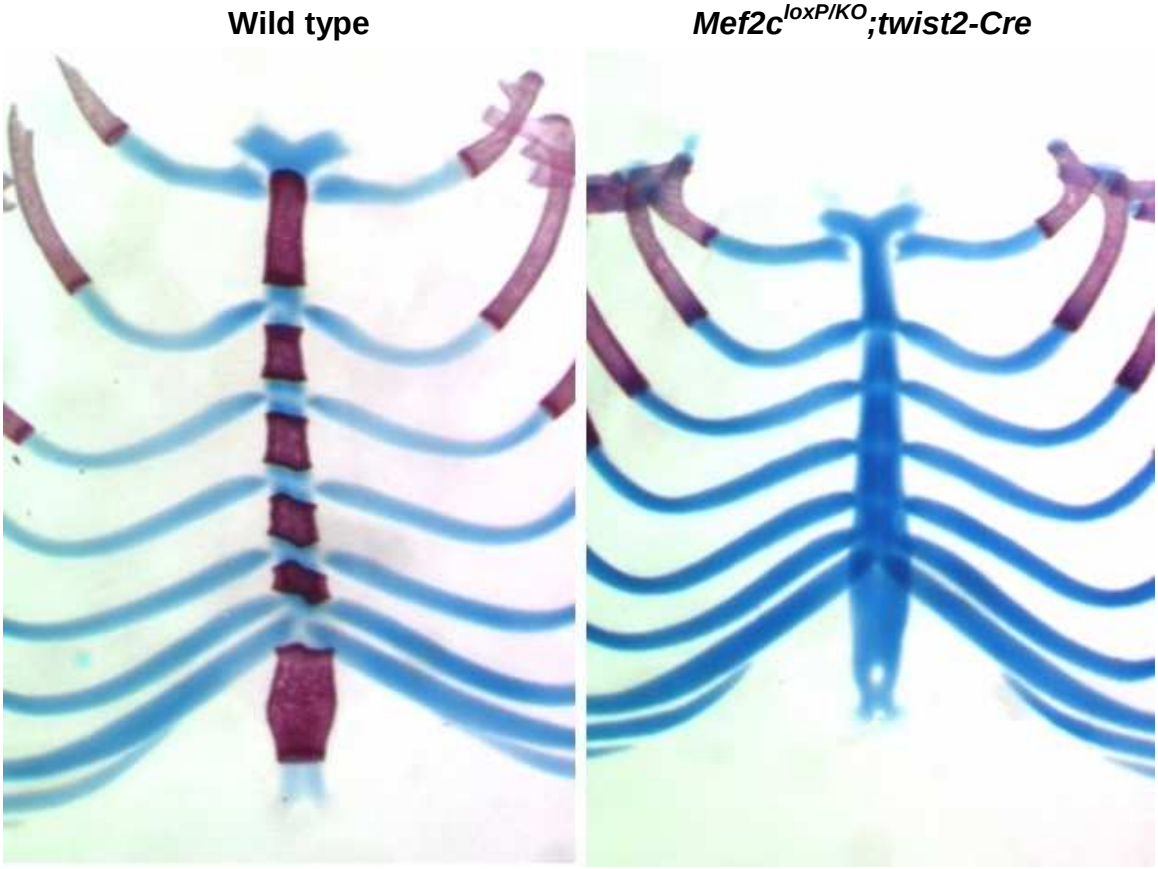

Figure III.4. Defects in Endochondral Ossification in *Mef2c* Mesoderm Mutants. Skeletons of wild type and *Mef2c*$^{loxP/KO}$*;twist2-Cre* mice at postnatal day one were stained for bone (Alizarin red) and cartilage (Alcian blue) and dissected to illustrate the sternum. The sternum of *Mef2c*$^{loxP/KO}$*;twist2-Cre* mice is fails to ossify at postnatal day one.

and scapula are all reduced in length, and Alcian blue staining of the cartilaginous growth plates in these bones can be seen within much of the length of these bones, especially the radius in which cartilage is present throughout its length (Figure III.5 panel D). The formation of the bone collars in the forelimb is also abnormal. Hypertrophic chondrocytes recruit osteoblasts to deposit the bone collar. Bone collars of mutant mice can be seen by staining for bone and cartilage to be unusually disorganized (Fig III.5 panels D and F). These defects may be a result of deletion of *Mef2c* from either osteoblasts or chondrocytes, and will be addressed later. Similar defects in endochondral ossification are also responsible for the shortening of the hind limbs of the mutant mice

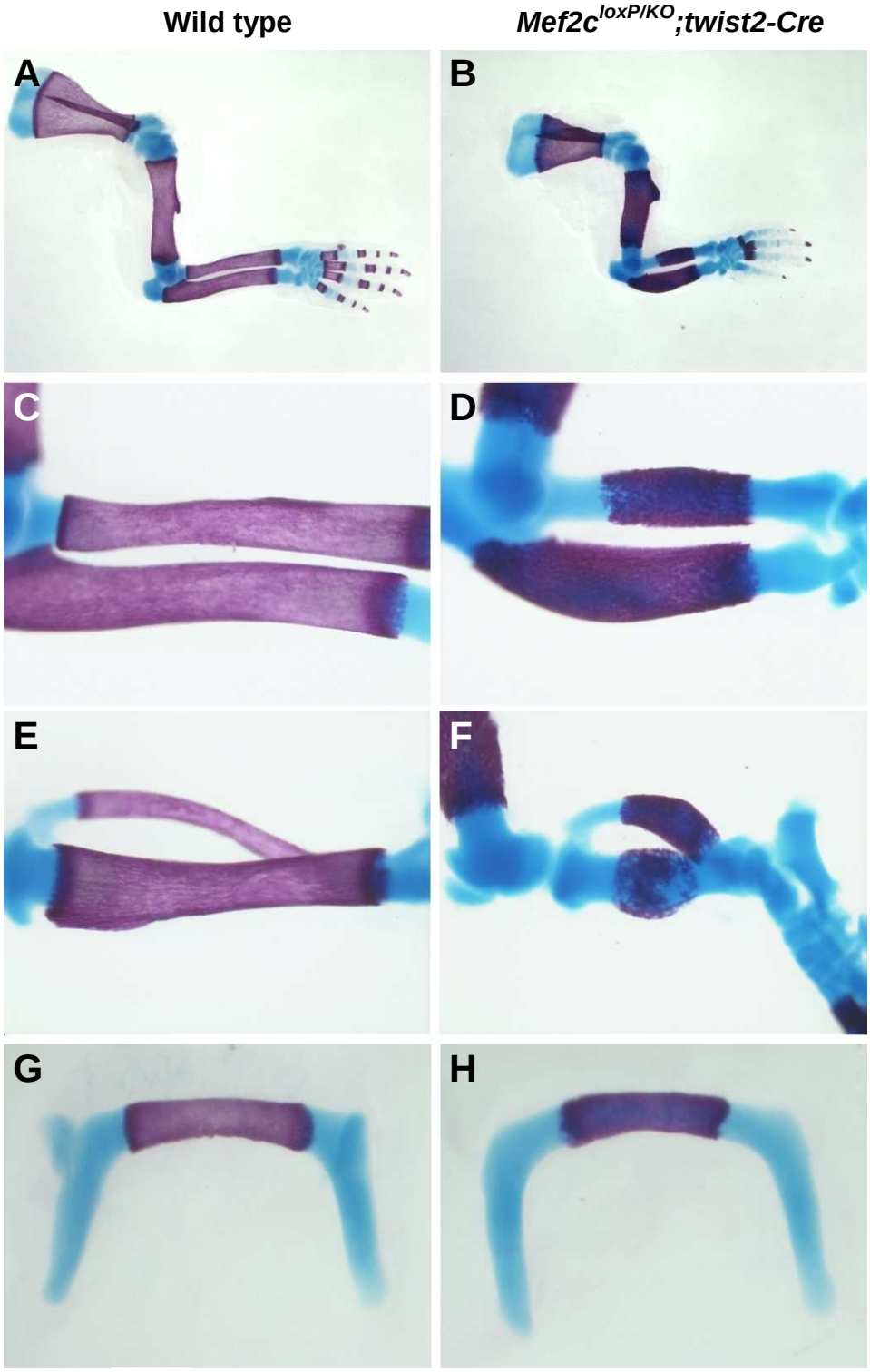

Figure III.5. Defects in Endochondral Ossification in *Mef2c* Mesoderm Mutants. Skeletons of wild type and *Mef2c*$^{loxP/KO}$*;twist2-Cre* mice at postnatal day one were stained for bone (Alizarin red) and cartilage (Alcian blue) and dissected to illustrate the arm (panels A and B), radius and ulna (panels C and D), tibia and fibula (panels E and F), and hyoid bones (panels G and H). Bones of *Mef2c*$^{loxP/KO}$*;twist2-Cre* mice are short and contain cartilaginous remnants of the growth plate.

(Figure III.5 panel F). Similarly, the hyoid bone ossifies, but contains cartilage throughout the ossified segment at postnatal day one (Figure III.5 panel H).

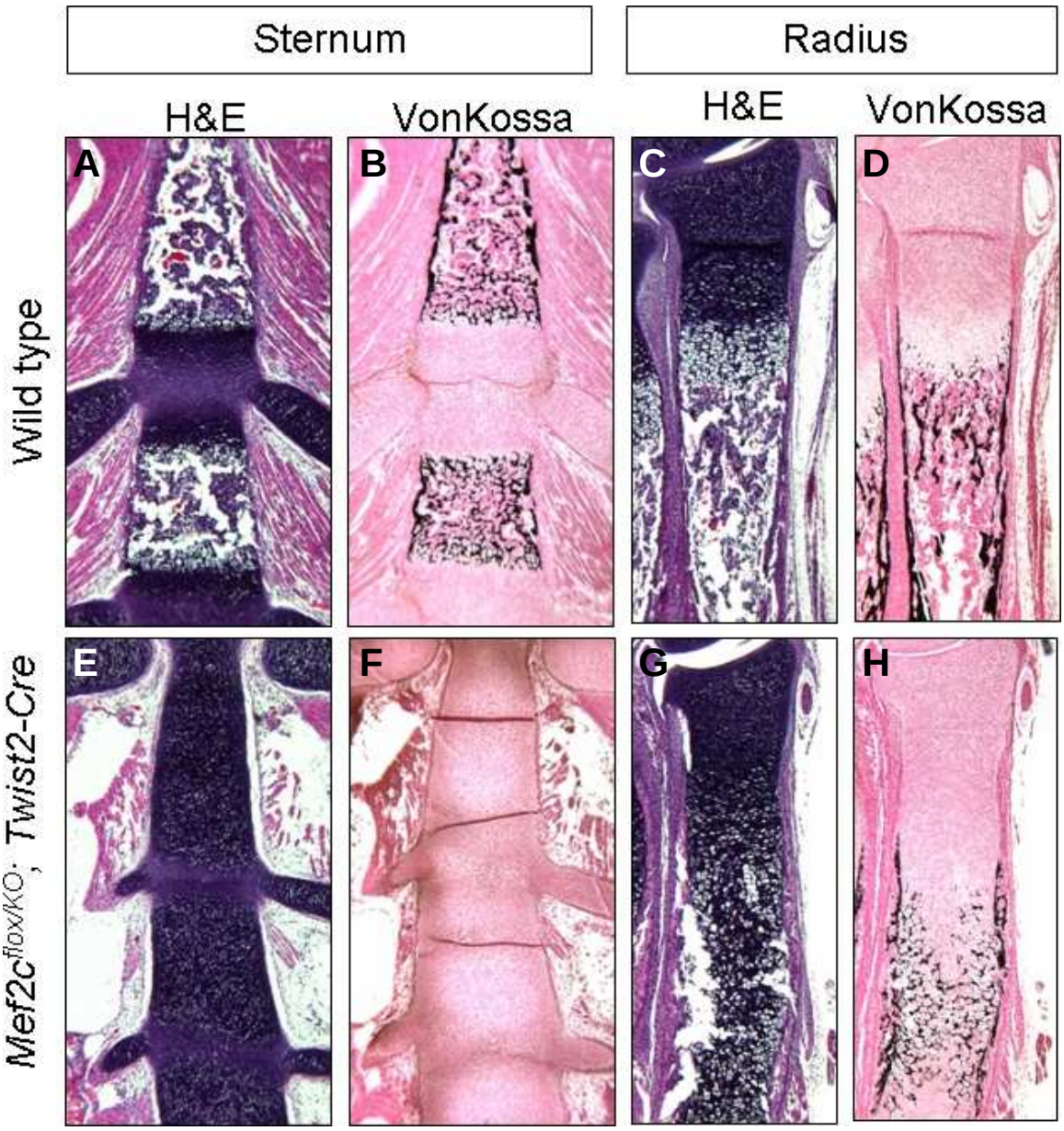

Figure III.6. Defects in Endochondral Ossification in *Mef2c* Mesoderm Mutants. Histological sections of indicated bones from wild type (panels A to D) or *Mef2c*$^{loxP/KO}$*;twist2-Cre* postnatal day one mice (panels E to H) were stained with hematoxylin and eosin (panels A, C, E and G) or for calcium deposits with VonKossa's method (black staining in panels B, D, F and H). Chondrocytes in bones of *Mef2c*$^{loxP/KO}$*;twist2-Cre* mice have failed to undergo chondrocyte hypertrophy and apoptosis, resulting in persistence of large amounts of growth plate cartilage, to the exclusion of trabeculated bone.

Sections of the sternum and radius from wild type and P1 *Mef2c$^{loxP/KO}$;twist2-Cre* mice reveal that the defects in endochondral ossification observed in *Mef2c$^{loxP/KO}$;twist2-Cre* mice result from defects in chondrocyte hypertrophy (Figure III.6). The sternum of wild type mice contains trabeculated bone within each sternebra, with growth plates at either end. The mature ossified bone is marked in VonKossa stained sections by black staining of calcium deposits (Figure III.6 panels A and B). Sections of the sternum of *Mef2c$^{loxP/KO}$;twist2-Cre* mice demonstrate that the sternebrae contain neither ossified bone nor growth plates Figure III.6 panels E and F). Chondrocyte hypertrophy within these bones has not been initiated at P1. Similarly, the radius of *Mef2c$^{loxP/KO}$;twist2-Cre* mice is seen to contain chondrocytes throughout its length, however chondrocytes in these bones have begun to initiate chondrocyte hypertrophy at a much lower rate. Chondrocytes in the bones of mutant mice appear smaller than hypertrophic chondrocytes in growth plates of wild type mice, yet these cells appear to reach late stages of chondrocyte hypertrophy as seen by VonKossa staining surrounding chondrocytes in the middle of the bone (compare Figure III.6 panels C and D to panels G and H). This pattern of VonKossa staining is characteristic of chondrocytes in growth plates of wild type mice just prior to apoptosis.

To determine if the delay in chondrocyte maturation observed in *Mef2c$^{loxP/KO}$;twist2-Cre* mice correlated with changes in gene expression, *in situ* hybridization to detect multiple markers of chondrocyte maturation was undertaken. In radius bones, significant changes were seen in the expression of *Collagen α1(II)*, a marker of proliferating and prehypertrophic chondrocytes (Figure III.7 panels F and M), and *Collagen α1(X)*, a specific marker of hypertrophic chondrocytes (Figure III.7 panels

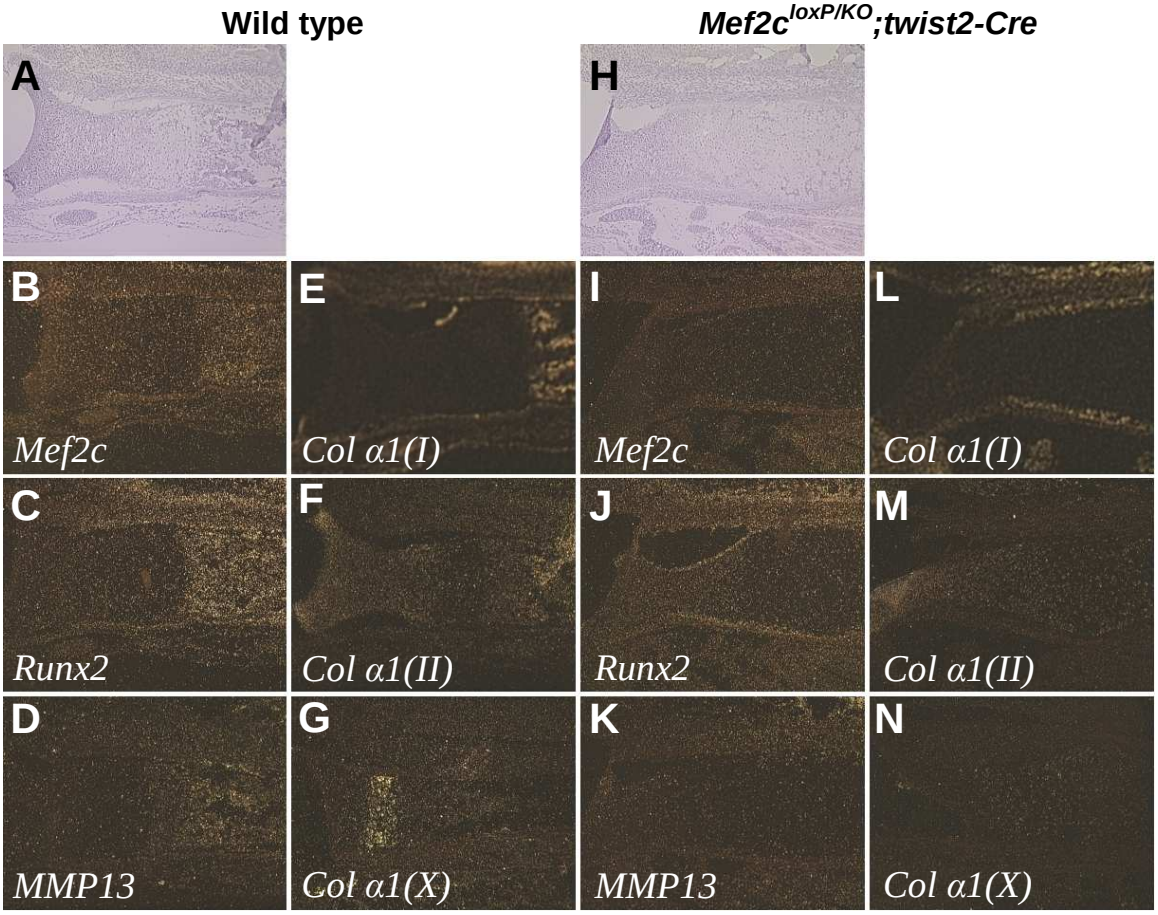

Figure III.7 Detection of Chondrocyte Gene Expression by *in situ* Hybridizaton. Sections of the radius bone of wild type (panels A to G) and *Mef2c$^{loxP/KO}$;twist2-Cre* (panels H to N) mice were hybridized with probes for *Mef2c* (panels B and I), *Runx2* (panels C and J), *MMP13* (panels D and K), *collagen α1(I)* (panels E and L), *collagen α1(II)* (panels F and M), and *collagen α1(X)* (panels G and N).

G and N). Chondrocytes of *Mef2c$^{loxP/KO}$;twist2-Cre* mice fail to robustly express *Collagen α1(X)*, and persist in expressing *Collagen α1(II)*, consistent with impaired maturation of chondrocytes in these mutants. Additionally, the expression of *Mef2c* in growth plates of wild type and *Mef2c$^{loxP/KO}$;twist2-Cre* was determined. In wild type bones, *Mef2c* is expressed in chondrocytes just prior to the initiation of chondrocyte hypertrophy, and is not expressed in chondrocytes of *Mef2c$^{loxP/KO}$;twist2-Cre* mice

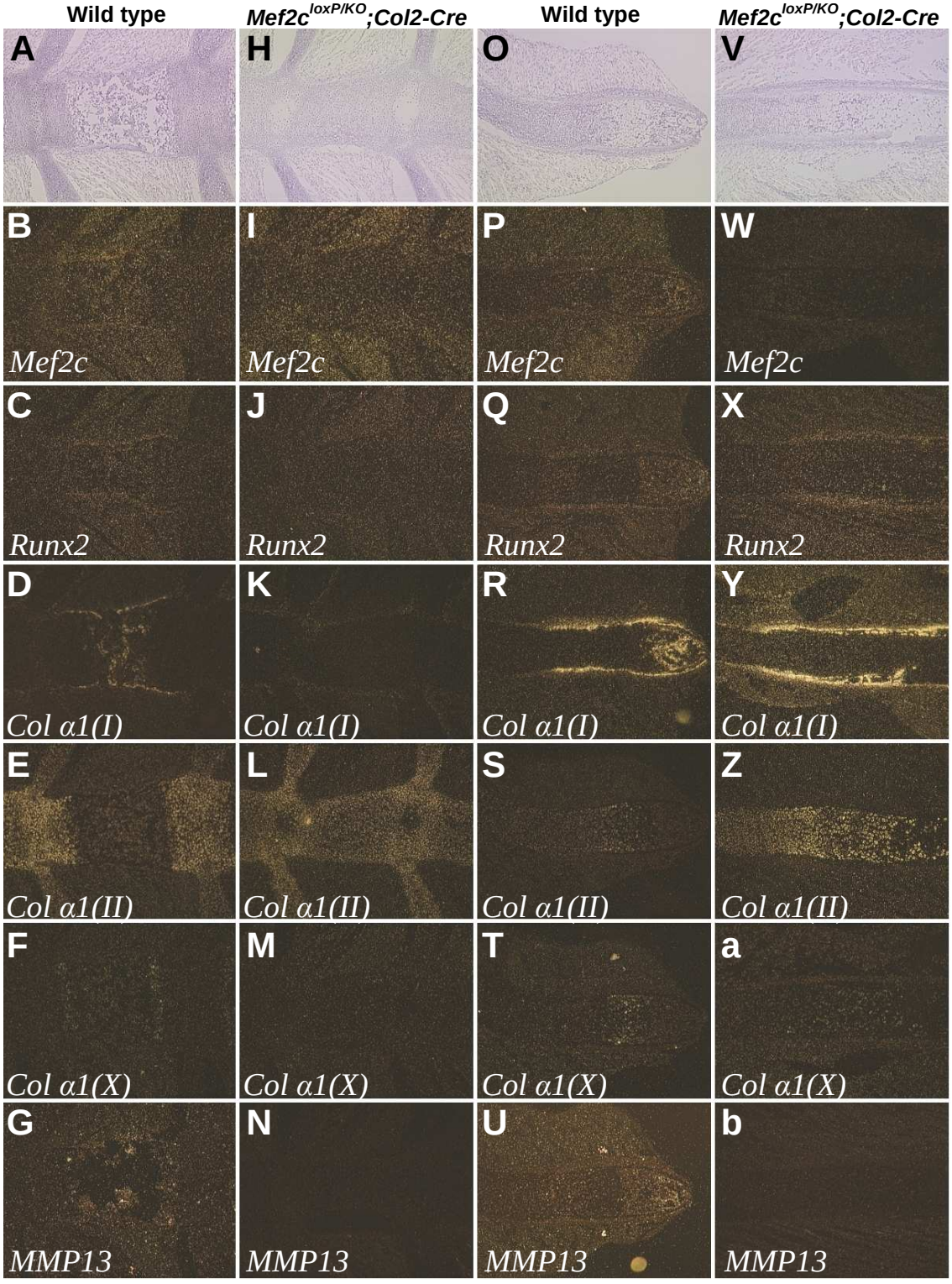

Figure III.8 Detection of Chondrocyte Gene Expression by *in situ* Hybridizaton. Sections of the sternum (panels A to N) or rib (panel O to b) bones of wild type (panels A to G and O to U) and *Mef2c*$^{loxP/KO}$*;twist2-Cre* mice (panels H to N and V to b) were hybridized with probes for *Mef2c*, *Runx2*, *collagen α1(1)*, *collagen α1(II)*, *collagen α1(X)*, and *MMP13*.

(Figure III.7 panels B and I). Similar results were seen in the sternum and rib bones (Figure III.8).

To determine whether the skeletal defects observed in *Mef2c$^{loxP/KO}$;twist2-Cre* and *Mef2c$^{loxP/KO}$;Wnt1-Cre* mice reflected a requirement for MEF2C in chondrocytes or osteoblasts, I specifically deleted *Mef2c* in proliferating endochondral cartilage using a Cre transgene controlled by the *Collagen α1(II)* promoter, called *Col2-Cre* (Long et al., 2001). The resulting mutants were identifiable at birth by shortened limbs, an absence of ossification of the sternum. The *Mef2c$^{loxP/KO}$;Col2-Cre* mice do differ from *Mef2c$^{loxP/KO}$;twist2-Cre* in that they are viable to adulthood (Figure III.9). *Mef2c$^{loxP/KO}$;Col2-Cre* mice are of similar overall length to littermates, however these mice are distinguishable by their waddling gait due to their shortened limbs. Bone and cartilage staining of adult skeletons of three month old mutant mice highlights the reduction in limb length of *Mef2c$^{loxP/KO}$;Col2-Cre* mice, which is caused by a reduction in the length of all long bones of the limb (Figure III.9). Significant amounts of cartilage and disorganized ossification is apparent in the sternebrae (Figure III.9 panel D), and small amounts of cartilage are also visible within the ends of the long bones when examined closely. The overall patterning of the limb bones is not significantly disturbed. However, the structure of several ribs in *Mef2c$^{loxP/KO}$;Col2-Cre* mice is dramatically altered; large swellings of the rib bones at the junction of the ossified bone and chondrocostal cartilage are apparent (Figure III.9 panel F). To better determine the architectural defects in the ribs, and more closely examine cartilaginous remnants in the long bones and sternum, histological sections were prepared of these regions of the skeleton. These sections reveal the presence of large remnants of the growth plates in

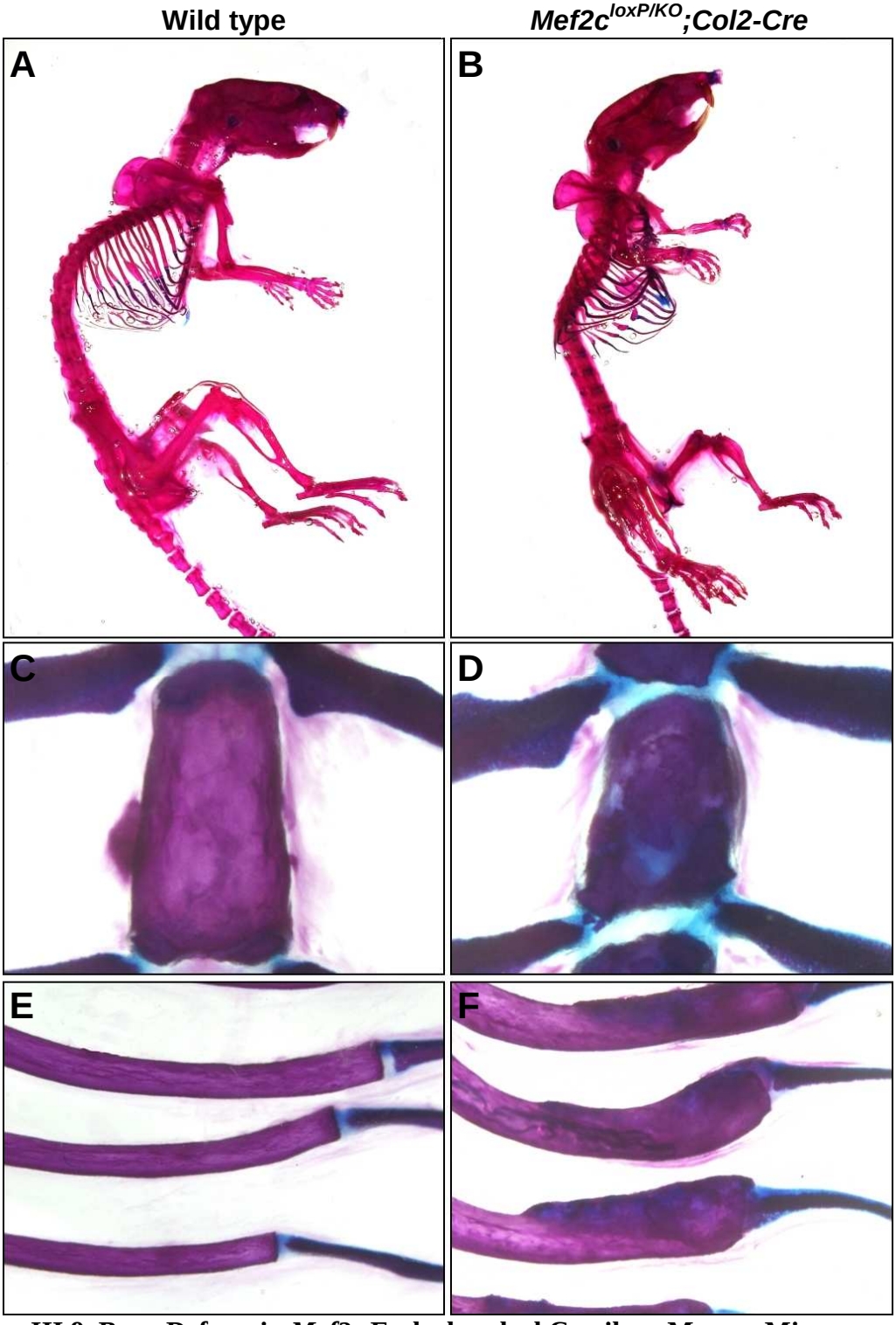

Figure III.9. Bone Defects in *Mef2c* Endochondral Cartilage Mutant Mice.
Skeletons of three month old wild type (panels A, C and E) and *Mef2c*$^{loxP/KO}$*;Col2-Cre* mice (panels B, D and F) were stained for bone (Alizarin red) and cartilage (Alcian blue). Whole skeletons (panels A and B), second sternebrae (panels C and D) and rib growth plates (panels E and F) are shown.

multiple endochondral bones, marbled with mineralized cartilaginous matrix (Figure III.10). In littermate wild type mice, the endochondral growth plates remain only as thin remnants of the proliferating chondrocytes, with few evident hypertrophic chondrocytes. The growth plate remnants in *Mef2c*$^{loxP/KO}$*;Col2-Cre* mice at three months of age are greatly increased in size (Figure III.10). Within the distal radius and ribs, chondrocytes of increased cell size are observed in large numbers. This collection of cells is assembled into disorganized or columns of cells, reminiscent of prehypertrophic chondrocytes despite their increased size. The groups of cells within these regions are interrupted by veins of mineralized matrix (Figure III.10 panels B and D), which is more typical of chondrocytes in the late stages of hypertrophy. This reflects the impaired maturation of these cells which has resulted in a disorganized and abnormally persistent growth plate and changes in bone architecture. Similarly, the entire length of the sternebrae contain cartilaginous remnants composed of enlarged cells and mineralized matrix, but are only occasionally interrupted by punctuate ossification as compared to the radius and ribs which maintain the polarity of the growth plate.

Examination of skeletons of *Mef2c*$^{loxP/KO}$*;Col2-Cre* mice stained for bone and cartilage at postnatal day one demonstrates identical defects in most bones compared to defects observed in *Mef2c*$^{loxP/KO}$*;twist2-Cre* mice. At P1, overall length of the *Mef2c*$^{loxP/KO}$*;Col2-Cre* mice is not observably shorter than wild type or *Mef2c* heterozygous littermates. However, the truncated limbs of these mice make them distinguishable from littermates, as are *Mef2c*$^{loxP/KO}$*;twist2-Cre* mice. As observed in *Mef2c*$^{loxP/KO}$*;twist2-Cre* mice, the limbs are reduced in length and contain excessive cartilage (Figure III.11). Similarly, formation of the bone collars in the limbs is

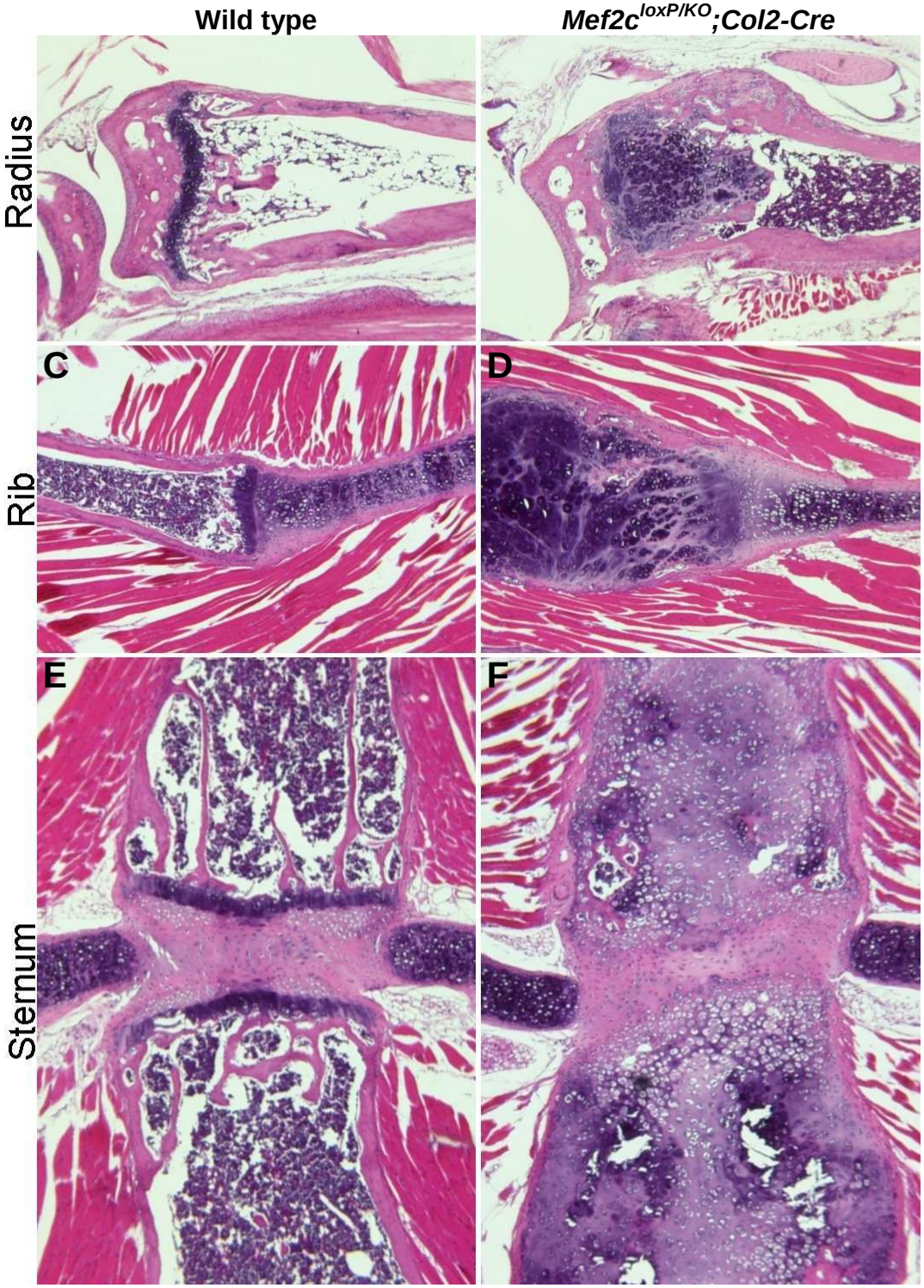

Figure III.10. Bone Defects in *Mef2c* Endochondral Cartilage Mutant Mice.
Histological sections of wild type (panels A, C and E) and *Mef2c*$^{loxP/KO}$*;Col2-Cre* (panels B, D and F) radius (panels A and B), rib (panels C and D) and sternum bones (panels E and F) were stained with hematoxylin and eosin. Bones from *Mef2c* chondrocyte mutants contain significant remants of the growth plate cartilage, which distort the shape of the ribs, and prevent ossification of the sternum.

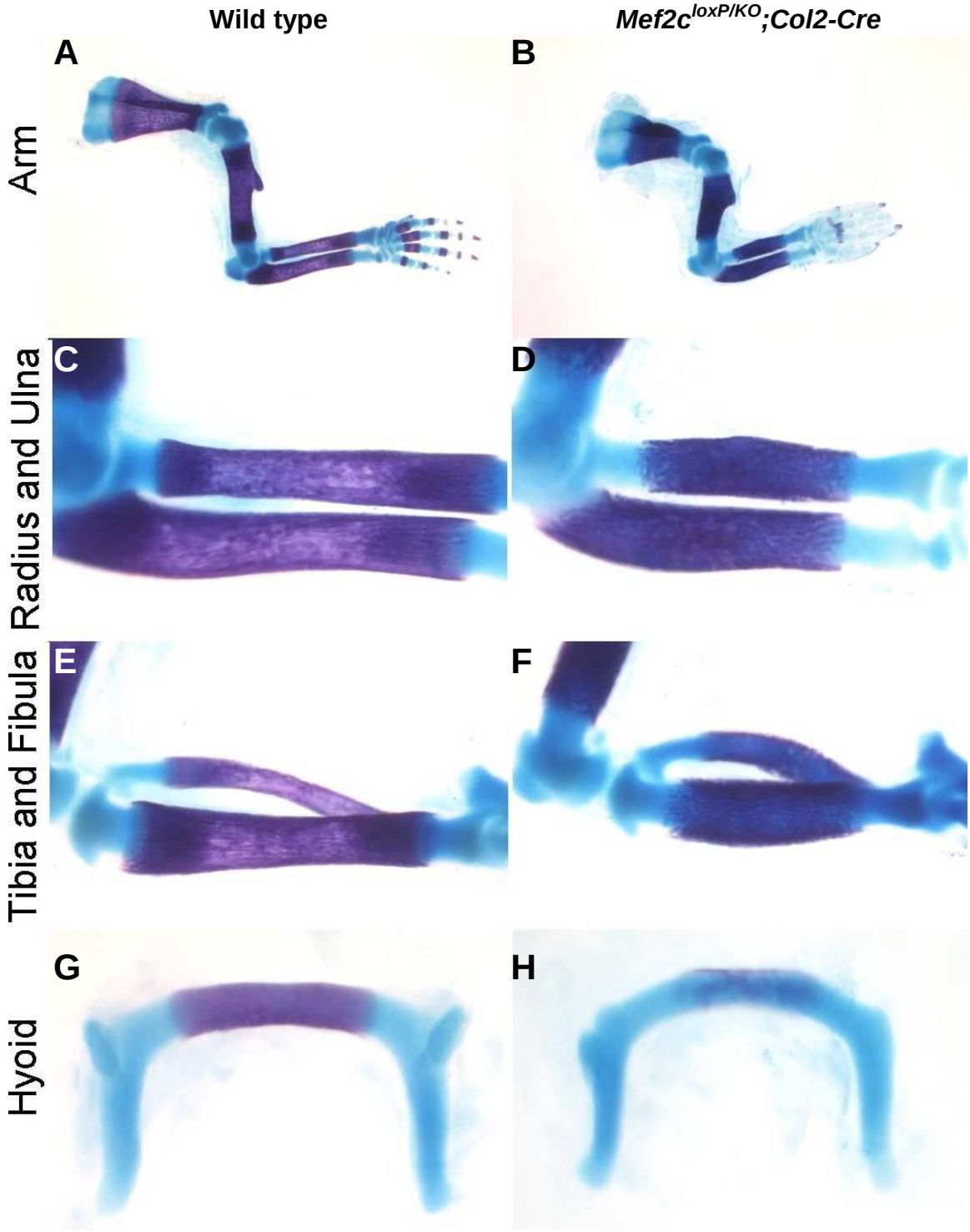

Figure III.11. Bone Defects in *Mef2c* Endochondral Cartilage Mutant Mice.
Skeletons of wild type and *Mef2c*$^{loxP/KO}$*;Col2-Cre* mice at postnatal day one were stained for bone and cartilage and dissected to illustrate the arm (panels A and B), radius and ulna (panels C and D), tibia and fibula (panels E and F), and hyoid bones (panels G and H). Bones of *Mef2c*$^{loxP/KO}$*;Col2-Cre* mice are short and contain cartilaginous remnants of the growth plate.

perturbed. Trabeculation of the forming bone collar is disorganized when compared to limbs of wild type animals. This demonstrates that *Mef2c* function in chondrocytes is required for orderly bone collar formation, and that abnormalities in bone collar formation when *Mef2c* is deleted from multiple mesoderm lineages by *twist2-Cre* result from defects in chondrocyte signaling as opposed to defects in osteoblast function. Other abnormalities seen in both *Mef2c*$^{loxP/KO}$*;Col2-Cre* mice and *Mef2c*$^{loxP/KO}$*;twist2-Cre* mice include an absence of ossification in the sternum and ventral vertebral bodies

The significant differences in the ossification defects seen in *Mef2c*$^{loxP/KO}$*;Col2-Cre* mice and *Mef2c*$^{loxP/KO}$*;twist2-Cre* mice relate to the tissues in which Cre recombinase is produced. Defects are not seen in the neural crest derived endochondral bones of *Mef2c*$^{loxP/KO}$*;twist2-Cre* mice since the expression of Cre is limited to mesoderm derivatives. *Collagen α1(II)-Cre* is expressed in endochondral bones derived from either mesoderm or neural crest, resulting in additional defects when compared to *Mef2c*$^{loxP/KO}$*;twist2-Cre* mice, best evidenced by a significant decrease in ossification of the hyoid bone in *Mef2c*$^{loxP/KO}$*;Col2-Cre* mice (compare Figure III.5 panel H and Figure III.11 panel H). The defects in in *Mef2c*$^{loxP/KO}$*;twistl2-Cre* mice is slightly more severe in the bones of the hind limb (compare Figure III.5 panel F and III.11 panel F). This may be related to the earlier expression of in *twist2-Cre*, or it could suggest a subtle role for *Mef2c* in osteoblast development.

Histological sections of bones from *Mef2c*$^{loxP/KO}$*;Col2-Cre* mice demonstrate similar changes in growth plate architecture and chondrocyte development when compared to *Mef2c*$^{loxP/KO}$*;twist2-Cre* mice. Deletion of *Mef2c* from chondrocytes impairs differentiation of chondrocytes to the same extent as deletion from mesoderm.

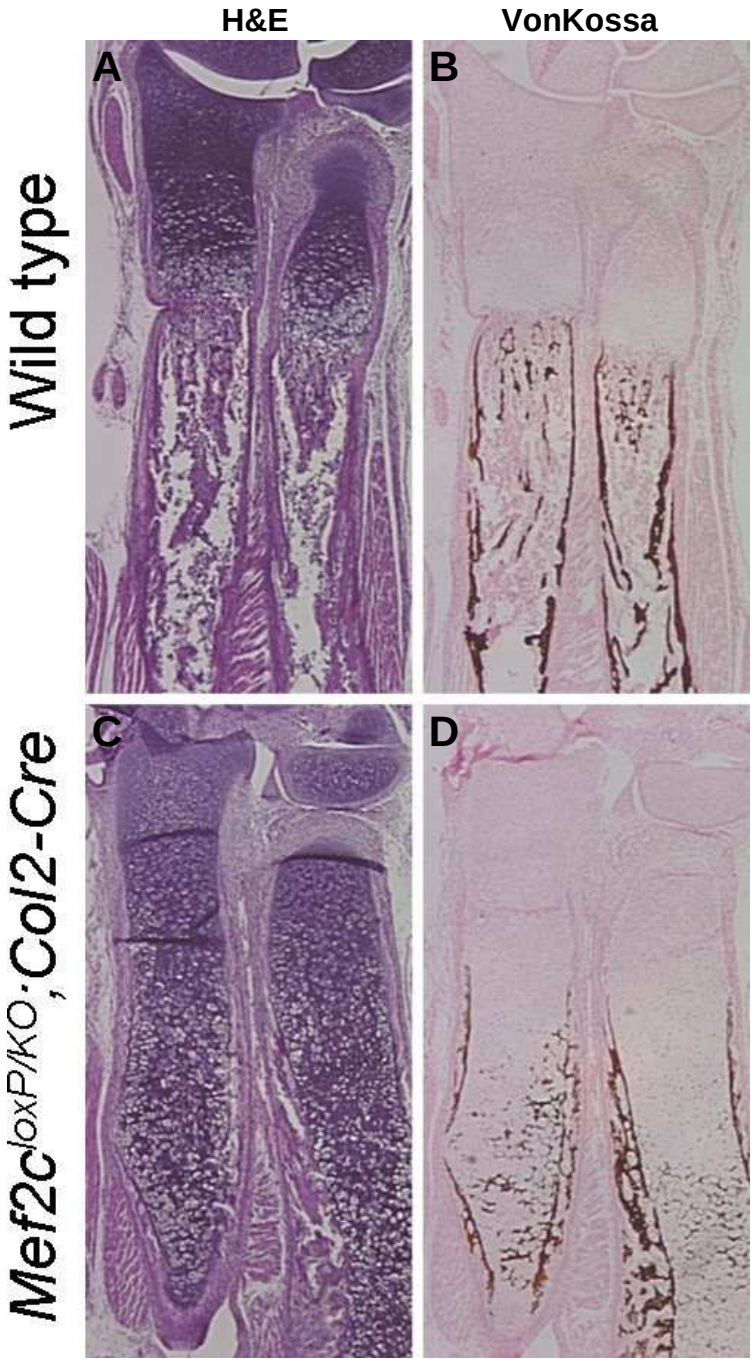

Figure III.12 Defects in Endochondral Ossification in *Mef2c* Chondrocyte Mutants. Histological sections of radius bones from wild type (panels A and B) or *Mef2c*$^{loxP/KO}$*;Col2-Cre* postnatal day one mice (panels C and D) were stained with hematoxylin and eosin (panels A and C) or for calcium deposits with VonKossa's method (black staining in panels B and D). Chondrocytes in bones of *Mef2c*$^{loxP/KO}$*;Col2-Cre* mice have failed to undergo chondrocyte hypertrophy and apoptosis, resulting in persistence of large amounts of growth plate cartilage, to the exclusion of trabeculated bone.

Staining of sections from the radius and sternum of *Mef2c*$^{loxP/KO}$*;Col2-Cre* mice with hematoxylin and eosin or VonKossa (Figure III.12) reveal identical changes in growth plate morphology observed in *Mef2c*$^{loxP/KO}$*;twist2-Cre* mice (Figure III.6). *Mef2c* is therefore required specifically in chondrocytes to promote hypertrophic differentiation. Examination of marker gene expression in bones of *Mef2c*$^{loxP/KO}$*;Col2-Cre* mice demonstrated an identical pattern to that observed in bones of *Mef2c*$^{loxP/KO}$*;twist2-Cre* mice, shown in Figures III.7 and III.8.

Functional Redundancy Among *Mef2* Family Members

Mice which lack *Mef2c* in endochondral cartilage display significant defects in bone development resulting from impaired chondrocyte hypertrophy. However, chondrocyte maturation is not completely abolished in these mice. One explanation for the ability of these chondrocytes to eventually complete maturation is the potential for functional redundancy among members of the *Mef2* family. The expression patterns of all four *Mef2* genes in the developing growth plate were therefore determined by *in situ* hybridization (Figure III.13). Of the four *Mef2* genes, *Mef2a* and *Mef2d* are expressed throughout chondrocyte development, confirming the potential for these genes to function redundantly in chondrocyte differentiation. These genes are all expressed at similar levels to their expression in skeletal muscle (lower right corner of each panel in Figure III.13). Functional redundancy of *Mef2* genes in endochondral bone development has since been confirmed *in vivo* by another member of the Olson lab, Yuri Kim, who has intercrossed the null alleles of *Mef2c* and *Mef2d* resulting in a significant exacerbation of the defects in endochondral ossification observed in *Mef2c* heterozygous mice.

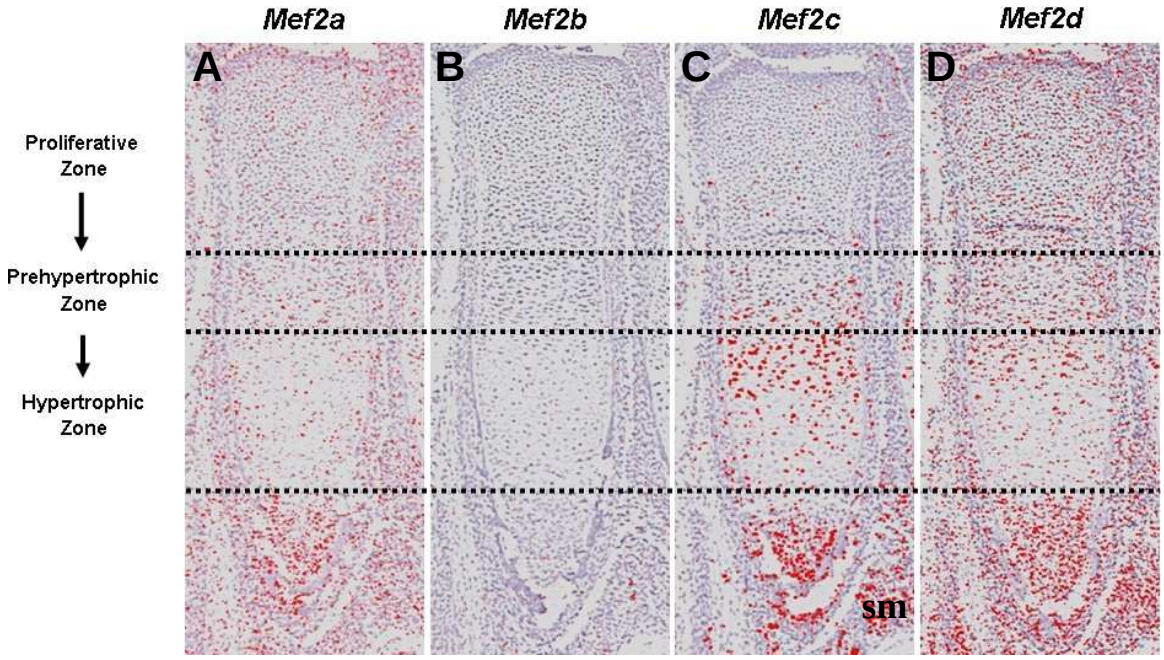

Figure III.13. Expression of *Mef2* Family Members in Endochondral Growth Plate. Expression of each member of the *Mef2* family was examined by *in situ* hybridization. Signal is pseudocolored red. *Mef2a, Mef2c* and *Mef2d* are each expressed during chondrocyte development. Skeletal muscle (sm) is marked in panel C.

The activity of all members of the MEF2 family can be inhibited in transfected cells by the expression of a fusion protein consisting of the MEF2 DNA binding domain and the *Drosophila* engrailed protein (Stanton et al., 2004). To block all transcriptional activity of the MEF2 transcription factors in endochondral cartilage, I cloned the MEF2C-engrailed coding sequence into a vector containing the promoter and enhancer of the *Collagen α1(II)* gene, which directs expression of the fusion protein in chondrocytes of transgenic mice (Vega et al., 2004). Expression of MEF2C-engrailed in endochondral cartilage of transgenic mice resulted in a substantial block in chondrocyte development at E18.5. As seen in Figure III.14, staining of *Collagen α1(II)-Mef2c-engrailed* embryos for bone and cartilage reveals multiple defects in endochondral ossification. Ossification in nearly every region of the endochondral skeleton is blocked, while formation of cartilage independent membranous bones remains unchanged. All endochondral bones

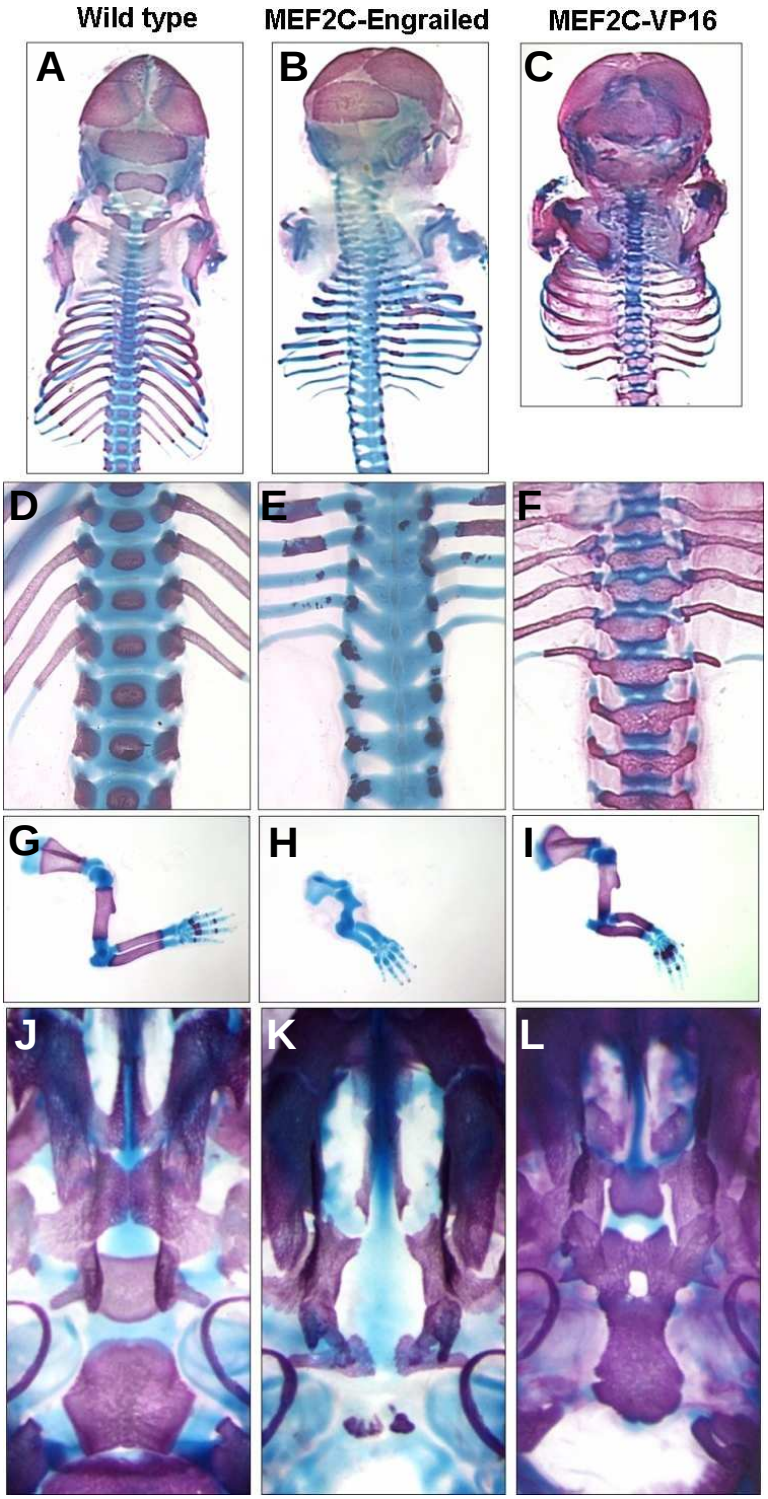

Figure III.14. Control of Endochondral Ossification by MEF2C Fusioin Proteins. Skeletons of transgenic mice expressing a fusion of the MEF2C DNA binding domain and Engrailed repressor driven by the *collagen α1(II)* promoter (panels B, E, H and K), or transgenic mice expressing a fusion of the MEF2C DNA binding domain and VP16 activation domain proteins driven by the *collagen α1(II)* promoter (panels C, F, I and L) were stained for bone and cartilage and compared to non-transgenic littermates at E 18.5.

are abnormally small, resulting in shortening of the limbs, spine and pelvis, and deformation of the rib cage. Milder defects are observed in transgenic mice which carry fewer copies of the transgene. Notably in the most strongly effected skeletons, the endochondral bones in the base of the skull, hyoid bone, limbs, sternum and pelvis remain entirely cartilaginous. However, patterning of these cartilaginous templates is normal (Figure III.14 panels B, E, H and K). The only difference in the shape of these bones is due to failed chondrocyte hypertrophy.

The activity of MEF2 proteins can also be "super-activated" *in vitro* and *in vivo* by fusion to the activation domain of VP16 (Molkentin et al., 1996, Xu et al, 2006). To over-activate MEF2 transcription activity in endochondral cartilage, I cloned a MEF2C-VP16 coding sequence into a vector containing the promoter and enhancer of the *Collagen α1(II)* (Vega et al., 2004). Expression of MEF2C-VP16 in endochondral cartilage of transgenic mice resulted in premature endochondral ossification at E18.5. These mice are also identifiable by their shortened limbs as a result of accelerated ossification, instead of the blockade of chondrocyte hypertrophy observed when MEF2C-engrailed is expressed in chondrocytes. Ossification of multiple bones has progressed to a stage characteristic of much later development. Growth plates in the sternum have fused, and the width of the ventral vertebral body has ossified to fuse with the lateral processes (Figure III.14 panels C, F, I and L). Growth plates in the limbs have advanced closer to the ends of the bones and the remaining growth plate cartilages at these sites are reduced in size. The premature nature of the ossification of these bones has altered the shape of these bones; the bones of the arm are more similar in shape to the unossified forelimb of the *Mef2c-engrailed* transgenic mice than the forearm of wild type mice.

MEF2 Directly Regulates Gene Expression in Hypertrophic Chondrocytes

The bone abnormalities resulting from *Mef2c* deletion and MEF2C-engrailed expression suggest that MEF2 proteins are required for activation of transcription in hypertrophic chondrocytes. To determine if chondrocyte gene expression was altered in the absence of *Mef2c*, the expression of several genes expressed during chondrocyte development was analyzed by *in situ* hybridization in samples collected from *Mef2c*$^{loxP/KO}$*:twist2-Cre* mice at P1. Of particular interest were potential changes in the expression of *Runx2*, a known regulator of chondrocyte and osteoblast development. Runx2 expression was examined in the sternum and radius of wild type and *Mef2c* chondrocyte mutant mice. These results were virtually identical to those seen in *Mef2c* mesodermal mutant mice (Figures III.7 and III.8). Published reports demonstrate that during embryonic development *Runx2* expression begins when chondrocyte hypertrophy is initiated, and continues to increase throughout chondrocyte hypertrophy. At P1, my data indicates that *Runx2* is strongly expressed in osteoblasts and expressed to a much lesser extent throughout chondrocyte differentiation (Figures III.7 panels C and J, and III.8 panels C, J, Q and X). In *Mef2c* mutant mice, the pattern of tissues in which Runx2 is expressed is unchanged (compare Figures III.7 panels C and J, and III.8 panels C, J, Q and X). Expression of Runx2 appears lower in the mutant bone only because sites occupied by osteoblasts in bones of wild type mice are occupied by chondrocytes in *Mef2c* mutant bones.

To identify the various stages of chondrocyte development in bones of both wild type and mutant mice, the expression of *Collagen α1(II)* which marks proliferating and

prehypertrophic chondrocytes, *Collagen α1(X)* which marks hypertrophic chondrocytes, *MMP13*, which is expressed in the late stages of chondrocyte hypertrophy and is highly expressed in osteoblasts (Stickens et al., 2004), was examined in the sternum and radius of wild type and mutant mice. Surprisingly, *MMP13* expression which is reported to mark late hypertrophic chondrocytes was not detected in wild type chondrocytes at P1, but was readily detectable in osteoblasts, limiting the usefulness of this probe. However, as expected the expression of *Collagen α1(II)* and *Collagen α1(X)* were readily detectable in wild type bones in proliferating and prehypertrophic chondrocytes, or hypertrophic chondrocytes, respectively. In *Mef2c* mutant mice, the expression of *Collagen α1(II)* and *Collagen α1(X)* were significantly altered. The sternum of mutant mice, which is composed entirely of prehypertrophic chondrocytes at P1 only expresses of *Collagen α1(II)* and not *Collagen α1(X)*. This result correlates with the stage of chondrocyte development observed in these bones. However in the radius, where chondrocytes are capable of reaching what appears to be later stages of chondrocyte development marked by VonKossa staining for mineralized cartilage matrix (Figures III.6 and III.12), *Collagen α1(II)* expression persists, and *Collagen α1(X)* expression is nearly absent, suggesting that the activation of *Collagen α1(X)* may be dependent on MEF2C.

The enhancer which drives *Collagen α1(X)* expression in hypertrophic chondrocytes is the only such enhancer identified (Gebhard et al., 2004). In the mouse genome, this region is contained within approximately four kilobases upstream of the *Collagen α1(X)* promoter. This genomic region was examined for consensus MEF2 binding sites which were conserved among higher vertebrates. Six consensus MEF2 binding sites were identified (Figure III.15), three of which are conserved between the

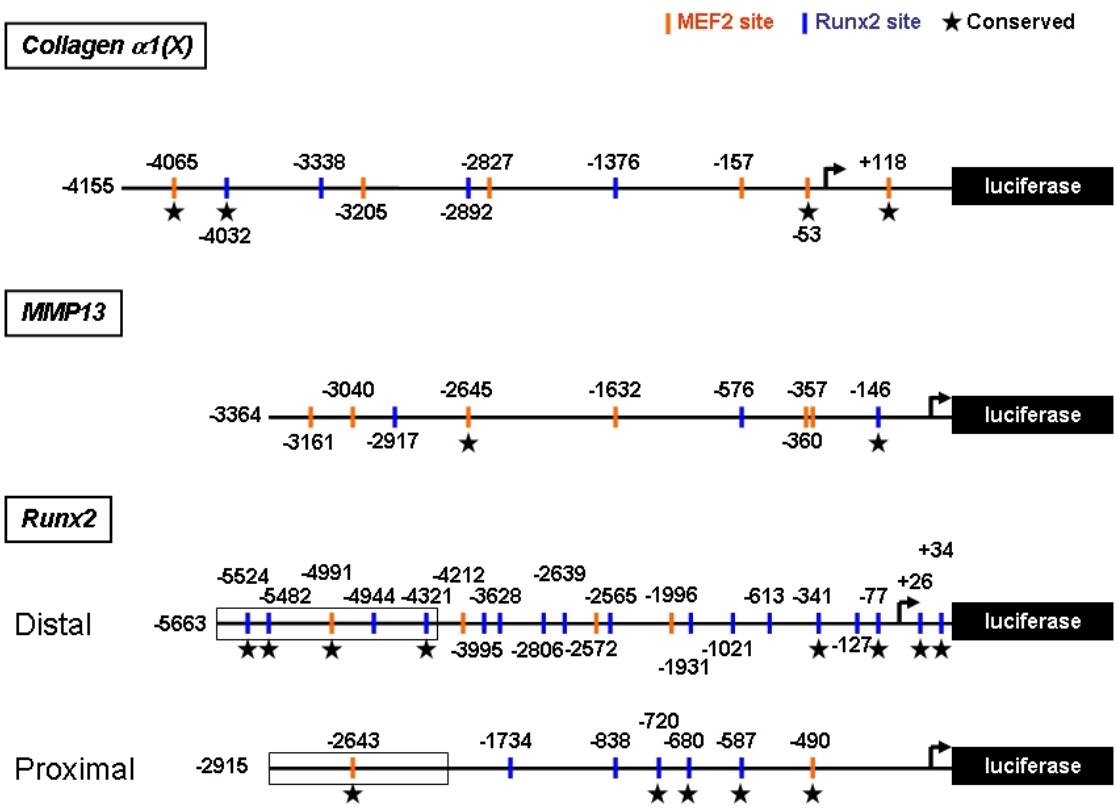

Promoter	Position	Sequence
Collagen α1(X)	-4065	ATAAAAATAG
Collagen α1(X)	-3205	CTATATTTAA
Collagen α1(X)	-2827	TTATAAATAT
Collagen α1(X)	-157	TTAAAAATAA
Collagen α1(X)	-53	CTATTAATAT
Collagen α1(X)	+118	GTATAAATAC
MMP13	-3161	GTAAAATTAA
MMP13	-3040	ATAAAAATAA
MMP13	-2645	ATAATTTTAA
MMP13	-1632	CTAATTTTAC
MMP13	-360	CTATTATTAT
MMP13	-357	TTATTATTAC
Runx2 Distal	-4991	TTAAATATAT
Runx2 Distal	-4212	ATAATTATAA
Runx2 Distal	-2572	ATAAATTTAA
Runx2 Distal	-1996	GTATAAATAT
Runx2 Proximal	-2643	TTATAAATAA
Runx2 Proximal	-490	TTATTTTTAA

Figure III.15 Promoter Structures of Chondrocyte Expressed Genes.
The genomic sequences upstream of the *Collagen α1(I)* and *Bone Sialoprotein* genes contain putative MEF2 binding sites (orange lines), including sequences where the MEF2 binding consensus sequence is conserved among mice and humans (star). Sequences of the potential MEF2 binding sites are listed with the position of the site relative to the start of transcription. These genomic regions are not activated by MEF2 in COS7 cells.

mouse and human genomes. The critical regulatory regions which are required for the expression of many genes in hypertrophic chondrocytes remain unidentified. To identify potential MEF2 dependent enhancers in genes reportedly expressed in hypertrophic chondrocytes, the genomic regions immediately upstream of Runx2 and MMP13 were examined. MEF2 binding sites that conform to the T A (T/A) (T/A) (T/A) (T/A) T A consensus, and Runx2 binding sites that conform to the (G/A) C C (G/A) C A consensus are shown in Figure III.15. Conserved MEF2 binding sites were identified within approximately 10kb of both promoters of Runx2, and the promoter of MMP13.

To determine if these genomic regions functioned as MEF2 responsive enhancer regions, portions of these regions were isolated by polymerase chain reaction (PCR) amplification and cloned upstream of the luciferase open reading frame as pictured in Figure III.15, and tested for responsiveness to MEF2C in COS7 cells. This work was performed in collaboration with Yuri Kim. Putative enhancer regions (boxed regions in Figure III.15) of the *Runx2* promoter were tested for activation by MEF2C. These genomic regions contained conserved MEF2 binding sites, but were not activated by MEF2C. This is consistent with my data that *Runx2* expression is not significantly altered in endochondral or membranous bones which lack *Mef2c*. However, genomic regions of either *Collagen α1(X)* or *MMP13* were activated by MEF2C, but not Runx2 (Figure III.16 panels A and B). The expression of MEF2C in a wide variety of cell types led me to expect that MEF2C would activate the expression of chondrocyte genes in cooperation with factors restricted to bone, such as Runx2. Surprisingly, MEF2C and Runx2 do not function cooperatively in activating the promoters of *Collagen α1(X)* or *MMP13* (Figure III.16 panels A and B), suggesting that MEF2C may function

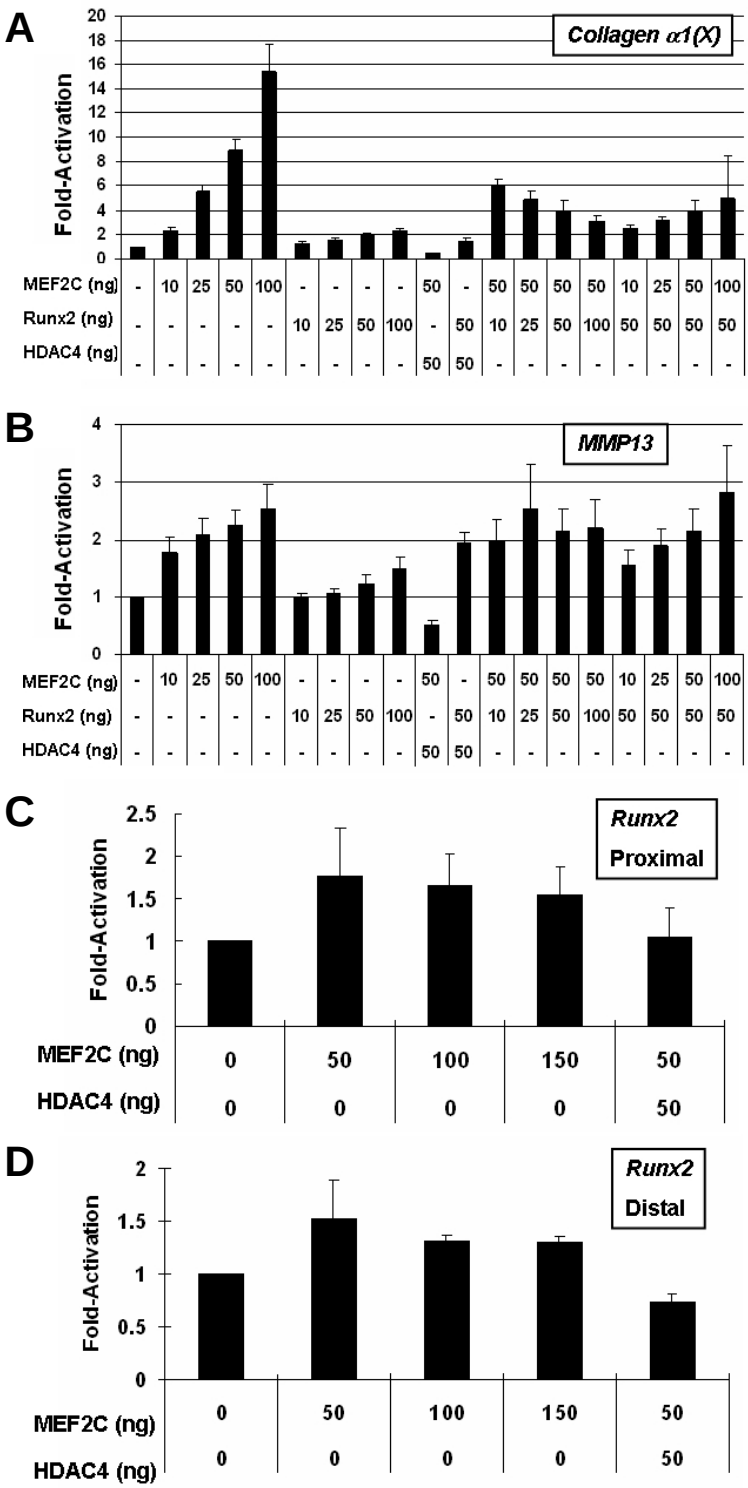

Figure III.16. Relative Activation of the *Collagen α1(X)* and *MMP13* Promoters.
The promoter regions of both *Collagen α1(X)* (panel A) and *MMP13* (panel B) can be activated by MEF2C but not by Runx2 in COS7 cells. Synergistic activation of these promoters by combinations of MEF2C and Runx2 is not observed. Putative enhancer regions (boxed regions in Figure III.15) of the proximal *Runx2* promoter (panel C) and the distal *Runx2* promoter (panel D) cannot be activated by MEF2C.

independently of Runx2, or cooperatively with yet identified co-factors

Activation of the *Collagen α1(X)* promoter by MEF2C is the strongest of the bone promoters tested here. Since this genomic region is also reported to drive reporter gene expression in all hypertrophic chondrocytes *in vivo* (Gebhard et al, 2004), I chose the *Collagen α1(X)* promoter for further study. To further demonstrate that activation of the *Collagen α1(X)* promoter by MEF2 is direct, all six consensus MEF2 binding sites in this reporter construct were mutated to sites which did not fit the MEF2 consensus (Table III.1). The resulting mutations abolished activation of the *collagen α1(X)* promoter by

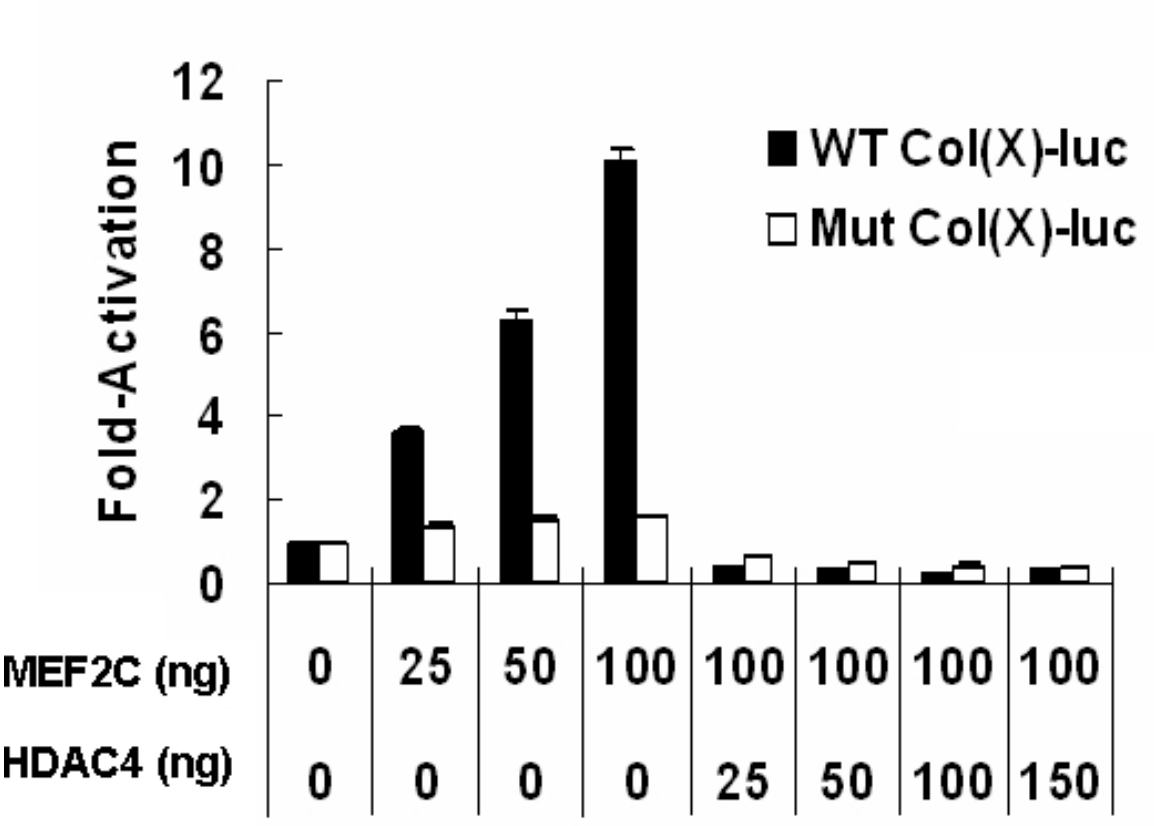

Figure III.17. Activation of the *Collagen α1(X)* Promoter by MEF2C Requires MEF2 Binding Sites.
Activation of the *Collagen α1 (X)* promoter by MEF2C can be repressed by HDAC4 (black bars), and depends on the presence of the consensus MEF2 binding sites (white bars).

MEF2C, suggesting that activation of this reporter is accomplished by direct binding of MEF2 (Figure III.17).

To confirm direct binding of MEF2C to sites in the *Collagen α1(X)* promoter, gel electromobility shift assays were preformed. Candidate MEF2 binding sites from the *Collagen α1(X)* promoter and the previously described MEF2 binding site in the promoter of the *srpk3* gene (Nakagawa et al., 2005) were analyzed for MEF2 binding activity (Figure III.18). MEF2 binding can be seen at two sites in the *Collagen α1(X)* promoter, -3205 and -53 which is conserved in the genomes of both mice and humans. To further examine the affinity of these sites for MEF2C, binding of MEF2C to the MEF2 site in the *srpk3* promoter was competed with unlabeled oligonucleotides containing the MEF2 sites of the *Collagen α1(X)* promoter. The two sites which were observed to bind MEF2 in the previous assay are the most capable of competing for MEF2 binding, and additional sites demonstrate lower affinities for MEF2 as evidenced by weaker competition with the *srpk3* oligonucleotide (Figure III.18)

Given the ability of MEF2 to bind and activate expression of a *Collagen α1(X)* promoter reporter *in vitro*, I confirmed the ability of this reporter to direct expression in hypertrophic chondrocytes *in vivo*. I constructed a transgene in which the region of the *Collagen α1(X)* promoter examined above was positioned upstream of a basal promoter and the LacZ gene. Consistent with a previous report (Gebhard et al., 2004), LacZ expression of the *Collagen α1(X) promoter-LacZ* transgenic mice recapitulates the expression pattern of endogenous *Collagen α1(X)* in nearly every endochondral bone (Figure III.19 panel A).

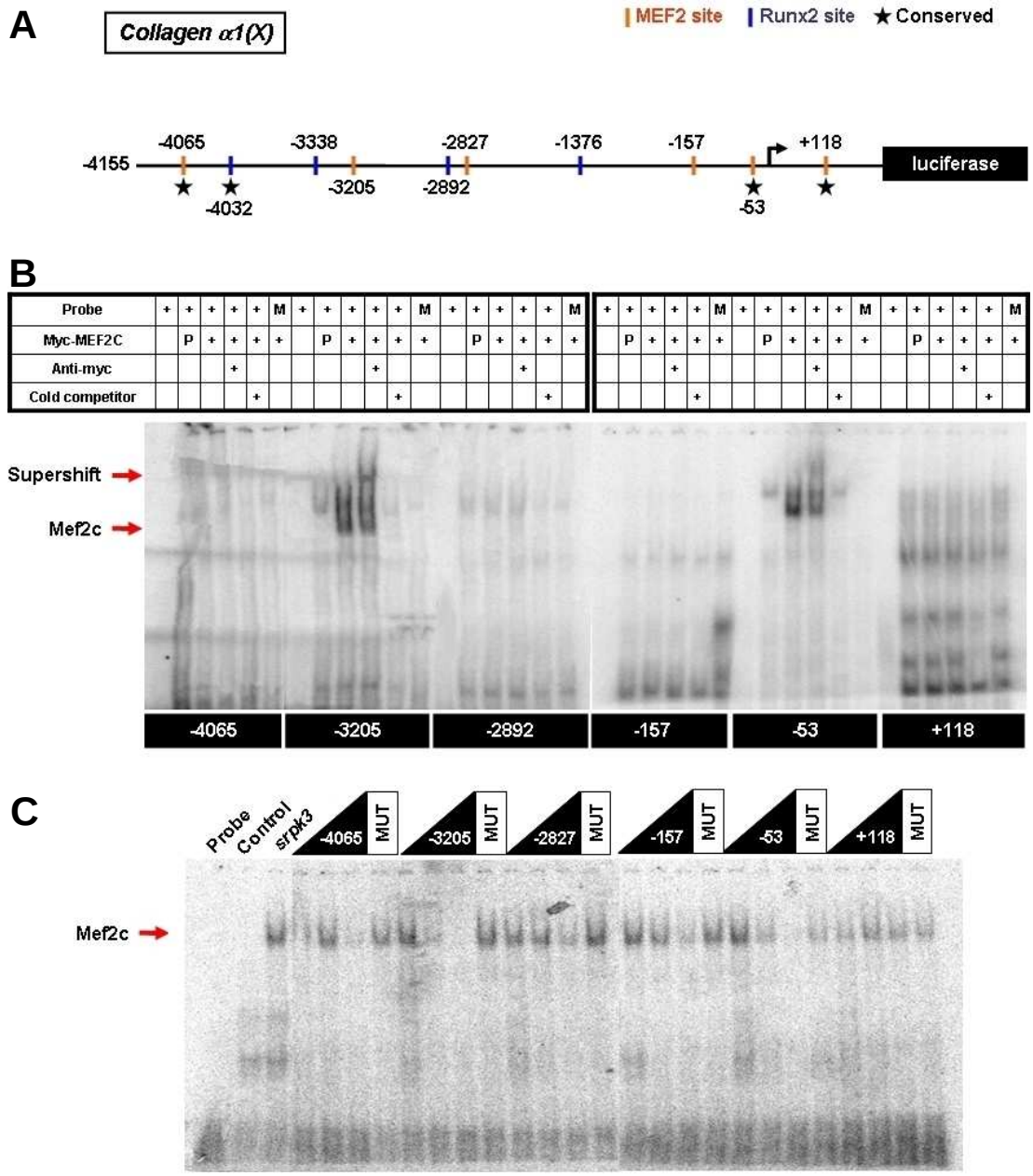

Figure III.18 MEF2C Binds to Sites in the *Collagen α1(X)* Promoter.
Oligonucleotides containing the potential MEF2 binding sites of the *Collagen (X)* promoter (panel A, sequences listed in Figure III.17) were labeled and assayed for binding to MEF2C (panel B). Each α-^{32}P labeled sequence was tested in binding reactions containing no protein, Myc tagged MEF2C, Myc tagged MEF2Cand an anti-Myc antibody, Myc tagged MEF2C and an unlabeled oligonucleotide containing the MEF2 binding site of the *srpk3* promoter "cold competitor", or a labeled probe containing a mutated MEF2C binding site was substituted "M", and incubated with Myc tagged MEF2C. The ability of these sites to compete for MEF2C binding with a α-^{32}P labeled oligonucleotide containing the MEF2 binding site of the *srpk3* promoter (panel C) was assayed at equal, 10 fold or 100 molar concentration of the labeled oligo, or with 100 molar excess with a mutated MEF2 binding site "MUT".

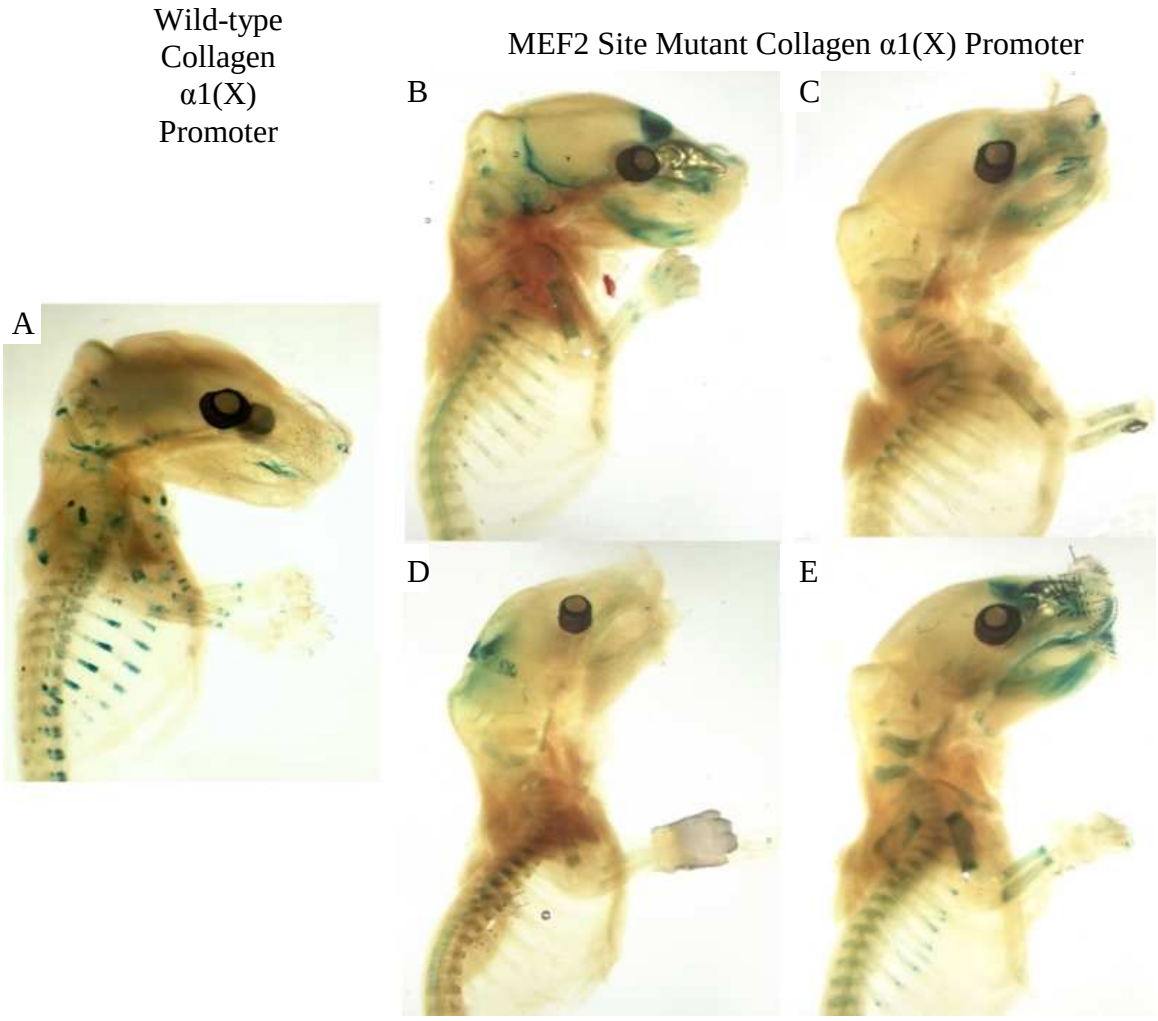

Figure III.19. A Genomic Region Upstream of the *Collagen α1(X)* Gene Can Drive Reporter Gene Expression in Hypertrophic Chondrocytes.
β-galactosidase staining of E18.5 embryos that is positive for a lacZ transgene which contains 4 kilobases of wild-type sequence of the *collagen α1(X)* genomic locus (panel A), or the same region of the *collagen α1(X)* genomic locus with mutations in each of the six MEF2 binding sites (panels B to E)

To determine if the in vivo expression of *Collagen α1(X)* promoter-lacZ is dependent on the consensus MEF2 binding sites, a *Collagen α1(X)* promoter-lacZ transgene was constructed containing mutations in all six consensus MEF2 binding sites; the same mutations which abolished *in vitro* activation of this reporter. The resulting transgenic mice were analyzed for β-galactosidase staining at E18.5. Mice positive for

the transgene in which the MEF2 binding sites are mutated show decreased levels of staining in endochondral growth plates. This demonstrates that MEF2 proteins are important in regulating the expression of this reporter, and may play a general role in regulating gene expression in hypertrophic chondrocytes.

Oligonucleotide Name	Sequence
Col X 4kb Promoter fwd SmaI	GGTTCCCGGGTTGGGCCTCCTGTTTCACGTAG
Col X Promoter rev XhoI	GGTTGTCGACGAGTCTTTGACATGACTTGAAATAGCTAGAACTTTCGAG
ColX -4032 mut up	CGAGGAAACACCCAGAATACCCCTAGTTTAATACACACAATTAG
ColX -4032 mut lw	CTAATTGTGTGTATTAAACTAGGGGTATTCTGGGTGTTTCCTCG
ColX -4032 gsmut up	GGGGAGGAAACACCCAGAATACCCCTAGTTTAATACACACAAT
ColX -4032 gsmut lw	GGGATTGTGTGTATTAAACTAGGGGTATTCTGGGTGTTTCCTC
ColX -4032 gs up	GGGGAGGAAACACCCAGAATAAAAATAGTTTAATACACACAAT
ColX -4032 gs lw	GGGATTGTGTGTATTAAACTATTTTTATTCTGGGTGTTTCCTC
ColX -3205 mut up	GATATAAAAGCTAGCGGTAAAACCAGGTATGACGGTACACTTCTG
ColX -3205 mut lw	GTACCGTCATACCTGGTTTTACCGCTAGCTTTTATATCAGTTTAG
ColX -3205 gsmut up	GGGAAACTGATATAAAAGCTAGCGGTAAAACCAGGTATGACGG
ColX -3205 gsmut lw	GGGCCGTCATACCTGGTTTTACCGCTAGCTTTTATATCAGTTT
ColX -3205 gs up	GGGAAACTGATATAAAAGCTATATTTAAAACCAGGTATGACGG
ColX -3205 gs lw	GGGCCGTCATACCTGGTTTTAAATATAGCTTTTATATCAGTTT
ColX -2827 mut up	TTCCAGCTTCTGTCTATTAGCCCTATGGCTGCTATGAACATAATG
ColX -2827 mut lw	TTATGTTCATAGCAGCCATAGGGCTAATAGACAGAAGCTGGAAAG
ColX -2827 gsmut up	GGGTCCAGCTTCTGTCTATTAGCCCTATGGCTGCTATGAACAT
ColX -2827 gsmut lw	GGGATGTTCATAGCAGCCATAGGGCTAATAGACAGAAGCTGGA
ColX -2827 gs up	GGGTCCAGCTTCTGTCTATTATAAATATGGCTGCTATGAACAT
ColX -2827 gs lw	GGGATGTTCATAGCAGCCATATTTATAATAGACAGAAGCTGGA
ColX -157 mut up	AGAATGTATTTTACCCCTAAAAAGGGTGAA
ColX -157 mut lw	TTCACCCTTTTTAGGGGTAAAATACATTCTTGTGTTATTTG
ColX -157 gsmut up	GGGAGAATGTATTTTACCCCTAAAAAGGGTGAA
ColX -157 gsmut lw	GGGTTCACCCTTTTTAGGGGTAAAATACATTCT
ColX -157 gs up	GGGAGAATGTATTTTAAAAATAAAAAGGGTGAA
ColX -157 gs lw	GGGTTCACCCTTTTTATTTTTAAAATACATTCT
ColX -53 mut up	ACAGCCGAAGCGCGGAATATATAATGGAGA
ColX -53 mut lw	TCTCCATTATATATTCCGCGCTTCGGCTGT
ColX -53 gsmut up	GGGACAGCCGAAGCTAGGCCTATATAATGGAGA
ColX -53 gsmut lw	GGGTCTCCATTATATAGGCCTAGCTTCGGCTGT
ColX -53 gs up	GGGACAGCCGAAGCTATTAATATATAATGGAGA
ColX -53 gs lw	GGGTCTCCATTATATATTAATAGCTTCGGCTGT
ColX +118 mut up	GAAGAAAACAGTAGCCCTACTCCAGGGCAG
ColX +118 mut lw	CTGCCCTGGAGTAGGGCTACTGTTTTCTTC
ColX +118 gsmut up	GGGGAAGAAAACAGTATAAATACTCCAGGGCAG
ColX +118 gsmut lw	GGGCTGCCCTGGAGTATTTATACTGTTTTCTTC
ColX +118 gs up	GGGGAAGAAAACAGTATAAATACTCCAGGGCAG
ColX +118 gs lw	GGGCTGCCCTGGAGTATTTATACTGTTTTCTTC
ColX seq up1	CTGGGTCACACTGCTGAGTCTACAG
ColX seq up2	GAGAGGCACTTGGACTACATGGAAG
ColX seq up3	GCTGAGAACATAGCAGAACAG
Col X seq up4	CAATATGAACTAACCAGTATCTCCAG
Col X seq up5	GCCAGAGTTCTTAACTGCTAAG
Col X seq up6	GATACAGAACTTGGTCTCTCAG
Col X seq up7	CATGCACCAGCTTCTAAGAG
MMP13 prom fwd KpnI	GGATCCGCCAACCTCAGCTCCATAGTGAGTTTGAG
MMP13 promoter rev XhoI	CTCGAGGTGCCCAGCAGTGCCTGGAGTCTCTCCTTCCCAG
MMP13 prom seq 1 fwd	ATGACCTTGGTCAGAGTCAGCAG
MMP13 prom seq 2 fwd	AATACGCATTAGAGTTGAGAAGTAG
MMP13 prom seq 3 fwd	GTGTGACAAGTTCCACAAACTGAG
MMP13 prom seq 4 fwd	GTTCTGTTTGTGATTCACTGAATACATAG
BSP prom up KpnI	GGTACCGCCTAGTCCATCATCAATGGGATGAGAAG
BSP prom lw (XhoI)	CTTGCCCATTACCTTAACCTTCCTTTCGGCAG
BSP seq up1	GAACGCTGTAACGTTCACAGTCAG
MEF2C tg geno lw	GAGGCCCTTCTTTCTCAATGTCTCCACAATGTCTGAG
MEF2C tg geno up	GATTCAGATTACGAGGATAATGGATGAGCGTAACAGACAG
MMP13 probe lw	GCTCATCTGTGGCTCCCCATACATGAACTCCTCACAATTTTCAAG
MMP13 probe up	GCCCATACAGTTTGAATACAGTATCTGGAGTAATCGCATTGTGAG

Oligonucleotide Name	Sequence
MSSK MEF2 gs lw	GGGTCACTCGCCTTTATAAATAGCCTCCCAGCT
MSSK MEF2 gs up	GGGAGCTGGGAGGCTATTTATAAAGGCGAGTGA
Runx2 Dist Prom fwd KpnI	GGTACCAGACCTCAATCCACAATAGCCTTTTCTGAACCCAATGAG
Runx2 Dist Enc rev XhoI	CTCGAGCTTGTATGACAGCTGAGGATGTGGCCAGACTAAAGCAG
Runx2 Dist Prom rev XhoI	CTCGAGCTTGTGGTTCTGTGGTTGTTTGTGAGGCGAATGAAG
Runx2 Dist prom seq 1	GTCTTTCCTTATCATCTAATACAATCTCTTAACATTATTTG
Runx2 Dist prom seq 2	CAATACAAGAACAATTCAAGTGAACAAGAGAG
Runx2 Dist prom seq 3	CACTCTTCAGAGAGCAATGCCTCACAATCAG
Runx2 Dist prom seq 4	GCCAAGTTCAAAATACTCTGTACTCACAACCAG
Runx2 Dist prom seq 5	GATATTACTATACTGTTATATTCACATGTCTTG
Runx2 Dist prom seq 6	GCAACCTCTACTAAACTCTTGTATCATGAGATACAG
Runx2 Dist prom seq 7	GTATAAATATCTGTTTTACAGTAAAACATGAG
Runx2 Dist prom seq 8	GAAAAATCCTCCATCGCTCCCAACTAATGAAAACAG
Runx2 Dist prom seq 9	CAATTCCTGACATTTGTTTTTTAAGATCTTCAAAG
Runx2 Dist prom seq 10	GCTACAGAGTTCTGCTCTCCAGAG
Runx2 Prox Enc rev SalI	GTCGACAAACTGACAGAACTGAGAAACGGCCCATGTTTCAAATAG
Runx2 Prox Prom fwd SmaI	CCCGGGCATTTCATGGCAGCAGTAAGGACGCATACACAAAAG
Runx2 Prox Prom rev SalI	GTCGACGCTAAAGCTGAGAAGCGGGAGAGCCTCAG
Runx2 Prox Prom seq 1	GGCCTGCATGTCTCATTATGCATCAAG
Runx2 Prox Prom seq 2	GTAACTCGCTCCACCTGTAATG
Runx2 Prox Prom seq 3	CTGCGCTAGGGAGGGTCATGACAG
Runx2 Prox Prom seq 4	GAAATCCCAGCCTCCAAAAACCACATTTTAG

Table III.1. Oligonucleotide Sequences.

Oligonucleotides utilized in generation and verification of reporter constructs, generation of mutant reporter constructs, gel electromobility shify assays, generation of ribonucleotide probe templates, and genotyping of transgenic mice.

Discussion

Summary

The results described in this chapter reveal an essential and unexpected role for MEF2C in chondrocyte hypertrophy and endochondral bone formation. During endochondral bone formation, MEF2C is expressed in prehypertrophic and hypertrophic cartilage. Hypertrophy of chondrocytes within endochondral bones is exquisitely sensitive to the level of MEF2C activity such that reduction of MEF2C expression by only 50% in *Mef2c*$^{+/-}$ mice results in a pronounced diminution in ossification of the sternebrae. The finding that this abnormality in ossification can be rescued in a dose dependent manner by removal of *HDAC4* alleles provides strong evidence for the association of MEF2C and HDAC4 in chondrocytes and demonstrates that bone development is dependent on the precise stoichiometry between these positive and negative transcriptional regulators, respectively.

Control of Chondrocyte Hypertrophy and Ossification by MEF2C

The lengthwise growth of endochondral bones depends on the growth plate dynamics of chondrocyte hypertrophy. The absence of HDAC4 results in premature growth plate fusion, restricting the growth of endochondral bones. This feature is prominent in the base of the skull, where premature fusion of the endochondral growth plates results in deformation of the cranial vault. The defects in ossification of these bones when *Mef2c* is deleted from the neural crest led me to investigate the role of *Mef2c* in endochondral cartilage development, especially the potential relationship of HDAC4 and MEF2C. My data identifies MEF2C as an essential and previously unknown

regulator of chondrocyte hypertrophy (Figure III.20). The absence of MEF2C from endochondral cartilage results in shortening of endochondral bones, most notably the limbs, and persistence of the growth plate cartilage. MEF2C is required for the development of endochondral bones of mesodermal origin, in addition to endochondral bones derived from neural crest precursors.

To determine if MEF2C is directly responsible for activating gene expression in hypertrophic chondrocytes, I examined a previously identified promoter and enhancer of the *Collagen α1(X)* gene which is sufficient to drive reporter gene expression in hypertrophic chondrocytes *in vivo*. MEF2C is capable of activating this promoter, and the promoter of *MMP13*, *in vitro*. Since MEF2C is expressed in a wide variety of cell types, I expected that MEF2C would activate the expression of a chondrocyte specific gene in cooperation with factors restricted to bone, such as Runx2. Surprisingly, MEF2C and Runx2 do not cooperate in activating the *Collagen α1(X)* promoter, suggesting that MEF2C may function independently of Runx2, or cooperatively via yet identified co-factors. Runx2 could potentially activate the expression of MEF2C. It will be important to identify the critical regulatory regions of *Mef2c* to determine if the activation of *Mef2c* in chondrocytes depends on Runx2.

Bone Development is Regulated by the Balance of MEF2C and HDAC4

I demonstrate that MEF2C and HDAC4 play antagonistic roles in the regulation of chondrocyte hypertrophy. Intercrosses of the null alleles of *HDAC4* and *Mef2c* demonstrate their antagonistic roles in bone development, highlighting the requirement for a balance of HDAC4 and MEF2C in normal bone development (Figure III.21).

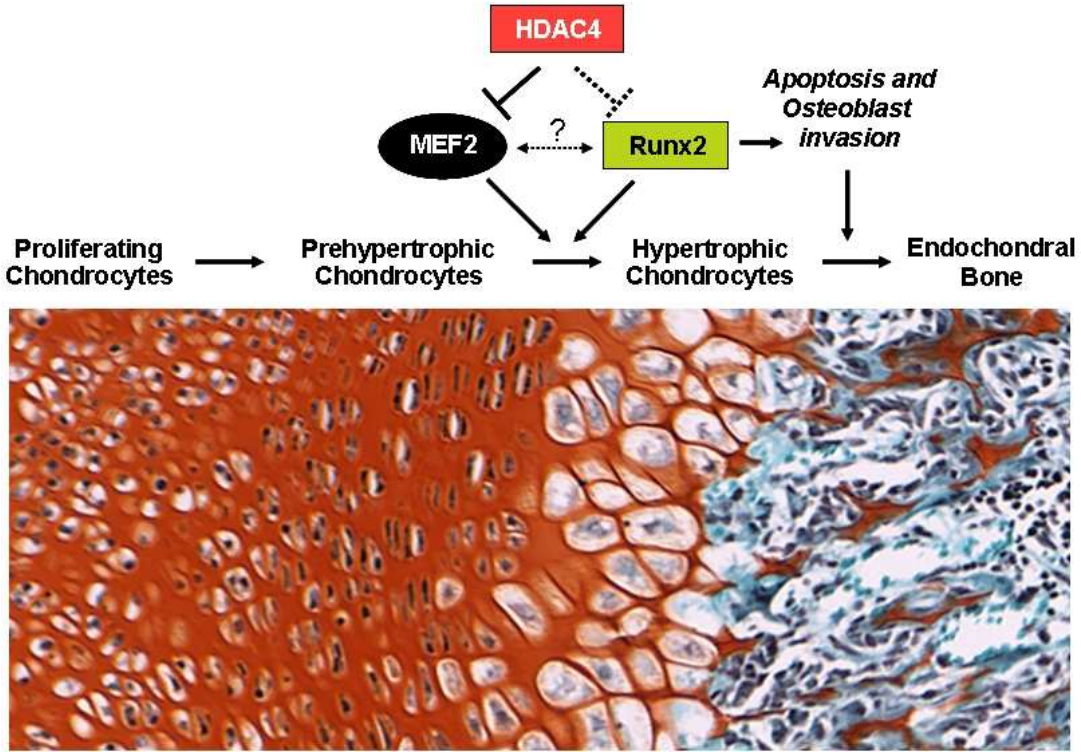

Figure III.20 MEF2 is an Essential Regulator of Chondrocyte Hypertrophy
MEF2 transactivation is essential for chondrocyte hypertrophy, and is a key mediator of HDAC4 repression in chondrocytes.

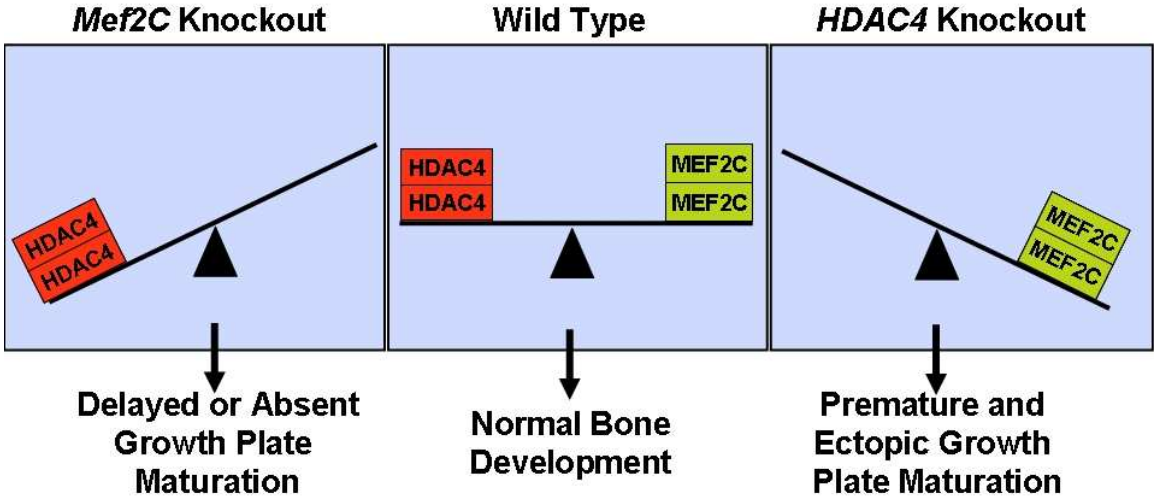

Figure III.21 Bone Development is Regulated by the Balance of MEF2C and HDAC4
The development of endochondral bones can be altered by the balance of HDAC4 repression and MEF2C transactivation. This balancing point may be a key control point downstream of pathologic signals which result in dwarfisms caused by either excessive activation of MEF2C, or failure to export HDAC4 from the nucleus and relieve repression of MEF2C.

The nearly identical phenotypes observed when *Mef2c* is deleted from several mesodermal lineages or specifically from chondrocytes demonstrates that defects observed in MEF2C deficient mice are due to defects in chondrocyte hypertrophy. The expression of HDAC4 in bone is restricted to chondrocytes (Vega 2004). My data demonstrates that MEF2C activity and its regulation by HDAC4 is a key control point in regulating chondrocyte gene expression.

Runx2 and Runx3 undoubtedly regulate chondrocyte maturation as evidenced by the block in chondrocyte hypertrophy in mice null for both *Runx2* and *Runx3*, however their repression by HDAC4 *in vivo* has not been demonstrated. *Mef2c* and *Runx2* interact genetically, enhancing the endochondral bone defects seen in *Mef2c* mice. However, this result, is complicated by the strong requirement for Runx2 in osteoblast development, and may require conditional deletion of Runx2 from chondrocytes. Further genetic investigations into the interactions of *HDAC4* and *Runx2* will face similar complications. It would be reasonable to expect that the defects in osteoblast differentiation observed in *Runx2* mutant mice would not be rescued by removal of *HDAC4*, since *HDAC4* is not expressed in osteoblasts. However, the ectopic ossification seen in *HDAC4* null mice might be diminished by removal of *Runx2* due to decreased osteoblast activity. It will be important to determine the extent of chondrocyte hypertrophy in mice null for both *HDAC4* and *Runx2* to determine the extent to which deletion of *Runx2* can rescue the premature and ectopic chondrocyte hypertrophy of *HDAC4* null mice.

Implications for Skeletal Disease

Misregulation of signaling pathways that influence growth plate dynamics are responsible for dwarfisms and bone deformations resulting from either premature maturation of the growth plate cartilage, characteristic of achondroplasia (Chen el al., 1999, Li et al., 1999, Reviewed in Horton 2006 and Ornitz 2005), or delayed or absent chondrocyte maturation, characteristic of many chondrodysplasia syndromes (Reviewed in Schipani and Provot 2003, Cohen 2002). My results demonstrate that growth plate dynamics can be modified by the balance of MEF2C and its repressor, HDAC4. The activation of MEF2C dependent transcription by a variety of signaling pathways, and the ability of MEF2C to directly activate chondrocyte gene expression demonstrates that MEF2C and HDAC4 control a key nodal point in chondrocyte hypertrophy and growth plate dynamics. Further investigation may identify molecules which can influence the interaction of MEF2C and HDAC4 in chondrocytes and make control of growth plate dynamics possible.

Methods

Transgenic mice.

Chondrocyte-specific transgenes were constructed by subcloning either an in-frame fusion of the MEF2C DNA binding domain (amino acids 1 to 105) and the engrailed repressor, or an in-frame fusion of MEF2C (amino acids 1 to 436) and the VP16 activation domain, between a 3-kb fragment of the *collagen α1(II)* promoter and its 3-kb chondrocyte-specific enhancer region (Zhou et al., 1998). Linearized transgenic constructs were injected into the pronuclei of fertilized oocytes.

Cell Culture, Reporter Plasmids and Transfection

COS7 cells were grown in DMEM with 10% FBS. Fugene 6 (Roche) was used for transient transfection according to the manufacturer's instructions. A reporter plasmid containing 4.5 kb of the collagen α1(X) locus was generated by PCR and cloned into pGL3. COS7 cells were transfected with pCNDA Myc-MEF2C or a Runx2 expression vector (Kern et al., 2001)). Reporter plasmids and mutants were generated by PCR using oligonucleotides in Table III.1 and cloned into pGL3-basic, or pGL3-TATA (Promega). Plasmids were co-transfected with 10ng of a CMV-β-galactosidase reporter plasmid to control for transfection efficiency. Transfections were preformed in collaboration with Yuri Kim.

Electromobility Shift Assays

Cell lysates containing MEF2C, were prepared from transfected COS7. In vitro binding analysis was performed as previously described (Wang et al., 2001), using

oligonucleotide fragments that contained a MEF2-binding site from the *collagen α1(X)* promoter, or the *srpk3* promoter (Nakagawa et al., 2005). Complimentary oligonucleotides designed with 5' overhanging guanine nucleotides, hybridized and overhanging sequences were made double stranded by incorporation of [α-^{32}P]-dCTP by the Klenow fragment of DNA polymerase I (New England Biolabs) and purified using G25 spin columns. Oligonucleotide sequences are listed in Table III.1. Assays were preformed in collaboration with Yuri Kim.

Tissue specific deletion of *Mef2c*

To generate mice that lack MEF2C in specific tissues, mice heterozygous for the null allele of *Mef2c* were mated to mice bearing the designated Cre transgene. The resulting mice were mated to mice heterozygous for the *Mef2c*^{loxP} allele to produce conditional null mice (*Mef2c*$^{loxP/-}$*;Cre)*. Mesoderm deletion of MEF2C was performed using *twist2-Cre* (Yu et al., 2003). Chondrocyte deletion was performed using *Col2-Cre* (Long et al., 2001). Mice heterozygous for the existing null allele of *Mef2c* (Lin et al., 1997) were mated to mice positive from each Cre line. Cre positive *Mef2c* heterozygous mice were mated to mice homozygous for the *Mef2c*^{loxP} allele. All animal experimental procedures were reviewed and approved by the Institutional Animal Care and Use Committees at the University of Texas Southwestern Medical Center.

Cartilage and Bone Staining

Euthanized mice were skinned, eviscerated, and fixed overnight in 100% ethanol. Adult animals were additionally incubated overnight in acetone to clear fatty tissues. All

specimens were then stained using Alcian blue. Soft tissues were removed by incubation in 2% KOH as needed, and specimens were stained with Alizarin red for 30 to 90 minutes as needed. Tissues were cleared in 1%KOH, 20% glycerol and photographed in 50% ethanol, 50% glycerol. Staining reagents were prepared as described in Chapter II.

Histology

Tissues were fixed in 10% phosphate-buffered formalin at 4°C. Samples were then embedded in paraffin, sectioned at 5 um, and stained with hematoxylin and eosin or Von Kossa's method as described in Chapter II. These protocols were executed by members of the laboratory of Dr. James Richardson.

***In situ* hybridization**

Tissue samples were fixed overnight in DEPC-treated 4% paraformaldehyde. Riboprobes were labeled with [α-^{35}S]-UTP using the MAXIscript in vitro transcription kit (Ambion, Austin, Texas). In situ hybridization of sectioned tissues was performed as previously described Shelton et al., 2000 and Chapter II. Hybridizations and slide development were executed by John Shelton, and other members of the laboratory of Dr. James Richardson.

LacZ Staining of Transgenic Mouse Bones

Transgenic embryos were collected at E18.5 and stained as described in Zhou et al, 1995. Samples were skinned, eviscerated and fixed in PBS supplemented with 4%

paraformaldehyde for 30 minutes on ice. Samples were then washed three times, each for 30 minutes, in PBS supplemented with 2mM $MgCl_2$, 0.2% NP40, and 0.1% deoxycholic acid. Samples were then stained in the dark for 48 hours in PBS supplemented with 2mM $MgCl_2$, 0.2% NP40, 0.1% deoxycholic acid, 5mM potassium ferrocyanide, 5mM potassium ferricyanide and 1mg/ml X-gal. Stained samples were then fixed overnight at room temperature in PBS supplemented with 4% paraformaldehyde. For photography, fixed samples were dehydrated into methanol by 30 minute washes in PBS with 25% (v/v) methanol, PBS with 50% methanol, PBS with 75% methanol and 100% methanol and cleared in 2:1 benzyl alcohol:benzyl benzoate for approximately 4 hours.

Bibliography

Chang S, McKinsey TA, Zhang CL, Richardson JA, Hill JA, Olson EN. (2004). Histone deacetylases 5 and 9 govern responsiveness of the heart to a subset of stress signals and play redundant roles in heart development. Mol Cell Biol. *24*, 8467-76.

Chen L, Adar R, Yang X, Monsonego EO, Li C, Hauschka PV, Yayon A, Deng CX. (1999). Gly369Cys mutation in mouse FGFR3 causes achondroplasia by affecting both chondrogenesis and osteogenesis. J Clin Invest. *104*, 1517-25.

Cohen MM Jr. Some chondrodysplasias with short limbs: molecular perspectives. (2002). Am J Med Genet. *112*, 304-13.

Dodou E, Verzi MP, Anderson JP, Xu SM, Black BL. (2004). Mef2c is a direct transcriptional target of ISL1 and GATA factors in the anterior heart field during mouse embryonic development. Development. *131*, 3931-42.

Ducy P, Zhang R, Geoffroy V, Ridall AL, Karsenty G. (1997). Osf2/Cbfa1: a transcriptional activator of osteoblast differentiation. Cell. *89*, 747-54.

Edmondson DG, Lyons GE, Martin JF, Olson EN. (1994). Mef2 gene expression marks the cardiac and skeletal muscle lineages during mouse embryogenesis. Development. *120*, 1251-63.

Fischle W, Emiliani S, Hendzel MJ, Nagase T, Nomura N, Voelter W, Verdin E. (1999). A new family of human histone deacetylases related to Saccharomyces cerevisiae HDA1p. J Biol Chem. *274*, 11713-20.

Flavell SW, Cowan CW, Kim TK, Greer PL, Lin Y, Paradis S, Griffith EC, Hu LS, Chen C, Greenberg ME. (2006). Activity-dependent regulation of MEF2 transcription factors suppresses excitatory synapse number. Science. *311*, 1008-12.

Gebhard S, Poschl E, Riemer S, Bauer E, Hattori T, Eberspaecher H, Zhang Z, Lefebvre V, de Crombrugghe B, von der Mark K. (2004). A highly conserved enhancer in mammalian type X collagen genes drives high levels of tissue-specific expression in hypertrophic cartilage in vitro and in vivo. Matrix Biol. *23*, 309-22.

Gossett LA, Kelvin DJ, Sternberg EA, Olson EN. (1989). A new myocyte-specific enhancer-binding factor that recognizes a conserved element associated with multiple muscle-specific genes. Mol Cell Biol. *9*, 5022-33.

Grozinger CM, Hassig CA, Schreiber SL. Three proteins define a class of human histone deacetylases related to yeast Hda1p. (1999). Proc Natl Acad Sci U S A. *96*, 4868-73.

Grozinger CM, Schreiber SL. Regulation of histone deacetylase 4 and 5 and transcriptional activity by 14-3-3-dependent cellular localization. (2000). Proc Natl Acad Sci U S A. *97*, 7835-40.

Han J, Jiang Y, Li Z, Kravchenko VV, Ulevitch RJ. (1997). Activation of the transcription factor MEF2C by the MAP kinase p38 in inflammation. Nature. *386*, 296-9.

Harada S, Rodan GA. (2003). Control of osteoblast function and regulation of bone mass. Nature. *423*, 349-55.

Hayashi S, McMahon AP. (2002). Efficient recombination in diverse tissues by a tamoxifen-inducible form of Cre: a tool for temporally regulated gene activation/inactivation in the mouse. Dev Biol. *244*, 305-18.

Hoch RV, Soriano P. (2006). Context-specific requirements for Fgfr1 signaling through Frs2 and Frs3 during mouse development. Development. *133*, 663-73.

Horton WA. (2006). Recent milestones in achondroplasia research. Am J Med Genet A. *140*, 166-9.

Jiang X, Rowitch DH, Soriano P, McMahon AP, Sucov HM. (2000). Fate of the mammalian cardiac neural crest. Development. *127*, 1607-16.

Kern B, Shen J, Starbuck M, Karsenty G. (2001). Cbfa1 contributes to the osteoblast-specific expression of type I collagen genes. J Biol Chem. *276*, 7101-7.

Kim Y, Phan D and Olson EN
Unpublished data.

Komori T, Yagi H, Nomura S, Yamaguchi A, Sasaki K, Deguchi K, Shimizu Y, Bronson RT, Gao YH, Inada M, Sato M, Okamoto R, Kitamura Y, Yoshiki S, Kishimoto T. (1997) Targeted disruption of Cbfa1 results in a complete lack of bone formation owing to maturational arrest of osteoblasts. Cell. *89*, 755-64.

Lefebvre V, Smits P. (2005). Transcriptional control of chondrocyte fate and differentiation. Birth Defects Res C Embryo Today. *75*, 200-12.

Li C, Chen L, Iwata T, Kitagawa M, Fu XY, Deng CX. (1999). A Lys644Glu substitution in fibroblast growth factor receptor 3 (FGFR3) causes dwarfism in mice by activation of STATs and ink4 cell cycle inhibitors. Hum Mol Genet. *8*, 35-44.

Lin Q, Lu J, Yanagisawa H, Webb R, Lyons GE, Richardson JA, Olson EN. (1998). Requirement of the MADS-box transcription factor MEF2C for vascular development. Development. *125*, 4565-74.

Lin Q, Schwarz J, Bucana C, Olson EN. (1997). Control of mouse cardiac morphogenesis and myogenesis by transcription factor MEF2C. Science. *276*, 1404-7.

Long F, Zhang XM, Karp S, Yang Y, McMahon AP. (2001). Genetic manipulation of hedgehog signaling in the endochondral skeleton reveals a direct role in the regulation of chondrocyte proliferation. Development. *128*, 5099-108.

Lu J, McKinsey TA, Zhang CL, Olson EN. (2000a) Regulation of skeletal myogenesis by association of the MEF2 transcription factor with class II histone deacetylases. Mol Cell. *6*, 233-44.

Lu J, McKinsey TA, Nicol RL, Olson EN. (2000b). Signal-dependent activation of the MEF2 transcription factor by dissociation from histone deacetylases. Proc Natl Acad Sci U S A. *97*, 4070-5.

Lyons GE, Micales BK, Schwarz J, Martin JF, Olson EN. (1995). Expression of mef2 genes in the mouse central nervous system suggests a role in neuronal maturation. J Neurosci. *15*, 5727-38.

Ma K, Chan JK, Zhu G, Wu Z. (2005). Myocyte enhancer factor 2 acetylation by p300 enhances its DNA binding activity, transcriptional activity, and myogenic differentiation. Mol Cell Biol. *25*, 3575-82.

McKinsey TA, Zhang CL, Lu J, Olson EN. (2000). Signal-dependent nuclear export of a histone deacetylase regulates muscle differentiation. Nature. *408*, 106-11.

McKinsey TA, Zhang CL, Olson EN. (2001). Control of muscle development by dueling HATs and HDACs. Curr Opin Genet Dev. 2001 *11*, 497-504.

Molkentin JD, Black BL, Martin JF, Olson EN. (1996). Mutational analysis of the DNA binding, dimerization, and transcriptional activation domains of MEF2C. Mol Cell Biol. *16*, 2627-36.

Molkentin JD, Olson EN. (1996). Combinatorial control of muscle development by basic helix-loop-helix and MADS-box transcription factors. Proc Natl Acad Sci U S A. *93*, 9366-73.

Mundlos S, Otto F, Mundlos C, Mulliken JB, Aylsworth AS, Albright S, Lindhout D, Cole WG, Henn W, Knoll JH, Owen MJ, Mertelsmann R, Zabel BU, Olsen BR. (1997). Mutations involving the transcription factor CBFA1 cause cleidocranial dysplasia. Cell. *89*, 773-9.

Nakagawa O, Arnold M, Nakagawa M, Hamada H, Shelton JM, Kusano H, Harris TM, Childs G, Campbell KP, Richardson JA, Nishino I, Olson EN. (2005). Centronuclear myopathy in mice lacking a novel muscle-specific protein kinase transcriptionally regulated by MEF2. Genes Dev. *19*, 2066-77.

Naya FJ, Wu C, Richardson JA, Overbeek P, Olson EN. (1999). Transcriptional activity of MEF2 during mouse embryogenesis monitored with a MEF2-dependent transgene. Development. *126*, 2045-52.

Naya FJ, Black BL, Wu H, Bassel-Duby R, Richardson JA, Hill JA, Olson EN. (2002). Mitochondrial deficiency and cardiac sudden death in mice lacking the MEF2A transcription factor. Nat Med. *8*, 1303-9.

Ornitz DM. (2005). FGF signaling in the developing endochondral skeleton. Cytokine Growth Factor Rev. *16*, 205-13.

Otto F, Thornell AP, Crompton T, Denzel A, Gilmour KC, Rosewell IR, Stamp GW, Beddington RS, Mundlos S, Olsen BR, Selby PB, Owen MJ. (1997). Cbfa1, a candidate gene for cleidocranial dysplasia syndrome, is essential for osteoblast differentiation and bone development. Cell. *89*, 765-71.

Schipani E, Provot S. (2003). PTHrP, PTH, and the PTH/PTHrP receptor in endochondral bone development. Birth Defects Res C Embryo Today. *69*, 352-62.

Shin CH, Liu ZP, Passier R, Zhang CL, Wang DZ, Harris TM, Yamagishi H, Richardson JA, Childs G, Olson EN. (2002). Modulation of cardiac growth and development by HOP, an unusual homeodomain protein. Cell. *110*, 725-35.

Srivastava D, Olson EN. (2000). A genetic blueprint for cardiac development. Nature. *407*, 221-6.

Stickens D, Behonick DJ, Ortega N, Heyer B, Hartenstein B, Yu Y, Fosang AJ, Schorpp-Kistner M, Angel P, Werb Z. (2004). Altered endochondral bone development in matrix metalloproteinase 13-deficient mice. Development. *131*, 5883-95.

Stanton LA, Sabari S, Sampaio AV, Underhill TM, Beier F. (2004). p38 MAP kinase signalling is required for hypertrophic chondrocyte differentiation. Biochem J. *378*, 53-62.

Subramanian SV, Nadal-Ginard B. (1996). Early expression of the different isoforms of the myocyte enhancer factor-2 (MEF2) protein in myogenic as well as non-myogenic cell lineages during mouse embryogenesis. Mech Dev. *57*(1), :103-12.

Takeda S, Bonnamy JP, Owen MJ, Ducy P, Karsenty G. (2001). Continuous expression of Cbfa1 in nonhypertrophic chondrocytes uncovers its ability to induce hypertrophic chondrocyte differentiation and partially rescues Cbfa1-deficient mice. Genes Dev. *15*, 467-81.

Vega RB, Matsuda K, Oh J, Barbosa AC, Yang X, Meadows E, McAnally J, Pomajzl C, Shelton JM, Richardson JA, Karsenty G, Olson EN. (2004). Histone deacetylase 4 controls chondrocyte hypertrophy during skeletogenesis. Cell. *119*, 555-66.

Verdel A, Khochbin S. (1999). Identification of a new family of higher eukaryotic histone deacetylases. Coordinate expression of differentiation-dependent chromatin modifiers. J Biol Chem. *274*, 2440-5.

Vong LH, Ragusa MJ, Schwarz JJ. (2005). Generation of conditional Mef2cloxP/loxP mice for temporal- and tissue-specific analyses. Genesis. *43*, 43-8.

Wu H, Rothermel B, Kanatous S, Rosenberg P, Naya FJ, Shelton JM, Hutcheson KA, DiMaio JM, Olson EN, Bassel-Duby R, Williams RS. (2001). Activation of MEF2 by muscle activity is mediated through a calcineurin-dependent pathway. EMBO J. *20*, 6414-23.

Xu J, Gong NL, Bodi I, Aronow BJ, Backx PH, Molkentin JD. (2006). Myocyte enhancer factors 2A and 2C induce dilated cardiomyopathy in transgenic mice. J Biol Chem. *281*, 9152-62.

Yoshida CA, Yamamoto H, Fujita T, Furuichi T, Ito K, Inoue K, Yamana K, Zanma A, Takada K, Ito Y, Komori T. (2004). Runx2 and Runx3 are essential for chondrocyte maturation, and Runx2 regulates limb growth through induction of Indian hedgehog. Genes Dev. *18*, 952-63.

Yu K, Xu J, Liu Z, Sosic D, Shao J, Olson EN, Towler DA, Ornitz DM. (2003). Conditional inactivation of FGF receptor 2 reveals an essential role for FGF signaling in the regulation of osteoblast function and bone growth. Development. *130*, 3063-74.

Zhang CL, McKinsey TA, Lu JR, Olson EN. (2001). Association of COOH-terminal-binding protein (CtBP) and MEF2-interacting transcription repressor (MITR) contributes to transcriptional repression of the MEF2 transcription factor. J Biol Chem. *276*, 35-9.

Zhang CL, McKinsey TA, Chang S, Antos CL, Hill JA, Olson EN. (2002). Class II histone deacetylases act as signal-responsive repressors of cardiac hypertrophy. Cell. *110*, 479-88.

Zhou G, Garofalo S, Mukhopadhyay K, Lefebvre V, Smith CN, Eberspaecher H, de Crombrugghe B. (1995). A 182 bp fragment of the mouse pro alpha 1(II) collagen gene is sufficient to direct chondrocyte expression in transgenic mice. J Cell Sci. *108*, 3677-84.

VITAE

Michael Andrew Arnold was born in Brockport, New York on December 3, 1976, son of Mary Anne and Andrew Daniel Arnold. A 1995 graduate of Hilton Central High School in Hilton, New York, he received a Bachelor of Science in Molecular Genetics with a distinction in research from the University of Rochester in Rochester New York in 1999. He entered the Medical Scientist Training Program at the University of Texas Southwestern Medical Center at Dallas in 1999, and joined the Graduate Program in Genetics and Development in the laboratory of Dr. Eric N. Olson in 2001. The 2006 Genetics and Development Nominee for the University of Texas Southwestern Graduate School Nominata Award, he completed his Ph.D. requirements in June of 2006 and continued his training in the Medical Scientist Training Program. He married Christina Avery Martinez-Smith on May 5th, 2003 and has a daughter, Madelyn Catherine, born February 3rd, 2006.

Permanent Address: 95 Dunbar Rd.
Hilton, NY 14468